

Role of NOS-like proteins found in bacteria

by

Andrea B. L. Dupont

A thesis
presented to the University of Waterloo
in fulfillment of the
thesis requirement for the degree of
Master of Science
in
Chemistry

Waterloo, Ontario, Canada, 2006

©Andrea Dupont 2006

AUTHOR'S DECLARATION

I hereby declare that I am the sole author of this thesis. This is a true copy of the thesis, including any required final revisions, as accepted by my examiners.

I understand that my thesis may be made electronically available to the public.

Andrea Dupont

Abstract

Nitric oxide (NO) is a molecule with diverse biological effects involved in both signaling and defense mechanisms in mammalian systems. The production of NO is catalyzed from L-Arginine by a family of enzymes known as nitric oxide synthases (NOS). All mammalian isoforms contain an active site oxygenase domain and an electron-donating reductase domain joined by a calmodulin binding region. Recently, prokaryotic homologues to the oxygenase domain of mammalian NOS enzymes have been identified. Although several bacterial NOS (bNOS) enzymes have been characterized, their function is still unknown. Possible roles for this enzyme could include: (i) intercellular signaling to coordinate cellular/infectious activity, (ii) regulation via NO -mediated posttranslational modifications, or (iii) nitration of compounds in different biosynthetic pathways. Efforts, contained in this thesis, to determine a probable role for this enzyme are two-fold: (i) via a search for possible interacting protein partners, and (ii) via a proteomic analysis of the effects of a knockout of the bNOS gene.

Bacterial-NOS knockouts in *Bacillus subtilis* and *Bacillus cereus* have been created. 2D-Differential in gel electrophoresis (DIGE) has been used to analyze the proteomic effects of the expression of this gene in *B. subtilis*. Thus far 16 proteins which exhibited significant changes in expression, with a p value ≤ 0.05 and fold change $\geq |2|$, have been isolated and identified by peptide mass fingerprinting (PMF) in order to shed light on the relevance of this bacterial NOS homologue. The proteins which have been identified thus far are involved in cellular metabolism, amino acid metabolism and nitrogen metabolism. The identification of further proteins is required for a broader view of the impact of the expression of this gene on the proteome.

Acknowledgements

I would like to thank my Supervisor, Dr. Guy Guillemette, for giving me this opportunity to study such an intriguing area of research. I am grateful for the diversity of the experience I've gained through this project and your guidance and encouragement throughout.

I would like to thank Andrea Spires, whose expertise in the 2D gel world has been invaluable in the setup of this technology in our lab.

I would like to thank my labmates and thesis-buddies for all your guidance and encouragement through this process.

I would like to thank my family, friends, housemates and training partners who all 'smiled and nodded' endlessly while listening to me talk about protein gels for the past 2 years.

Finally, I would like to thank all of you for your love and support of all my dreams.

Dedication

I would like to dedicate this thesis to all those bacteria out there who still don't know what their NOS is used for.

Table of Contents

Author's Declaration.....	Error! Bookmark not defined.
AUTHOR'S DECLARATION FOR ELECTRONIC SUBMISSION OF A THESIS	ii
Abstract.....	iii
Acknowledgements.....	iv
Dedication.....	v
Table of Contents.....	vi
List of Figures.....	x
List of Tables	xii
List of Abbreviations	xiii
Chapter 1 : Introduction.....	1
1.1 Mammalian NOS.....	2
1.1.1 NOS Isoforms.....	2
1.1.2 Domain Architecture	2
1.1.2 Crystal Structure Highlights.....	4
1.1.2 NOS Mechanism.....	6
1.2 Bacterial NOS	10
1.2.1 Prevalence of bNOS in prokaryotic systems	10
1.2.2 Crystal Structure.....	14
1.2.3 Characterization.....	16
1.2.4 Potential Roles.....	17

1.3 Overview of the Thesis	23
Chapter 2 : Attempts to identify electron donating partners for bNOS	25
2.1 Introduction	25
2.1.1 Possible bNOS Electron Donating Partners	25
2.1.2 Possible Docking Position Electron Donor for bNOS.....	29
2.1.3 Approach	30
2.2 Procedures	32
2.2.1 Strain and Growth Conditions	32
2.2.2 Cell Disruption	33
2.2.3 MonoQ/Sephacryl 300 Chromatography	33
2.2.4 2'5' ADP-sepharose/L-Arginine-sepharose	34
2.2.5 Metal-Chelating Chromatography	34
2.2.6 ProFound™ Pull-Down PolyHis Protein:Protein Interaction Kit	35
2.2.7 Magnetic Resin	35
2.2.8 Protein Detection	36
2.2.9 Determination of Nitric Oxide Production	37
2.3 Results and Discussion.....	37
2.3.1 Bacterial NOS Expression.....	37
2.3.2 Attempts at Isolation of Intact bNOS Protein Complex	38
2.3.3 Probing Protein-Protein Interactions of bNOS.....	43
2.3.4 Bacterial NOS Activity.....	47

2.4 Concluding Remarks	48
2.5 Future Directions	49
2.5.1 Expression of Tagged-bNOS in Native Conditions	49
2.5.2 Yeast 2 Hybrid System for <i>B. subtilis</i>	51
Chapter 3 : Investigations into the Role of bNOS	52
3.1 Introduction	52
3.1.1 Gene Knockout	53
3.1.2 2D Gel Methodology and Limitations	55
3.1.3 DIGE	55
3.2 Procedures	58
3.2.1 Bacterial Strains and Growth Conditions	58
3.2.2 Knockout Vector	59
3.2.3 PCR Mutagenesis	60
3.2.4 Gene Knockout	61
3.2.5 Verification of Knockouts	61
3.2.6 Expression Test	61
3.2.7 Griess Assay	62
3.2.8 Fluorometric Nitrite Assay	63
3.2.9 2D Electrophoresis Sample Preparation	63
3.2.10 IPTG-Induction of Downstream Elements	66
3.2.11 MS Sample Prep and Analysis	66

3.3 Results	68
3.3.1 Knockout Characterization	68
3.3.2 2D Gel Trouble Shooting	72
3.3.3 Differential in-gel Electrophoresis Analysis	75
3.3.4 Protein Identification	80
3.4 Discussion	86
3.4.1 2D Electrophoresis	86
3.4.2 Perspectives on the Role of NOS in Bacteria	90
3.5 Future Directions	97
3.5.1 *NO-mediated Posttranslational Modification	98
Appendix A	101

List of Figures

Figure 1.1– Linear alignment of the three mammalian NOS isoforms.....	3
Figure 1.2– Model of mammalian NOS dimer showing intermolecular electron transfer.	6
Figure 1.3– Overall reaction for mammalian Nitric oxide synthase (NOS).	7
Figure 1.4– Model for [•] NO synthesis catalyzed by NOS via two mono-oxygenation reactions.	8
Figure 1.5– Model for the dissociation of the Fe ³⁺ -NO complex during NOS catalysis.....	9
Figure 1.6– Linear alignment of the oxygenase domain.....	12
Figure 1.7– Taxonomic tree of distribution of bcNOS in prokaryotic systems.....	13
Figure 1.8- Crystal structure comparison of bcNOS and mouse iNOS.	16
Figure 2.1- Crystal structure of <i>Staphylococcus aureus</i> NOS.	30
Figure 2.2 – Fractionation of <i>B. cereus</i> lysate using MonoQ (A) and Sephacryl 300 (B) columns.	39
Figure 2.3– <i>B. cereus</i> lysate fractionated using ADP-sepharose and L-Arg sepharose consecutively.....	41
Figure 2.4– Pull-down experiment using bcNOS bound to Ni ²⁺ -chelating column.	44
Figure 2.5 – Pull-down experiment using bcNOS bound to Co ²⁺ -chelating column.	45
Figure 2.6– Purification fractions from magnetic resin.	46
Figure 3.1– Schematic of homologous recombination of pMUTIN4 and with the targeted chromosomal DNA resulting in insertional mutagenesis.	54

Figure 3.2-Structure of Cy3 (A) and Cy5 (B) fluors used in differential in-gel eletrophoresis.	56
Figure 3.3 – PCR verification of NOS knockout.....	68
Figure 3.4– Expression of yfIM during cell growth cycle exhibited by the β -galactosidase reporter gene activity.	71
Figure 3.5– Analytical trouble shooting 2D gel image.....	74
Figure 3.6 – 2D Preparative gel of wild type sample with IPTG.	75
Figure 3.7– Screen capture of the match table of the DeCyder 2D gel analysis software.....	77
Figure 3.8– Screen capture of the Protein table view of the DeCyder 2D gel analysis software.....	78
Figure 3.9– Tricolour comparison of the change in protein expression due to bNOS knockout in <i>Bacillus subtilis</i>	80
Figure 3.10– Comparison of two protein spots which resulted in the same MS identification.	85
Figure 3.11– 2D gel of <i>B. subtilis</i> pH 4-7 demonstrating both horizontal and vertical streaking.....	87
Figure 3.12 – Summary of metabolic pathways affected by the yfIMd knockout.....	92

List of Tables

Table 2.1– Summary of coexistence of putative electron donating partners for bacterial NOS in selected bacterial species.	26
Table 2.2- Summary table of efforts to isolate intact bNOS protein complexes from native sources.....	42
Table 2.3– Summary table of pull-down experiments using His-tagged bcNOS as bait immobilized on different metal-chelating resins.	47
Table 2.4– Bacillus expression vectors.....	50
Table 3.1– Bacterial strains and plasmids.....	59
Table 3.2 – Primers used for cloning, mutagenesis, and knockout verification.	60
Table 3.3– Proteins determined to change significantly due to the knockout of bNOS in <i>B. subtilis</i>	82

List of Abbreviations

*NO – Nitric oxide
AARS - Aminoacyl-tRNA synthetase
Ab - antibody
acoB - Acetoin dehydrogenase
AI - Autoinhibitory domain
argC - N-acetyl-glutamate-semialdehyde dehydrogenase
aroA - Chorismate mutase
baNOS - *Bacillus anthracis* nitric oxide synthase
bcNOS - *Bacillus cereus* nitric oxide synthase
B-gal - B-galactosidase
bNOS – Bacterial nitric oxide synthase
bsNOS - *Bacillus subtilis* nitric oxide synthase
BVA - Biological variation analysis
CaM - Calmodulin
carB - Carbamoyl-phosphate synthase
citH - Malate dehydrogenase
Cys - Cysteine
deiNOS - *Deinococcus radiodurans* nitric oxide synthase
deiTrpRS II - *Deinococcus radiodurans* Tryptophanyl tRNA synthetase
dhaS - Aldehyde dehydrogenase
DIA - Differential in-gel analysis
DIGE - Differential in gel electrophoresis
DTT - Dithiothreitol
eNOS – Endothelial nitric oxide synthase
etfB - Electron transfer flavoprotein
FAD - Flavin adenine dinucleotide
FMN - Flavin mononucleotide
GAR-HRP - Goat anti rabbit horse raddish peroxidase
gsNOS - *Geobacillus stearothermophilus* nitric oxide synthase
H₄B - Tetrahydrobiopterin
hutG - Formimino glutamase
hutU - Urocanate hydratase
IEF - Isoelectric focusing
iNOS – Inducible nitric oxide synthase

IPG - Immobilized pH gradient
L-Arg - L-Arginine
L-Cit - L-Citrulline
L-NOHA - N-hydroxy-L-arginine
luxS - Probable autoinducer-2 production protein
Lys - Lysine
mNOS – Mammalian nitric oxide synthase
MS - Mass spectrometry
mtnK - Methylthioribose kinase
mtnS - Methylthioribose-1-phosphate isomerase
MW - Molecular weight
NADPH - Nicotinamide adenine dinucleotide phosphate
nNOS – Neuronal nitric oxide synthase
noc - Nocardia nitric oxide synthase
NOS – Nitric oxide synthase
nusA - Transcription termination factor
P450 BM-3 - Cytochrome P450 BM-3
PMF - Peptide mass fingerprinting
Pspac - IPTG inducible promoter
PTM - Posttranslational modification
rocG - Glutamate dehydrogenase
samNOS - *Samonella typhimurium* nitric oxide synthase
saNOS - *Staphylococcus aureus* nitric oxide synthase
sdhA - Succinate dehydrogenase
serA - Phosphoglycerate dehydrogenase
sGC - Soluble gyanylyl cyclase
SiR-FP - Sulfite reductase flavoproteins
SONO - Sensors of nitric oxide
stNOS - *Streptomyces turgidiscabies* nitric oxide synthase
THF - Tetrahydrofolate
Trp - Tryptophan
TrpRS - Tryptophanyl tRNA synthetase
Tyr - Tyrosine
yflM – *Bacillus subtilis* nitric oxide synthase
yflMd – *Bacillu subtilis* strain 168 with yflM disrupted
ykuN, ykuP - *Bacillus subtilis* flavodoxins

Chapter 1: Introduction

Nitric oxide (NO) is a molecule with diverse biological effects that has been shown to play significant roles in signaling and defense mechanisms in mammalian systems. This free radical is biologically important due to its highly reactive nature and ability to readily permeate membranes (Snyder and Brecht, 1992). Not only can NO react with NO receptors, it can also mutate DNA, inhibit DNA repair and synthesis, inhibit protein synthesis, and regulate protein activity via protein posttranslational modification of amino acid residues or metal centers (Bogdan, 2001).

The production of NO is catalyzed by a family of enzymes known as Nitric Oxide Synthases (NOS). Although NOS homologues have been shown to be prevalent across the genomes of eukaryotic organisms (Ghosh and Salerno, 2003), efforts thus far have focused on mammalian NOS enzymes (mNOS) due to their importance in both physiological and pathological processes. Recently, it has been noted that many prokaryotic genomes contain NOS-like proteins (bNOS) which show significant sequence homology to the oxygenase domain of mNOS isozymes. This is of particular interest due to the fact that mammalian systems produce NO to defend the host against bacterial infection (Bogdan, 2001).

This thesis will first highlight some key aspects of mNOS isozymes and the current knowledge of prokaryotic NOS-like proteins. Potential roles for these intriguing proteins will be suggested. Studies to determine the physiological role of bNOS enzymes will then follow in later chapters.

1.1 Mammalian NOS

1.1.1 NOS Isoforms

There are three isoforms of NOS found in mammalian systems: neuronal (nNOS), endothelial (eNOS), and inducible (iNOS). Both eNOS and nNOS produce *NO that acts as a second messenger by activation of soluble guanylyl cyclase (sGC) in the cardiovascular and nervous system, respectively (Li and Poulos, 2005). These two isoforms are collectively known as the cNOS enzymes because they are constitutively expressed and are regulated by intracellular levels of Ca^{2+} . The iNOS isoform produces cytotoxic levels of *NO in response to cytokine production. It is active at basal intracellular levels of Ca^{2+} and is instead transcriptionally regulated.

1.1.2 Domain Architecture

All NOS isoforms have similar domain architecture, consisting of both an active site oxygenase domain and an electron donor reductase domain joined by a calmodulin (CaM) binding region (Mungrue, Bredt *et al.*, 2003). Figure 1.1 shows a linear alignment of the three mammalian isoforms, highlighting binding domains for specific enzyme cofactors and sites of posttranslational modification.

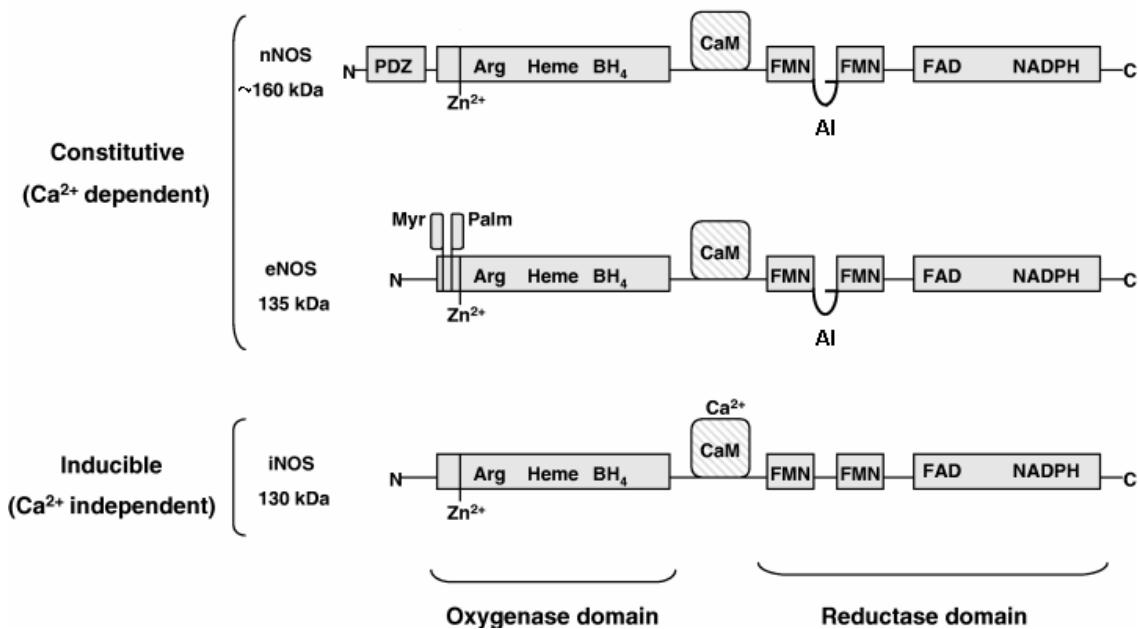


Figure 1.1– Linear alignment of the three mammalian NOS isoforms.

The catalytic oxygenase domain and reductase domain are represented showing the important binding domains, regulatory elements and localization factors (taken from Mungrue, et al., 2003). PSD-95 discs large/ZO-1 (PDZ) domain, myristoylation (Myr) and palmitoylation (Palm) sites, are all involved in cellular localization. Binding domains for the substrate L-Arginine (Arg) and the coenzymes Tetrahydrobiopterin (BH₄), Heme, flavin mononucleotide (FMN), flavin-adenine dinucleotide (FAD), nicotinamide adenine dinucleotide phosphate (NADPH) are indicated. The calmodulin binding domain (CaM) and the autoinhibitory (AI) regulatory element are also identified in this figure and described in the text.

The C-terminus loop is a 20-40 amino acid segment that is thought to interact with the reductase domain. This interaction regulates the electron flow through the flavin (FAD and FMN) domains in iNOS and the electron transfer between the flavin and heme domains in the cNOS isoforms (Sagami, Sato *et al.*, 2002). The flow of electrons from the flavin mononucleotide (FMN) to the heme is controlled by an additional regulatory element in the FMN domain of the cNOS isoforms, and is known as the autoinhibitory (AI) element (Salerno, Harris *et al.*, 1997). The binding of CaM prevents the interaction of these regulatory elements with the reductase domain and alters the structure of NOS for efficient

electron transfer (Li and Poulos, 2005). Once freed from the AI element, the FMN domain is believed to swing freely between the flavin-adenine dinucleotide (FAD) and the heme domains for efficient electron transfer (Garcin, Bruns *et al.*, 2004). In this state, the AI domain is accessible to proteolytic cleavage (Roman, Martasek *et al.*, 2002). Removal of the AI element results in tighter binding of CaM and possibly closer FMN to heme contacts leading to more efficient electron transfer (Li and Poulos, 2005).

1.1.2 Crystal Structure Highlights

The structure of the catalytically important sites are highly conserved throughout the three isoforms. Crystal structures obtained for the oxygenase domain indicate that all residues that are important for substrate and cofactor binding sites are highly conserved (Crane, Arvai *et al.*, 1997; Crane, Arvai *et al.*, 1998; Li and Poulos, 2005). The substrate binding pocket is maintained except for the residues that interact with the substrate carboxyl group, which is aspartate in nNOS and iNOS and asparagine in eNOS. However, this change has no apparent effect on substrate binding affinity. The cofactor tetrahydrobiopterin (H₄B) plays a key role in NOS catalysis and dimer formation. This pterin molecule is sandwiched between tryptophan (Trp) and phenylalanine residues at the dimer interface of adjacent monomers (Li and Poulos, 2005) and is maintained in all three isoforms.

The highly conserved nature of the active site constitutes a challenge for the design of NOS isoforms specific drug therapies. However, other sites, such as the substrate access channel, can be targeted for isoform-selective inhibitors (Li and Poulos, 2005).

A crystal structure for full-length mNOS has yet to be published due to difficulties in obtaining crystals; this could be due to flexibility in catalytically important regions as described above for the mobile elements such as the CaM binding region and the AI domain (Garcin, Bruns *et al.*, 2004). In attempts to build a structural model of the active protein, the known structures of proteolytic fragments have been combined. It has been widely accepted for some time that the oxygenase domain exists as an active dimer (Andrew and Mayer, 1999). Mutational studies aimed at disrupting the dimer interface confirm this fact by showing a decrease in enzymatic activity (Li and Poulos, 2005). The reductase domain was believed to exist as a monomer until Garcin *et al.* reported the crystal structure for a dimerized reductase domain in 2004.

The current model of NOS from Garcin and coworkers (2004) is based on crystal structures obtained for isolated reductase domains aligned with previously obtained structures for oxygenase domains. Garcin *et al.* have proposed the model shown in Figure 1.2 based on knowledge that electrons flow through the reductase domain of one subunit to the oxygenase domain of the adjacent subunit (Siddhanta, Presta *et al.*, 1998).

Figure 1.2 illustrates the flow of electrons through the reductase domain to the oxygenase domain. Not shown in this diagram is the proposed mobility of the FMN domain. The great distance (approximately 30 Å) between the FMN and the Heme domains illustrate the necessity for mobility of the FMN domain for efficient electron transfer. Garcin and coworkers suggest that the FMN domain is mobile and swings from an electron accepting position to an electron donating position in close proximity to the FAD and heme domains,

respectively. This is thought to be the rate determining step in the catalytic mechanism of NOS.

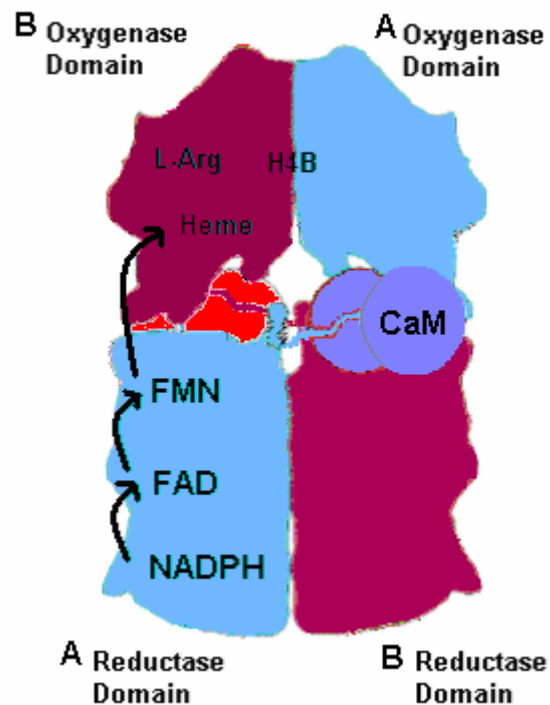


Figure 1.2– Model of mammalian NOS dimer showing intermolecular electron transfer. Binding domains for the substrate L-Arginine (Arg) and the coenzymes Tetrahydrobiopterin (BH₄), Heme, flavin mononucleotide (FMN), flavin-adenine dinucleotide (FAD), nicotinamide adenine dinucleotide phosphate (NADPH), calmodulin (CaM), are all indicated. The electrons flow through the reductase of one subunit to the heme centre in the oxygenase domain of the adjacent subunit is illustrated by curved arrows (Adapted from Garcin *et al.*, 2004).

1.1.2 NOS Mechanism

All NOS isoforms catalyze the conversion of L-Arginine (L-Arg) to [•]NO and L-Citrulline (L-Cit) via the intermediate N-hydroxy-L-Arginine (NOHA), as shown in Figure 1.3.

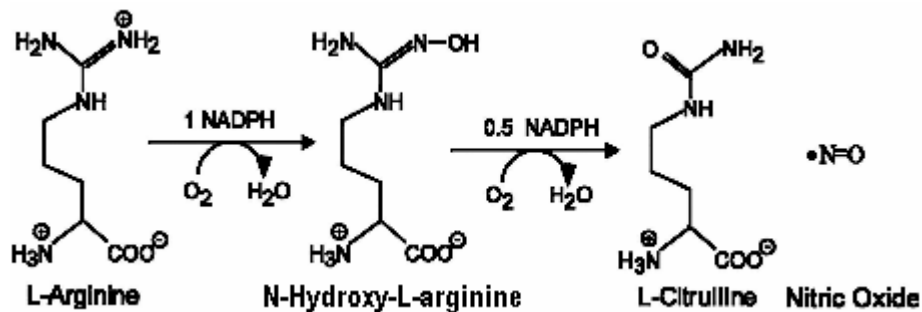


Figure 1.3– Overall reaction for mammalian Nitric oxide synthase (NOS).

[•]NO production from L-Arginine and NADPH catalyzed by NOS through the intermediate N-Hydroxy-L-Arginine.

The catalytic mechanism of NOS involves two successive mono-oxygenation reactions. The first cycle involves the hydroxylation of the guanidino nitrogen of L-Arg to form the intermediate L-NOHA. The second cycle involves the oxidation of the L-NOHA to L-Cit and [•]NO.

A catalytic model of NOS activity is illustrated in Figure 1.4. The reductase domain provides the first reducing equivalent to the heme domain through the flavins, which are initially reduced via a hydride transfer from nicotinamide adenine dinucleotide phosphate (NADPH). This is thought to be the slowest step during catalysis (Garcin, Bruns *et al.*, 2004). The reduced heme binds O₂ and is further reduced by a second electron either derived from H₄B or from the reductase domain in the absence of H₄B (Adak, Wang *et al.*, 2000). Fast and efficient electron transfer is important at this step to prevent superoxide release. Superoxide is a highly reactive free radical which reacts with proteins, DNA, and lipids, causing damage which is referred to as oxidative stress. The reduced heme binds O₂ enabling the hydroxylation of the substrate, L-Arg. It is important to note that H₄B is not

consumed during catalysis. H_4B is subsequently regenerated from an electron derived from the reductase domain, suspected to be mediated through a reduced heme site (Stuehr, Wei *et al.*, 2005).

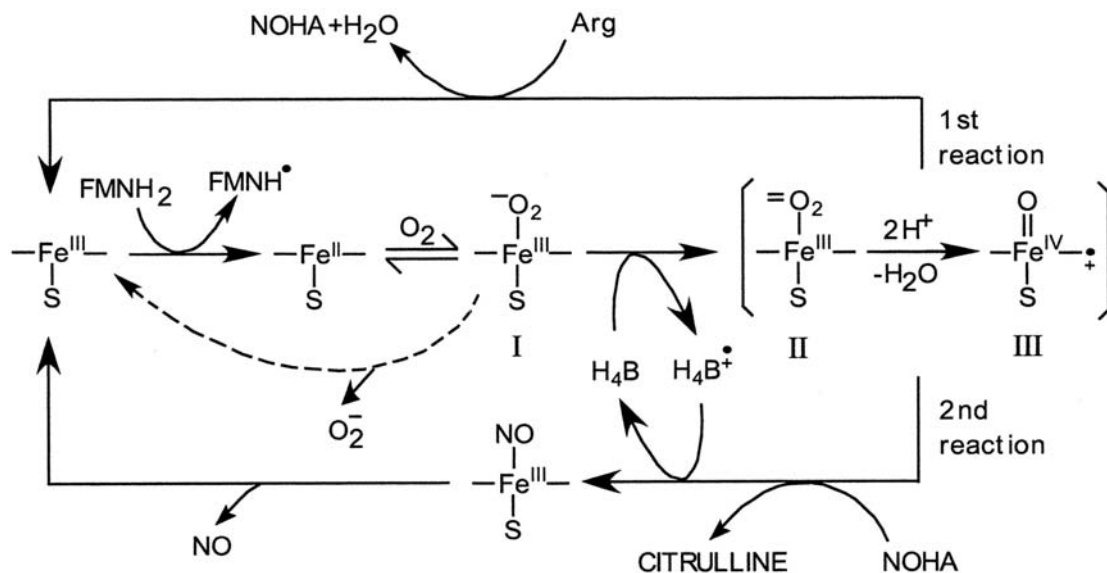


Figure 1.4– Model for NO synthesis catalyzed by NOS via two mono-oxygenation reactions. Details are given in text. Figure taken from Stuehr *et al.*, 2004.

During the second catalytic cycle, the heme is again first reduced by the reductase domain, followed by binding of O₂ and heme reduction by H₄B. The reduced heme is then able to oxidize the L-NOHA resulting in release of L-Cit and the formation of a ferrous heme-NO complex. The H₄B is regenerated in this case by a downstream reactive intermediate, most likely the heme-bound NOHA tetrahedral intermediate (Adak, Wang *et al.*, 2000; Li and Poulos, 2005). In the absence of H₄B, the ferrous heme-NO complex builds up and oxidative products are released instead of NO.

*NO has a high affinity for heme, and thus under normal conditions is slowly released from the heme-NO complex. An unproductive side reaction, referred to as futile cycling, can occur in the presence of O₂, yielding non-productive nitrogen oxide species such as NO₂⁻ and NO₃⁻. Figure 1.5 illustrates the kinetic constants that result in the distribution between the productive and futile cycle.

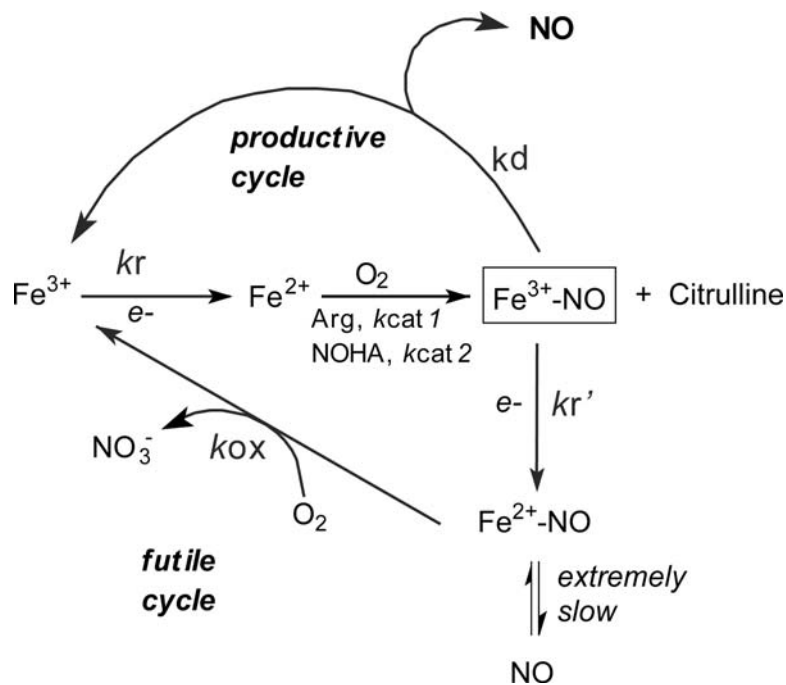


Figure 1.5– Model for the dissociation of the Fe³⁺-NO complex during NOS catalysis.

Both the productive cycle and the futile cycles of NOS catalysis are illustrated with the heme center shown as Fe. The productive cycle results in the fast release of NO from the NO-Fe³⁺ complex. A low k_d of the Fe³⁺-NO complex results in futile cycling via reduction of the heme center to NO-Fe²⁺ and subsequent release of oxidative products of NO. Figure taken from Wang, *et al.*, 2004.

The differences between the O₂ and NO binding affinities account for the differential rates of *NO production for different isoforms (Stuehr, Santolini *et al.*, 2004). It has been suggested that bNOS enzymes may kinetically favor futile cycling to limit the antimicrobial effects of

the productive cycle (Stuehr, Santolini *et al.*, 2004; Wang, Wei *et al.*, 2004; Li and Poulos, 2005).

1.2 Bacterial NOS

Recently, several prokaryotic genomes have been shown to contain a genetic homologue to the oxygenase domain of mNOS enzymes. Bacteria are known to produce *NO as an intermediate of denitrification; however, the enzymes involved are both structurally and mechanically distinct from bNOS (Bird, Ren *et al.*, 2002). The actual function of bNOS enzymes is still unknown, since the standard signaling and defense mechanisms mNOS enzymes would have no purpose in prokaryotic organisms. Due to the cytotoxic effects of this molecule, bacteria control *NO concentrations at nanomolar levels by tight binding of this intermediate during nitrogen cycling (Bird, Ren *et al.*, 2002). This thesis will explore the prevalence of bNOS proteins and suggest possible roles for such a protein. Efforts to elucidate this role will be discussed in chapter 3.

1.2.1 Prevalence of bNOS in prokaryotic systems

1.2.1.1 Oxygenase domain

The degree of homology between the oxygenase domain of mammalian NOS isoforms and putative bNOS enzymes is surprising. Figure 1.6 shows a linear alignment of the oxygenase domain of the three mNOS isoforms with four bNOS proteins; *Bacillus cereus* (bcNOS), *Bacillus subtilis* (bsNOS), *Staphylococcus aureus* (saNOS), *Deinococcus*

radiodurans (deiNOS). Based on alignments done to human iNOS oxygenase domain using the program ClustalW, these proteins show between 37-44% sequence identity and 56-64% sequence similarity (Altschul, Gish *et al.*, 1990).

The bNOS enzymes bsNOS, saNOS and deiNOS have previously been expressed, purified, and characterized. The bcNOS protein has recently been expressed, purified, and characterized in our lab. bcNOS is of interest due to its high degree of homology, 97% identical and 100% similar, to the equivalent bNOS protein found in *Bacillus anthracis* (baNOS) (Altschul, Gish *et al.*, 1990). Due to the high degree of homology between these two genomes, studies using *B. cereus* may provide insights into understanding this highly infectious species, *B. anthracis*.

```

bcNOS      1 : -----MSKTKQLIEE[SHFITICYKEL-NK
bsNOS      - : -----
SANOS      1 : -----MLFKE[QAFIENMYKEC-HY
deiNOS     1 : -----MSCPA[AVLTPDMRAFLLRF
miNOS     77 : QYVRIKNWGSGEILHDLHKKATSDFTCKSKSCLGSIINPKSLTRGPRDKPTPLEELPH[IEFINQY[GSFKEA
hnNOS     304 : RFLKVKNWETEVLTDTLHLKSTLETGCTEYICMGSIMHPSQHARRPE-DVRTKGLFPL[KEFIDQY[SSIKRF
beNOS     69 : KFPRVKWELSGSIYDYLCAQSQDGPCTPRCCLSGLVLPKRLQTRPSPGPPAEQLLSQ[RDFINQY[SSIKRS

bcNOS     25 : E-QFIEE[RMKEIRV[IEK[GT[YEHTFELVH[SR[MAWRNSNRC[IGRL[FWSK[H[LDA[REVNDEEGVYNALIH[H[K
bsNOS      1 : ---MKDELADIKSEIDL[TSYVHTKBELEH[SA[MAWRNSNRC[IGRL[FWNS[IN[VIDR[DVRTKKEVRDALPH[H[E
SANOS     20 : ETQIINK[ELHDI[EL[EIK[ET[GT[YHTHE[ELIY[SA[MAWRNSNRC[IGRL[FWDS[IN[VIDA[RDVTDEASFLSSIT[YHIT
deiNOS     21 : HEEMGEP[PLPARLRA[VEEA[GLWMP[TSAB[ELTWSA[VAWRNSNRC[IGRL[FWYEA[LSVR[DLRELNTAQAVYEA[LQHL[D
miNOS     152 : KIEEHLAR[LEAVTK[EIET[GT[YQLTLD[ELIFAT[MAWRNAPRC[IGRI[OWSN[IQV[FDARN[CSAQEMFQHICR[H[L
hnNOS     378 : GSKAHME[LEEVNKE[IDT[ST[YQLKDT[ELIY[SA[MAWRNAPRC[IGRI[OWSK[IQV[FDARD[CTTAHGFMFYICNH[V[K
beNOS     144 : GSQAHEE[SLQVEEA[VAST[GT[YHLRES[ELV[SA[MAWRNAPRC[IGRI[OWGK[IQV[FDARD[CSAQEMFTYICNH[H[K

bcNOS     99 : YATNDCKV[KP[ITIT[FKQYQGEENIRI[VNHQ[LR[IRYAGYKTE-MGVI[GD[SHSAV[TFDFCQE[LCWQGE[GTNFDV[LPL
bsNOS     72 : TATNNGT[TRP[ITIT[PPPEEK[GEKQVE[VNHQ[LR[IRYAGY[ESD-GERI[GD[PA[SCSL[IAA[EEEL[GW[RGERTDFD[LPL
SANOS     95 : QATNEGK[LPY[ITIT[YPKDG[---KIE[NNQ[LR[IRYAGY[DN---CGDPAE[KEV[RLANHL[GWK[KGTFDVLPL
deiNOS     96 : DAFCGH[ER[EVISV[FGP-----GVR[LE[NPQ[LR[IRYA-----DDE[INAD[EV[DKLRR[FGWQ[ERGERF[VLP
miNOS     227 : YATNNGN[ERSAI[TVFP[QRSDG[KHDFR[LVNSQ[LR[IRYAGY[QMPD[GTIR[SDA[ATLE[FTQL[CID[EGW[KPRYGRF[VLP
hnNOS     453 : YATNKG[ERSAI[TVFP[QRSDG[KHDFR[LVNSQ[LR[IRYAGY[QMPD[GTIR[SDA[ATLE[FTQL[CID[EGW[KPRYGRF[VLP
beNOS     219 : YATNKG[ERSAI[TVFP[QRSDG[KHDFR[LVNSQ[LR[IRYAGY[QMPD[GTIR[SDA[ATLE[FTQL[CID[EGW[KPRYGRF[VLP

bcNOS     173 : VFSIDG-KAPIYKEI[PKEEV[KEVP[IEH[EY[IP-ISSL[GAKW[GV[PMISDMR[LEIGGISYTAAB[FNGWY[MGTEIGAR
bsNOS     146 : NFRMKGDEQ[VWYEL[PRSLV[EVPT[TH[EDIEAF[SDLELKW[GV[PMISDMR[LEIGGISYTAAB[FNGWY[MGTEIGAR
SANOS     161 : IYQLPN-ESVKFYEY[PTSLI[KEVP[IEH[NHY[PKLRLK[LVAVP[PMISDMR[LEIGGISYTAAB[FNGWY[MGTEIGAR
deiNOS     155 : LIEVNG--RAELFSL[PPQAV[QEVAT[HEVCLGIGEL[GLRW[HALP[VISDMH[LDIGGLHLP-CAFS[GWY[QTEIAAR
miNOS     302 : VLQADG-QDPEVFEI[PPDLV[LEVPT[MEH[EKYEW[QELGLK[WY[ALPAV[ANMLLE[VGGLFFPAC[FNGWY[MGTEIGAR
hnNOS     528 : LLQANG-NDPELFQI[PPDLV[LEVPT[MEH[EKYEW[QELGLK[WY[ALPAV[ANMLLE[VGGLFFPAC[FNGWY[MGTEIGAR
beNOS     294 : LLQAPD-EAPDLFV[LPPELV[LEVPT[MEH[EKYEW[QELGLK[WY[ALPAV[ANMLLE[VGGLFFPAC[FNGWY[MGTEIGAR

bcNOS     246 : NLA[PHDRY[NL[PAVA[EMMDLDT[SRNGT[LWKD[KALVEL[NVAVLHSE[KKQGV[SIVD[HHTA[AQO[FQF[EKQ[BAACGRV
bsNOS     221 : NLADEKRY[DKKKV[ASVIGIAADYNTD[LWKD[QALVEL[NKAVLHSE[KKQGV[SIVD[HHTA[ASQ[ERFEEQ[EEAAGRK
SANOS     235 : NFIDDRY[NL[LEKVADAF[EFDTLKNN[SFNKD[RALVEL[NYAVYHSE[KKQGV[SIVD[HHTA[AKO[ELFERNEA[QOGRQ
deiNOS     227 : DLADVGRY[DQ[PAVARA[IGLDT[SRERT[LWRD[RALVEL[NVAVLHSE[DAAGV[KIAD[HHTVTAHVRFEBE[ARAGRE
miNOS     376 : DFCDTQRY[NL[LEEVGRRM[GLEHTLAS[LWKD[RAVTE[INAVLHSE[QKQNV[IMD[HHTA[SESE[MKHMQN[BYRARGG
hnNOS     602 : DYCDSRY[NL[LEEVAKKMN[LDMRKT[SSLWKD[QALVEL[NIAVLYSE[QSDKV[IVD[HHTA[TESE[IKHMEN[BYRCRGG
beNOS     368 : NLC[PHRY[NL[LEEDVAV[CMDLDT[TRTSS[LWKD[KAAVE[INLAVLHSE[QLAKV[IVD[HHTA[TVSE[MKHLDN[EQKARGG

bcNOS     321 : VTGNWVW[IVPPIS[PAATHIY[HKPY[PNELK[PNFFHK-----
bsNOS     296 : LTGDWVW[IVPPIS[PAATHIY[HKPY[PNELK[PNFFHK-----
SANOS     310 : VTGNWVW[IVPPIS[PAATHIY[HKPY[PNELK[PNFFHK-----
deiNOS     302 : VTGNWVW[IVPPIS[PAATHIY[HKPY[PNELK[PNFFHK-----
miNOS     451 : CPADWVW[IVPPIS[PAATHIY[HKPY[PNELK[PNFFHK-----
hnNOS     677 : CPADWVW[IVPPIS[PAATHIY[HKPY[PNELK[PNFFHK-----
beNOS     443 : CPADWVW[IVPPIS[PAATHIY[HKPY[PNELK[PNFFHK-----

bcNOS      - : -----
bsNOS      - : -----
SANOS      - : -----
deiNOS     - : -----
miNOS     525 : KVMASRV[RA[TVLFA[TE[TKSEALARDL
hnNOS     752 : QAMAKRV[KATILYAT[ETGKSQAYAKTL
beNOS     514 : TLMAKRV[KATILYAS[ETGRAQSYAQQL

```

Figure 1.6– Linear alignment of the oxygenase domain.

Alignment of the three mNOSd to NOS-like protein found in *Bacillus cereus* NOS (bcNOS), *Bacillus subtilis* NOS (bsNOS), *Staphylococcus aureus* NOS (saNOS), *Deinococcus radiodurans* NOS (deiNOS) performed using ClustalW. Degree of shading is indicative of sequence homology.

Homology searches done with putative bacterial NOS sequences reveal an abundance of NOS-like proteins in bacterial genomes (Altschul, Gish *et al.*, 1990). Figure 1.7 shows a taxonomic tree illustrating the distribution of NOS-like proteins found in prokaryotic systems. The distribution of bNOS is thus far limited to the gram-positive organisms and is particularly prevalent in the in the *Bacillus* genus.

```

Bacteria - 38
Firmicutes - 32
  Bacillales - 31
    Bacillaceae - 16
      Bacillus anthracis - 1
      Bacillus cereus (strain ATCC 10987) - 1
      Bacillus cereus (strain ATCC 14579 / DSM 31) - 1
      Bacillus cereus (strain ZK / E33L) - 1
      Bacillus cereus G9241 - 1
      Bacillus cereus subsp. cytotoxis NVH 391-98 - 1
      Bacillus clausii (strain KSM-K16) - 1
      Bacillus halodurans - 1
      Bacillus licheniformis (strain DSM 13 / ATCC 14580) - 1
      Bacillus sp. NRRL B-14911 - 1
      Bacillus subtilis - 1
      Bacillus thuringiensis subsp. konkukian - 1
      Bacillus weihenstephanensis KBAB4 - 1
      Exiguobacterium sibiricum 255-15 - 1
      Geobacillus kaustophilus - 1
      Oceanobacillus iheyensis - 1
    Staphylococcus - 15
      Staphylococcus aureus - 1
      Staphylococcus aureus (strain COL) - 1
      Staphylococcus aureus (strain MRSA252) - 1
      Staphylococcus aureus (strain MSSA476) - 1
      Staphylococcus aureus (strain MW2) - 1
      Staphylococcus aureus (strain Mu50 / ATCC 700699) - 1
      Staphylococcus aureus (strain N315) - 1
      Staphylococcus aureus (strain NCTC 8325) - 1
      Staphylococcus aureus (strain USA300) - 1
      Staphylococcus aureus (strain bovine RF122) - 1
      Staphylococcus aureus subsp. aureus JH1 - 1
      Staphylococcus aureus subsp. aureus JH9 - 1
      Staphylococcus epidermidis (strain ATCC 12228) - 1
      Staphylococcus epidermidis (strain ATCC 35984 / RP62A) - 1
      Staphylococcus haemolyticus (strain JCSC1435) - 1
    Lactobacillales - 1
      Lactobacillus plantarum - 1
  Actinobacteria - 5
    Actinomycetales - 5
      Streptomyces avermitilis - 2
      Streptomyces acidiscabies - 1
      Streptomyces scabies - 1
      Streptomyces turgidiscabies - 1
  Deinococcus-Thermus - 1
    Deinococcus radiodurans - 1

```

Figure 1.7– Taxonomic tree of distribution of bNOS in prokaryotic systems.
(Hulo, Bairoch *et al.*, 2006)

A link has yet to be drawn between those bacteria that contain a bNOS gene and a specific phenotypic trait. This list is by no means complete and will certainly increase with subsequent bacterial genomes being sequenced. Perhaps with a fuller list, the link to a phenotypic trait will be more evident.

1.2.1.2 Reductase Domain

Since bNOS proteins contain only the NOS oxygenase domain, a surrogate reductase domain would be required for catalytic activity. Several putative reductase domains have been suggested for such a role and the specifics of these will be discussed in Chapter 2. The number of potential electron-donating partners is very high. Meanwhile, in order to characterize the activity of these enzymes, recombinantly expressed bNOS enzymes have been reconstituted with mNOS reductase domains. The identity of this surrogate reductase domain would not only allow for a more accurate determination of the catalytic properties of bNOS enzymes but could also shed light on the possible role of these enzymes. Attempts at the elucidation of possible surrogate reductase domains are described in Chapter 2.

1.2.2 Crystal Structure

The structures of bNOS proteins, bsNOS, saNOS, and *Geobacillus stearothermophilus* NOS (gsNOS), have been solved by X-ray crystallography (Bird, Ren *et al.*, 2002; Pant, Bilwes *et al.*, 2002; Pant and Crane, 2006; Sudhamsu and Crane, 2006). An additional structure has been suggested for deiNOS, based on threading algorithms (Adak, Bilwes *et al.*, 2002). The dimeric structures obtained for bNOS like enzymes are remarkably

similar to structures obtained for the oxygenase domain of mNOS. The main difference between the bacterial and mammalian NOS structures is found along the dimer interface and at the N-terminus. The N-terminal hook extension, which has been shown to be required for dimer formation and activity in mNOS isozymes, is missing in bNOS enzymes. Deletions in the bNOS enzymes appear to be primarily surface-exposed loops in eukaryotic NOS structures, and do not alter the protein's conformation (Pant, Bilwes *et al.*, 2002). Other residues thought to be important for dimerization in mNOS enzymes are also missing from bNOS proteins. The conserved cysteine residues required for zinc binding and dimerization in mammalian systems (Mitchell, Erwin *et al.*, 2005) are absent, and not required for dimerization in bNOS enzymes.

Although the residues involved in the substrate and pterin binding sites are generally conserved between eukaryotic and prokaryotic NOS proteins, the absence of the N-terminal extension results in a more open structure and a wider substrate access channel (Bird, Ren *et al.*, 2002). Figure 1.8 shows a comparison of mouse iNOS and bsNOS. The missing N-terminal residues, highlighted in mauve, result in a more open structure for binding larger pterin molecules such as Tetrahydrofolate (THF). This feature is important since some prokaryotes which contain bNOS enzymes are unable to produce H4B, but are able to synthesize other pterins such as THF.

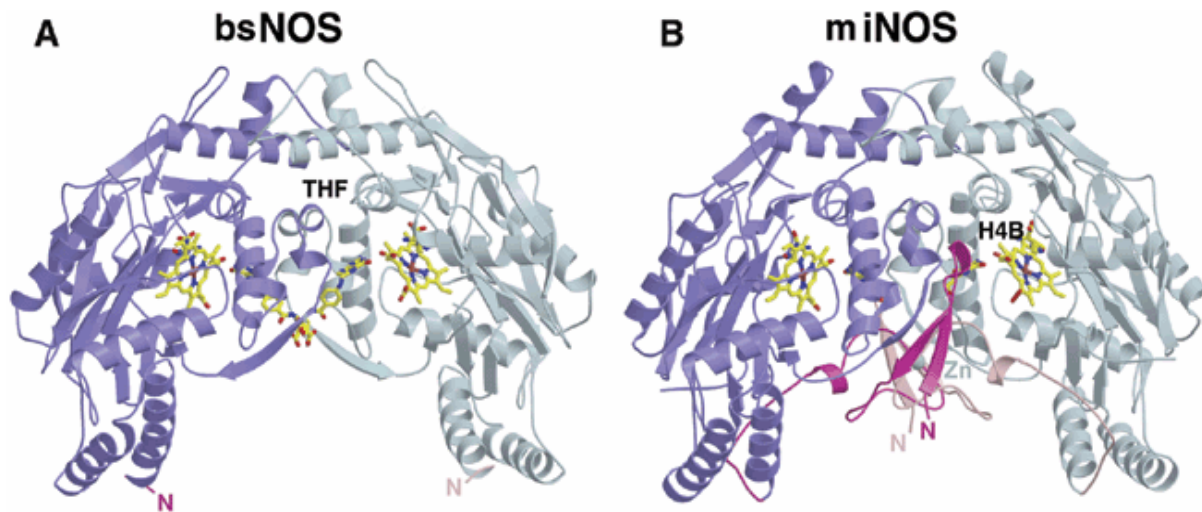


Figure 1.8- Crystal structure comparison of bsNOS and mouse iNOS.

The N-terminal hook extension which is missing in the bsNOS structure is highlighted in mauve. The overall structure of bsNOS is more open at the dimer interface than mouse iNOS, allowing for binding of a larger pterin cofactor. The pterin molecules are shown bound to the appropriate structure, THF in bsNOS and H₄B in mouse iNOS (Pant, Bilwes *et al.*, 2002).

Another conserved difference between eukaryotic and prokaryotic NOS is a valine to isoleucine switch found near the substrate binding pocket. Wang and coworkers (2004) showed that this conserved residue switch causes a 10-20 fold decrease in [•]NO dissociation rate in bNOS enzymes. They suggested that this residue switch may help to regulate [•]NO release in prokaryotic systems by decreasing the dissociation constant of [•]NO and thus increasing the proportion of futile cycling, as previously illustrated in Figure 1.5 (Wang, Wei *et al.*, 2004).

1.2.3 Characterization

Several bNOS proteins have been isolated and characterized. NOS-like proteins from *Nocardia* (nocNOS), saNOS, deiNOS, bsNOS, baNOS, and gsNOS have all shown to

produce L-Cit and ^1NO from L-Arg. Both nocNOS and saNOS were purified from crude cell extracts (Chen and Rosazza, 1995; Choi, Chang *et al.*, 1997), and were shown to produce ^1NO (or NO_2^- , NO_3^-) in the presence of L-Arg or NOHA, NADPH and H_4B without the requirement of a reductase domain. Several bacterial NOS enzymes including baNOS, bsNOS, deiNOS, saNOS, *Streptomyces turgidiscabies* (stNOS), and gsNOS have been recombinantly expressed and purified. These enzymes were shown to produce minimal levels of nitrite in the presence of either H_2O_2 or a rat nNOS reductase domain acting as surrogate electron donors (Adak, Aulak *et al.*, 2002; Adak, Bilwes *et al.*, 2002; Sudhamsu and Crane, 2006). Significant ^1NO production by bNOS has not been shown in bacterial systems. The relevance of ^1NO production using a mNOS reductase domain has yet to be shown. The ability of this bNOS enzymes to produce ^1NO would more appropriately be demonstrated if either bNOS enzymes were shown to produce ^1NO *in vivo* or if a bacterial electron-donating protein partner was found to interact with bNOS enzymes *in vivo* and provide the means to produce ^1NO .

The deiNOS, bsNOS, baNOS, and gsNOS enzymes were further shown to have high affinity for the substrate L-Arg and the cofactor H_4B (Midha, Mishra *et al.*, 2005). The deiNOS and bsNOS enzymes have both been shown to productively bind both H_4B and THF (Adak, Aulak *et al.*, 2002; Adak, Bilwes *et al.*, 2002).

1.2.4 Potential Roles

If these bNOS proteins are conclusively shown to produce ^1NO , it is intriguing to consider the possible roles for such proteins. Recall that mNOS enzymes are involved in

signaling and defense mechanisms, neither of which would be probable functions for prokaryotic organisms. Even more striking is the possibility of the catalytic product being cytotoxic to the organism. Thus, if this protein produces NO in vivo, this reaction would need to be tightly regulated or possibly coupled to another reaction.

Possible roles for bNOS proteins could include inter/intracellular signaling or involvement in biosynthetic pathways. These roles could be manifested in microorganisms by NO production resulting in NO release for signaling purposes, protein posttranslational modifications, or production of nitrosylated products.

1.2.4.1 Intercellular Signaling

Although it has long been thought that unicellular organisms act independently of one another, competing for nutrients within a niche, recent discoveries suggest that bacteria are quite social and depend on chemical signals to communicate. This regulative process, termed quorum-sensing, allows population based regulation of genetic competence, conjugative plasmid transfer, sporulation, cell differentiation, biofilm formation, virulence response, as well as production of antibiotics, antimicrobial peptides and toxins and bioluminescence (Kleerebezem and Quadri, 2001).

Presently, there are two basic quorum-sensing models. The first, found most commonly in gram-negative bacteria, is based on direct binding of the pheromone to the transcriptional factor to control this regulative process (Waters and Bassler, 2005). The second, found most often in gram-positive bacteria, is based on the pheromone binding to a receptor involved in a two-component phosphorelay signal transduction system that results in

gene regulation (Strume, Kleerebezem *et al.*, 2002). Both processes allow the cell to respond to environmental stimuli in a concentration dependent manner.

Although the current model for quorum-sensing is limited to larger molecule pheromones such as acylhomoserine lactones and small peptides, perhaps small molecules such as NO could also contribute to quorum-sensing. Akin to the two-component phosphorelay signal transduction system found in quorum-sensing gram-positive bacteria, some bacterial systems contain a specific NO receptor found in an operon that encode genes for a two-component, histidine kinase, signal transducing system. These receptors are prokaryotic homologues to sGC and have been found in *Clostridium botulinum* (Nioche, Berka *et al.*, 2004), *Vibrio cholerae* (Karow, Pan *et al.*, 2004), and *Thermoanaerobacter tengcongensis* (Karow, Pan *et al.*, 2004). The sensors of NO (SONO) have been expressed and characterized in vitro and were shown to have extremely high affinity for NO (Nioche, Berka *et al.*, 2004). It has been suggested that this sensor could aid the bacteria in avoiding this cytotoxic material by inducing chemotaxis. Although the signal transducing potential of this sensor has not been proven, it was suggested from amino acid sequence comparisons to mammalian sGC homologues. The possible chemotaxis role of this sensor in the avoidance of this toxic substance by bacteria was also suggested based on the ability of mammalian sGC to confer a chemoattractive response to dendrites and axons (Nioche, Berka *et al.*, 2004).

The possibility of SONO proteins contributing to the virulence has been suggested due to evidence of transcriptional down regulation of this gene in *V. cholerae* cells shed by

infected individuals. This evidence suggests that the SONO may be important for bacterial virulence within the host.

1.2.4.2 Intracellular Signaling

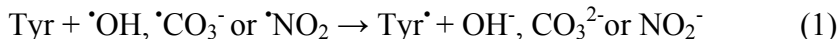
Another possible function for bNOS proteins found in bacteria is the involvement in intracellular signaling. The nitration of proteins has been shown to significantly alter protein conformation and function. In mammalian systems, the nitration of aromatic protein residues has been implicated in neurodegenerative diseases, atherosclerosis, infections, inflammation, and cancer (Buddha, Tao *et al.*, 2004). It is still unclear whether the increased formation of nitrated species is a causal agent or the result of the pathogenic onset of these diseased states (Schopfer, Baker *et al.*, 2003). Although most studies on protein nitration have focused on diseased states, there is increasing evidence suggesting that [•]NO-mediated posttranslational modification (PTM) is involved in cellular signaling. It has been suggested that if this highly regulated process were altered that it could result in disease.

[•]NO-mediated protein nitration can occur via NO-heme complex formation, the S-nitrosylation of cysteine (Cys) residues, or the C-nitration of tyrosine (Tyr) and Trp residues (Ischiropoulos, 2003). These PTMs can mark proteins for degradation, regulate protein function, or contribute to amino acid metabolism. The following criteria have been suggested by Koeck *et al.* (2005) to be required for [•]NO-mediated PTMs to be considered physiologically relevant to signaling: (i) the modification should be specific, (ii) the modification should be reversible, (iii) the modification should occur on a physiologically relevant time scale, and (iv) should alter the activity of the target (Green, Wagner *et al.*,

1982; Koeck, Stuehr *et al.*, 2005). $\cdot\text{NO}$ -mediated PTM of metal centers, S-nitrosylation of Cys residues, and C-nitration of Tyr have shown to meet the criteria required for signaling (Green, Wagner *et al.*, 1982; Schopfer, Baker *et al.*, 2003; Koeck, Stuehr *et al.*, 2005).

Although very little work has been done on Trp nitration, it has been suggested to have a similar mechanism and physiological relevance as Tyr nitration (Yumakura and Ikeda, 2006).

PTMs involving $\cdot\text{NO}$ can either be a result of $\cdot\text{NO}$ reacting directly with the target or via a secondary reaction involving a protein residue and a product of $\cdot\text{NO}$ oxidation. $\cdot\text{NO}$ can react with metal centers or reduced thiols to produce nitrosylated proteins. Equations 1 and 2 illustrate the formation of nitrotyrosine using oxidative products of $\cdot\text{NO}$.



$\cdot\text{NO}$ oxidative products, $\cdot\text{NO}^2$, ONOO^- , and N_2O_3 , are more reactive and toxic than $\cdot\text{NO}$, and can mediate S-nitrosylation (Ravi, Brennan *et al.*, 2004) and C-nitration (Radi, 2004). There are several possible mechanisms by which proteins can react with reactive nitrogen species (RNS) and become nitrated. The predominant species implicated in mediation of protein nitration are $\cdot\text{NO}_2$ and the carbonate radical ($\cdot\text{CO}_3^-$) (Radi, 2004). Tyr nitration depends on the concomitant production of $\cdot\text{NO}_2$ and Tyr radicals. As illustrated in the above equations, the Tyr radical can be generated from several species. The production of peroxynitrite and the Tyr radical result in protein nitration.

Some examples of enzymes involved in $\cdot\text{NO}$ -mediated PTMs: Heme modification in sGC (Ignarro, Degnan *et al.*, 1982), denitrase in mitochondria (Aulak, Koeck *et al.*, 2004), S-

nitrosylation of eNOS (Ravi, Brennan *et al.*, 2004), iNOS (Mitchell, Erwin *et al.*, 2005) and nNOS (Jaffrey, Erdjument-Bromage *et al.*, 2001), C-nitration of Trp in Mn superoxide dismutase (MacMillan-Crow, Crow *et al.*, 1996).

NO modification can occur through a variety of mechanisms but have all shown to meet the criteria required for signaling pathways.

Work on \cdot NO-mediated PTM in bacteria has focused on the effect of nitrosative stress of a host on bacterial systems (Rhee, Erdjument-Bromage *et al.*, 2005). Further studies are required to determine if \cdot NO-mediated PTM occur in bacterial cells under normal conditions. Future studies should address the possibility of \cdot NO-mediated PTMs playing a role in signaling mechanisms in bacterial systems.

1.2.4.3 Biosynthetic Pathways

Another alternative for a physiological role of bNOS proteins is involvement in biosynthetic pathways. Coupling of the production of \cdot NO to a biosynthetic reaction would allow the bacteria to direct reactivity and limit the toxicity of this product. The bNOS protein found in *S. turgidiscabies* (stNOS) was shown to be involved in the nitration of a dipeptide phytotoxin required for plant pathogenicity (Kers, Wach *et al.*, 2004). Kers *et al.* (2004) suggested that stNOS is responsible for the nitration of the 4-nitrotryptophanyl moiety of the phytotoxin thaxtomin. A knockout of this gene resulted in the bacteria lacking the ability to produce the phytotoxin, thaxtomin. Similarly, the addition of known L-Arg-based NOS inhibitors resulted in decreased production of the phytotoxin. Subsequently, Buddha *et al.* (2004) suggested that a tryptophanyl tRNA synthetase from *D. radiodurans* (deiTrpRS II)

interacts with deiNOS. Buddha et al. (2004) showed that TrpRS II increases the solubility, substrate binding and stimulates deiNOS activity (Buddha, Keery *et al.*, 2004). Since *D. radiodurans* possesses another tryptophanyl tRNA synthetase (TrpRS I) with higher charging activity and with greater sequence homology to TrpRSs found in organisms that only contain one TrpRS, it was suggested that the TrpRS II is auxiliary to the protein synthesis machinery and possibly involved in production of biosynthetic products. Further investigation of the deiNOS and deiTrpRS II complex showed that it was not only able to catalyze the production of $\cdot\text{NO}$ but also the regioselective nitration of tryptophan at the 4-position. In this system, Trp was shown to stimulate nitrite production, while the Trp nitration reaction was inhibited by H₄B (Buddha, Tao *et al.*, 2004). It was suggested that Trp may occupy the same site as and substitute for H₄B as an electron donor in order to stimulate the production of $\cdot\text{NO}$ from L-Arg (Buddha, Tao *et al.*, 2004). It also follows that H₄B would act as a competitive inhibitor for Trp in the nitration reaction. Thus, coupling the nitration of an amino acid to a bNOS protein would limit the potential toxic effects of the $\cdot\text{NO}$ product.

1.3 Overview of the Thesis

Although many roles have been suggested for this intriguing enzyme, there has yet to be a consistent trend found between the existence of this enzyme and any specific physiological or pathological trait. A trend of coexistence between bNOS and SONOs, trpRS II, or protein nitration has not been conclusively shown. This work endeavors to shine light on the potential role of bNOS.

Chapter 2 shows the attempts to isolate possible electron-donating protein partners for bNOS enzymes. Although it is evident that bNOS requires a physiological electron donating partner, none have been identified. Methods used here to probe the interactions between bcNOS and any interacting protein partners include: (i) attempts at isolation of intact protein complexes from native sources and (ii) using previously purified bNOS as bait to fish-out any interacting partners from cell lysate solutions. Determining the identity of electron donating partners for bNOS could shed light into the role of this intriguing enzyme.

Chapter 3 is a proteomic view of the change in protein expression due to the knockout of the bNOS gene in *B. subtilis*. This chapter outlines the methods used for generation of bNOS knockouts in *B. subtilis* and *B. cereus*. The introduction of DIGE technology into our lab and the optimization of sample specific parameters are described. A detailed summary of the procedures for 2D-DIGE comparison of the knockout and wild type strains is also provided. The change in protein expression due to the bsNOS knockout is discussed, with the goal of elucidation of a functional role for bNOS enzymes.

Chapter 2: Attempts to identify electron donating partners for bNOS

2.1 Introduction

One of the remaining enigmas in the bacterial NOS (bNOS) realm is to determine the physiological electron donor for this system. According to the mNOS mechanism, electrons must be transferred to the oxygenase domain in order for catalysis to occur. It has been shown that recombinantly expressed rat nNOS and human iNOS reductase domains are able to transfer electrons to bNOS enzymes eliciting minimal ¹⁴N¹⁵O production (Adak, Aulak *et al.*, 2002; Adak, Bilwes *et al.*, 2002; Buddha, Tao *et al.*, 2004). Although this is an interesting observation, the physiological relevance is quite limited. The most we can infer from this observation is that bNOS enzymes are able to accept electrons from an electron donating partner. The determination of a probable electron donor to this enzyme is key to understanding the role and possibly regulation of NOS-like enzymes found in prokaryotic systems.

2.1.1 Possible bNOS Electron Donating Partners

Several proteins have been suggested as possible electron donors for bNOSs, including sulfite reductase flavoproteins (SiR-FP), cytochrome P450 BM-3 (P450 BM-3) and

Flavodoxins. These potential surrogates have been suggested for this role based on homology to the mNOS reductase domain and their coexistence with bNOS in bacterial systems. Another possible interacting partner for bNOS could be a TrpRS II. As mentioned in 1.2.4.3, this interaction was suggested after Δ stNOS was shown to inhibit the production of a nitrated dipeptide required for plant pathogenicity (Kers, Wach *et al.*, 2004). The coexistence of these putative electron donors with bNOS is summarized in Table 2.1.

Table 2.1– Summary of coexistence of putative electron donating partners for bacterial NOS in selected bacterial species.

Organism*	SiR-FP	P450 BM-3	Flavodoxin	Flavodoxin-like	TrpRS II
<i>B. subtilis</i>	+	+	+	+	-
<i>B. halodurans</i>	+	-	-	+	-
<i>O. iheyensis</i>	+	-	+	+	-
<i>S. aureus</i>	+	-	-	+	-
<i>S. epidermidis</i>	+	-	-	+	-
<i>B. anthracis</i>	-	+	-	+	-
<i>B. cereus</i>	-	+	-	+	-
<i>D. radiodurans</i>	-	-	-	+	+

*All organisms contained in this table encode a bNOS gene. The coexistence of bacterial NOS with these putative electron donating partners is indicated by a '+'.
(Zemojtel, Wade *et al.*, 2003; Buddha and Crane, 2005; Hulo, Bairoch *et al.*, 2006)

2.1.1.1 Sulfite Reductase

Sulfite reductase is a soluble oligomeric protein made up of two types of subunits in $\alpha_8\beta_4$ stoichiometry. The α subunit is a FAD-FMN-containing flavoprotein (SiR-FP) and the β subunit is a siroheme and an Fe_4S_4 cluster (Murataliev, Feyereisen *et al.*, 2004). Analogous to mNOS reductase, the SiR-FP transfers six electrons from 3 molecules of NADPH to the active site. The coexistence of SiR-FP and bNOS was noted by Zemojtel *et al.* in 2003. As illustrated in Table 2.1, SiR-FP is found in many, but not all, bacteria that code for bNOS. A solution structure of a bacterial flavoprotein moiety of a sulfite reductase found in *E. coli* has

been obtained and was found to be homologous in structure to cytochrome-P450 reductase and nitric oxide synthase reductase domain (Sibille, Blackledge *et al.*, 2005). Although the transfer of electrons from SiR-FP to cytochrome c and to a cytochrome-P450 enzyme have been demonstrated (Sibille, Blackledge *et al.*, 2005), there have been no reported attempts to transfer electrons to NOS enzymes.

2.1.1.2 Cytochrome P450 BM-3

Cytochrome P450 BM-3 has analogous domain architecture to mNOS enzymes and thus has also been suggested as candidates for surrogate electron donors for bNOS enzymes (Zemojtel, Wade *et al.*, 2003). Similar to mNOS enzymes, the reductase domain is comprised of NADPH, FAD, and FMN binding domains; however, unlike mNOS, P450 BM-3 catalyzes fatty acid hydroxylation (Gustafsson, Roitel *et al.*, 2004). There is no evidence of interaction of P450 enzymes with bNOS enzymes. However, the ability of Cytochrome P450 reductase to donate electrons to P450 BM-3 suggests the possibility of interaction with other analogous enzymes (Sibille, Blackledge *et al.*, 2005). The coexistence of P450-BM3 enzymes in bacterial systems with bNOS, similar to other suggested electron-donating partners, does not show a consistent trend.

2.1.1.3 Flavodoxin

Another possibility for a surrogate electron donor for bNOS enzymes are short chain flavodoxins (Murataliev, Feyereisen *et al.*, 2004). Flavodoxins bind one molecule of FMN and act as an electron transfer protein in many electron transfer systems (Hulo, Bairoch *et al.*,

2006). In 2004, Lawson *et al.* cloned, overexpressed, and purified two *B. subtilis* flavodoxin proteins, ykuN and ykuP, in *E. coli*. They showed that ykuN and ykuP both bound FMN and supported lipid hydroxylation catalyzed by a cytochrome-P450 enzyme. However, no interaction with NOS was reported (Lawson, Wachenfeldt *et al.*, 2004).

Flavodoxin-like proteins are similar in domain architecture to flavodoxin proteins but have a more divergent sequence (Hulo, Bairoch *et al.*, 2006). Flavodoxin-like proteins are found to coexist in all the bNOS containing organisms listed in Table 2.1, and they might possibly function as electron donating partners for bNOS enzymes.

2.1.1.4 Tryptophanyl-tRNA synthetase II

Tryptophanyl-tRNA synthetase II is an aminoacyl-tRNA synthetase (AARSs) that is able to charge tRNA synthetase with nitro-tryptophan (Buddha and Crane, 2005). Generally AARSs function to attach one of the standard 20 amino acids to tRNAs with the appropriate anticodon. Most organisms only code for one AARS per amino acid, presumably to protect against the proliferation of mutations that would result in coupling inappropriate analogues. *D. radiodurans* contains two TrpRS enzymes. The most divergent of the two, TrpRS II, was shown to interact with deiNOS (Buddha and Crane, 2005). Buddha, Keery, *et al.* (2004) coexpressed deiTrpRS II and deiNOS in *E. coli* and showed that the use of copurification techniques significantly enhances the solubility of deiNOS (Buddha, Keery *et al.*, 2004). Dimeric deiNOS was shown to bind dimeric deiTrpRS II in a 1:1 ratio, thereby increasing its affinity for the substrate L-Arg. Buddha, Tao, *et al.* (2004) showed that this interaction was able to stimulate the regioselective nitration of Trp (Buddha, Tao *et al.*, 2004). The addition

of ADP was shown to stimulate production of 4-nitro-Trp, whereas the addition of H₄B inhibits the nitration reaction and promotes the production of [•]NO. Although TrpRS II are found in many bacteria, the specific residues suggested by Buddha and Crane in 2005 to be required for Trp modification are not found in any other Trp RS II which coexist with bNOS. The authors suggested that specific mutations in the TrpRS II active site are required to reorient the substrate to allow for the nitration reaction.

2.1.2 Possible Docking Position Electron Donor for bNOS

Regardless of which protein proves to interact with bNOS, ultimately the protein must donate electrons to the active site of bNOS enzymes. A probable docking position has been suggested for these potential surrogate electron donors (Bird, Ren *et al.*, 2002). Three residues on the exposed heme edge that are conserved across bNOS sequences have been suggested as a probable site of interaction for an electron donating partner. The following figure shows the dimeric structure of saNOS with the conserved residues along the exposed heme edge, Leu66, Phe67, and Gln297, highlighted in turquoise.

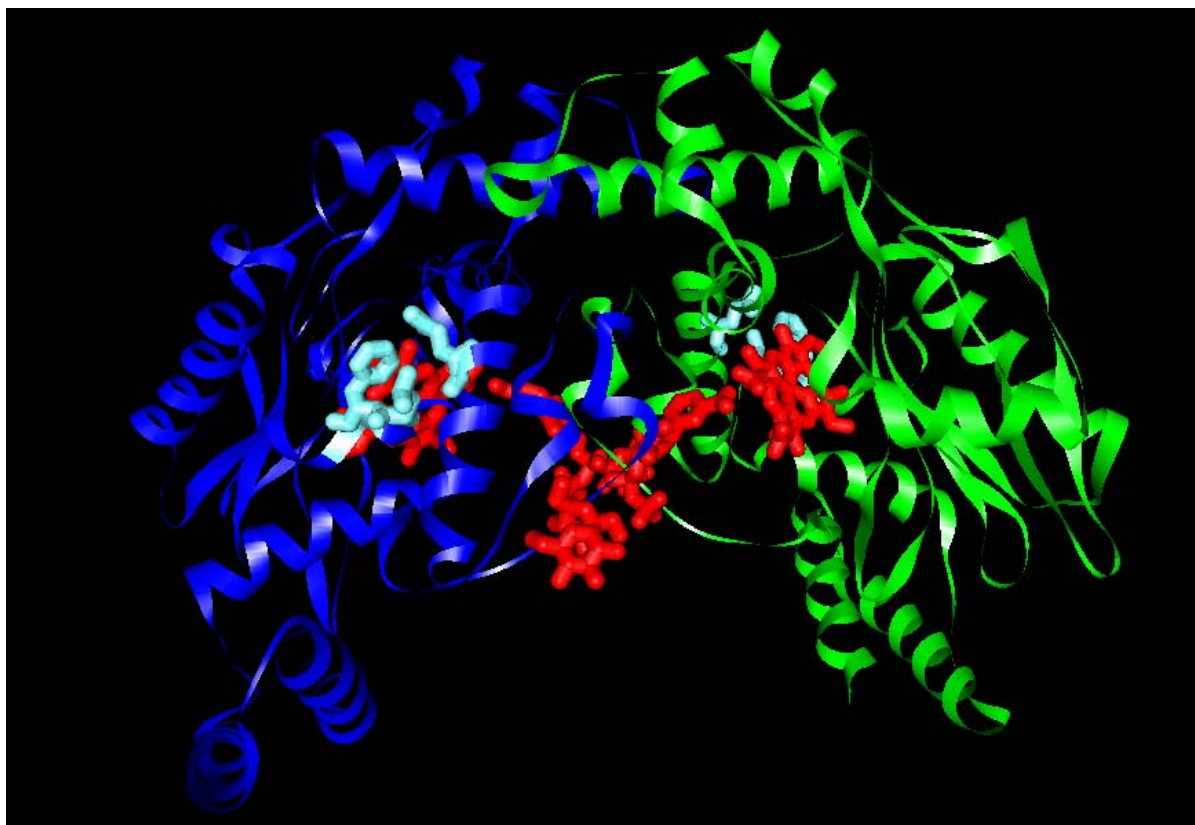


Figure 2.1- Crystal structure of *Staphylococcus aureus* NOS.

The possible docking site for bNOS electron donating partner is highlighted. The three residues that sit at the proposed docking site along the exposed heme edge are highlighted in turquoise and detailed in the text (Bird, Ren *et al.*, 2002).

2.1.3 Approach

All of these candidate proteins have yet to be shown to interact with bNOS under native conditions *in vivo*. It does not take long to realize many possible candidates for the role of electron donor exist within bacterial systems. Two experimental approaches were tried to identify potential electron donating protein partners for bNOS in *B. cereus*: (i) Isolate intact bNOS protein complexes from native sources using conventional chromatography

methods or (ii) Fish-out the electron donor using affinity-tagged recombinantly expressed bNOS protein as a bait protein.

The three chromatographic methods that have been previously used to isolate bNOS from native sources include (i) MonoQ column followed by Superose 12R (Choi, Oh *et al.*, 2000), (ii) MonoQ column followed by 2'5'ADP-agarose and then a Superdex 200HR column (Hong, Kim *et al.*, 2003), and (iii) 2'5'ADP-agarose column followed by hydroxylapatite chromatography (Chen and Rosazza, 1995). These methods were used in the current studies. Two methods were used in our attempts to isolate intact bNOS-electron donor protein complexes: (i) MonoQ column followed by Superdex 300 column and (ii) 2'5'-ADP-sepharose column followed by an L-Arg sepharose column.

Alternatively, previously purified bcNOS was bound to different metal-chelating chromatography columns and used as bait in efforts to fish-out interacting proteins from the bacterial cell lysate. Three different metal-chelating resins were used to probe these potential interactions: (i) Ni²⁺-chelating resin, (ii) Co²⁺-chelating resin, and (iii) Co²⁺-chelating magnetic resin.

Nickel-based metal-chelating chromatography tends to be the most common form of metal-chelating chromatography due to its high affinity to His-tags. Higher affinity properties allows for a more specific isolation of a target protein, which is a desirable trait when isolating recombinantly expressed His-tagged proteins. For our purposes, higher affinity for the bait protein could allow for elution of potentially interacting partners prior to the elution of the bait protein.

Cobalt-based metal-chelating chromatography allows for purification of His-tagged proteins using less stringent elution conditions. This is a desirable feature for pull-down experiments as it allows the elution of both the bait protein and potential interacting partners simultaneously. The metallic resin is a spherical and monosized resin, with defined and highly controllable physical and chemical characteristics allowing for highly reproducible results.

2.2 Procedures

2.2.1 Strain and Growth Conditions

The *Bacillus cereus* strain ATCC 10987 and the bcNOS enzyme cloned from this strain were used for all the following protocols. The bcNOS gene from ATCC 10987 was cloned into pET28a, expressed as a His-tagged fusion protein and purified by Ni²⁺-chelating chromatography. Cells were grown in 2XSG media (16 g Difco Bacto Nutrient Broth, 2 g KCl, 0.5 g MgSO₄·7 H₂O, pH to 7.0 with 1 M NaOH, autoclaved, cooled to 55°C, then 1 mM CaCl₂, 0.1 mM MnCl₂·H₂O, 1 uM FeSO₄ were added). One liter cultures were grown in 4 L flasks containing 2XSG media with and without the addition of 0.125 % methanol. Cultures were inoculated from a saturated overnight culture with a 1% inoculum and were grown at 30°C for 18-48 hours, as indicated. Cells were harvested at 8,000xg at 4°C for 10 min. Cells were stored at -80°C until further processing.

2.2.2 Cell Disruption

Cell lysate was prepared by resuspending the frozen cell pellet of 2-3L of *B. cereus* liquid culture in approximately 40 mL of the appropriate buffer specified for each chromatographic technique. The cells were disrupted by homogenization using Emulsiflex-C5 (Avestin) and centrifuged for 20,000xg for 30 min at 4°C.

2.2.3 MonoQ/Sephacryl 300 Chromatography

Approximately 40 mL of cell lysate in 40 mM Tris-HCl, pH 7.5, 1 mM EDTA, 1 mM DTT was loaded onto a MonoQ column (Pharmacia) equilibrated with Buffer A (40 mM Tris-HCl, pH 7.5, 1 mM EDTA, 1 mM DTT, 2 μ M H₄B, 2 μ M FAD, 2 μ M FMN). The column was washed with 5 column volumes of Buffer A and the protein was eluted with a linear gradient (0-0.75 M NaCl) in 10 column volumes. The column was then washed with 2 column volumes of Buffer B (0.75 M NaCl in Buffer A), 5 column volumes of H₂O and 5 column volumes of 20 % EtOH. The protein peak that was eluted between 0.2-0.5 M NaCl was pooled, concentrated to ~1 mL and dialyzed into Buffer C (40 mM Tris-HCl, pH 7.5, 5 % glycerol, 1 mM DTT, 250 mM NaCl) before loading onto a Sephacryl 300 column (Pharmacia). The 24 mL column was eluted with 4 column volumes of Buffer C and then eluted with 4 column volumes Buffer C. The column was washed with 8 column volumes of water and stored in 20 % Ethanol. The eluted peak was pooled and stored at -20°C.

2.2.4 2'5'ADP-sepharose/L-Arginine-sepharose

Both the ADP- and L-Arg-sepharose columns (GE Healthcare) were regenerated 3 times using alternating high pH buffer (0.1 M Tris-HCl, 0.5 M NaCl, pH 8.5) and low pH buffer (0.1 M Sodium acetate, 0.5 M NaCl, pH 4.5) regeneration buffers and then equilibrated with 5 column volumes of ADP wash buffer (10 mM Tris-HCl, 1 mM EDTA, 1 mM DTT, 2 μ M H₄B, pH 7.5). Approximately 40 mL of cell lysate in ADP wash buffer was incubated with the resin with slow rotation for 1 hr at 4°C and then packed into the column. The column was washed with 5 column volumes ADP wash buffer, 5 column volumes ADP salt wash buffer (10 mM Tris-HCl, 1 mM EDTA, 1 mM DTT, 2 μ M H₄B, 500 mM NaCl, pH 7.5) and eluted in 20 mL with 10 mM 2'AMP and 500 mM NaCl in ADP wash buffer. The eluate was concentrated, dialyzed into ADP wash buffer and loaded onto L-Arg sepharose resin by rotating in a centrifuge tube for 1 hr at 4°C before transferring to a column. The column was washed with 5 column volumes wash buffer and the protein was eluted in 20 mL wash buffer containing 1 M L-Arg. The eluted fraction was concentrated 20 fold before analysis.

2.2.5 Metal-Chelating Chromatography

12.5 mg of previously purified His-tagged protein was dialyzed into Wash buffer (40 mM Tris-HCl, 10 % glycerol, 1 mM L-Arg, 250 mM NaCl). The bait protein was loaded onto the 20 mL NTA-Ni²⁺ agarose column (Novagen) by gravity and washed with 5 column volumes of wash buffer. Approximately 40 mL of cell lysate in wash buffer containing 0.55

mg/mL Lysozyme (Roche) and 0.1 mg/mL DNase I (Roche) was loaded onto the column with the bound bait protein by slowly rotating the mixture in a centrifuge bottle for 1 hr at 4°C. The column was washed with 5 column volumes of wash buffer, and subsequently with wash buffer containing 0.5, 50, 100, 200 mM imidazole, successively.

2.2.6 ProFound™ Pull-Down PolyHis Protein:Protein Interaction Kit

Immobilized Co²⁺-chelate resin was equilibrated using 1:1 ProFound™(PIERCE Biotechnology) wash solution of TBS:ProFound™ Lysis Buffer containing 40mM imidazole and 75 mM NaCl and 1% proprietary nonionic detergent. 650 µg of bait protein was diluted to 800 µL and then loaded onto the 50 µL column bed by slowly rotating the mixture for 30 min at 4°C. The resin was washed 5 times with 800 µL wash buffer. The cell lysate of a 1 L culture in 15 mL of ProFound™ wash solution was then loaded by rotating the mixture in a centrifuge tube for 1 hr at 4°C. The column was washed 5 times with 800 µL ProFound™ wash buffer before successive elutions with 100, 250, 500 mM NaCl in ProFound™ wash solution. The final elution was performed with 500 mM NaCl with 290 mM imidazole in ProFound™ wash solution as recommended by the manufacturer.

2.2.7 Magnetic Resin

Approximately 2 mg (50 µL) of immobilized Co²⁺-chelate resin from DYNAL® Biotech was equilibrated with 3 volumes of 100 µL of Talon™ Wash Buffer (50 mM sodium phosphate, pH 8.0, 300 mM NaCl, 0.01 % Tween-20) by separation of the resin with the use of a magnet. 100 µg of the bait protein was diluted to 700 µL with Talon™ wash buffer and

then loaded onto the magnetic resin by slowly rotating the mixture for 30 min. The resin was washed 3 times with 700 μ L Talon™ wash buffer and then 15 mL of the cell lysate was loaded by rotating the mixture in a centrifuge tube for 1 hr at 4°C. The resin was then washed 3 times with 700 μ L of Talon™ wash buffer. Fractions were eluted successively in 100 μ L of 500 mM NaCl and 150 mM Imidazole in Talon™ wash buffer.

2.2.8 Protein Detection

A series of 10 % SDS-PAGE gels were run on eluted fractions to determine the distribution of proteins within the samples. Approximately 20 μ g of protein was loaded for each sample in separate lanes. Gels were stained with Coomassie R-250.

Western blots were performed by transferring proteins onto PVDF membranes overnight in a BIO-RAD electrophoretic transfer cell at 10 V at 4°C. The primary antibody (1°Ab) obtained from Transduction Laboratories was raised to a 21 kDa fragment corresponding to the C-terminal NADPH binding domain (residues 961-1144) of mouse iNOS. Membranes were blocked with 1 % BSA in TBS-T for 2 hrs. The membranes were incubated in a 1:5,000 solution of 1°Ab (Anti-iNOS Rabbit pAb) for 1 hr. The membranes were washed 3 times in TBS-T before incubating in a 1:10,000 solution of secondary antibody (2°Ab) Goat Anti-Rabbit IgG, (H+L), Peroxidase conjugate for 1 hr. The membranes were washed 3 times in TBS-T and then blotted dry. ECL detection solution (2 mL solution A & 50 μ L solution B) was poured over the surface of the membranes, wrapped in plastic wrap and incubated at room temperature for 5 min before visualizing.

Chemiluminescence was detected for 15-60 min using the Alpha innotech Flurochem 8000 Chemiluminescence and visible imaging system.

2.2.9 Determination of Nitric Oxide Production

Production of nitric oxide in fractions was determined using the Griess Assay (Griess, 1864; Ignarro, Buga *et al.*, 1987) modified for use in a microtiter plate reader. 20 μ L of purification samples were incubated at 37°C for 25 min in the presence of 50 μ M H₄B, 1 mM L-Arg, or 20 μ M NOHA, 20 μ M CaM, 200 μ M Ca₂Cl₂, 10 μ M FAD, 10 μ M FMN, 200 μ M DTT, as indicated. 100 μ L Griess reagents were added directly to the sample mixture. The Griess reagents comprise a 1:1 ratio of freshly prepared 0.1 % naphthylethylenediamine (N5889, Sigma-Aldrich Canada Ltd., Oakville, ON) in MQ water and freshly prepared 1 % sulphanilamide (S9251, Sigma-Aldrich Canada Ltd., Oakville, ON) in 5 % phosphoric acid (Fisher Scientific, Nepean, ON). Reaction mixture was allowed to react for 10 min at 25°C before reading at 540 and 630 nm using a SPECTRAMax PLUS 384. A standard curve was generated using 0-20 μ M sodium nitrite.

2.3 Results and Discussion

2.3.1 Bacterial NOS Expression

It was previously reported that bNOS expression can be induced by applying stress to the culture either by addition of methanol or by starvation (Choi, Seo *et al.*, 1998). However, expression tests, determined by β -gal activity, revealed that the bcNOS gene was expressed

late in exponential phase (see section 3.3.1.2) and that the presence of methanol did not significantly influence its expression. Therefore, cells were grown in media without methanol and harvested according to bcNOS expression.

2.3.2 Attempts at Isolation of Intact bcNOS Protein Complex

The anion exchange/size exclusion conditions were modeled after studies used to purify NOS from *Salmonella typhimurium* (Choi, Oh *et al.*, 2000). These studies characterized the elution of bcNOS using qualitative NO analysis. In the partially purified sample, a protein of 93 kDa was identified using an antibody raised against the C-terminus of iNOS (NADPH binding domain) (Choi, Oh *et al.*, 2000). Application of the same chromatographic purification scheme to a *B. cereus* lysate yielded protein bands of 30, 32, 42, 60, & 66 kDa identified by Coomassie staining. Although these fractions lacked the characteristic heme colour for NOS proteins, the 42 kDa protein could possibly be bcNOS and the other proteins are potential interacting partners. The lack of characteristic heme colour for the eluted fractions could be a result of the protein releasing its heme during the purification process. The other proteins may not necessarily interact with this 42 kDa protein, they could merely elute in the same fraction because they have similar binding properties for these columns. These methods are not specific and yield many potential interacting proteins. With no way of differentiating true interacting proteins, other methods were pursued to isolate interacting protein partners for bcNOS.

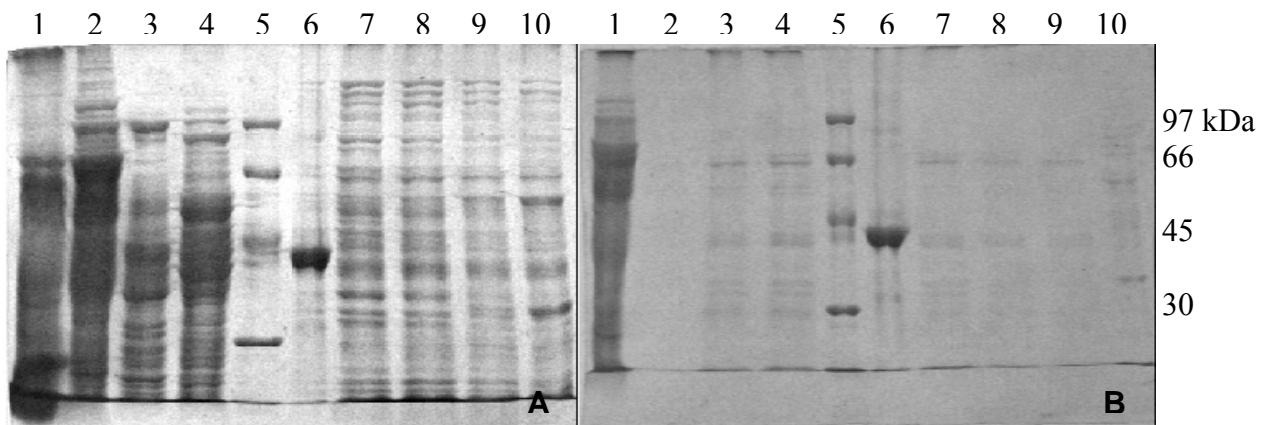


Figure 2.2 – Fractionation of *B. cereus* lysate using MonoQ (A) and Sephacryl 300 (B) columns.

MonoQ gel (A) lane 1 unfractionated cell lysate, lanes 2-4, 7-10 eluted fractions, lane 5 low molecular weight marker, lane 6 purified bcNOS. Sephacryl 300 gel (B) lane 1 MonoQ flowthrough, lane 2-4, 7-10 eluted fractions, lane 5 low molecular weight marker, lane 6 purified bcNOS. Gel stained with Coomassie R-250.

The ADP/L-Arg sepharose column conditions were modeled after the conditions used to purify NOS from *S. aureus* and *Nocardia*, in conjunction with the binding properties attributed to the bNOS enzymes. In this system, the first column should bind NADPH-binding proteins and the second column should bind proteins with an L-Arg binding pocket. Previous work isolating saNOS from native sources showed NOS activity using both a NO Analyzer (Model 7020, Antek Instruments) as previously described by Choi *et al.* in 2000 and radioactive L-[³H]Arginine assay methods (Hong, Kim *et al.*, 2003). The saNOS was found to be a heterodimer with masses of 64 and 67kDa determined by SDS-PAGE (Hong, Kim *et al.*, 2003). The *Nocardia* studies showed NOS activity via L-[³H]Arginine and the Griess assay. *Nocardia* NOS was isolated as a homodimer of 51.9 kDa (Chen and Rosazza, 1995).

The ADP/L-Arg sepharose columns yielded varying results. The eluates from both the ADP and the L-Arg sepharose columns had to be concentrated 20 fold to be detectable on

SDS-PAGE with Coomassie. The ADP-sepharose column alone isolated proteins of 30, 40, 42, 44, 60 and 97 kDa. The combination of ADP-sepharose followed by the L-Arg sepharose column gave two protein bands of approximate size 38 and 64 kDa. Upon Western blot analysis, faint bands indicated reactivity with proteins of molecular mass 30, 34, 40, and 42 kDa. Some of these protein bands were too dilute to be detected with Coomassie but the immunoblot using mouse iNOS 1° Ab was able to detect their presence. The bands exhibited in the immunoblot could be products of protein degradation, since they are all smaller than the 42 kDa bcNOS band and are all similarly immunoreactive. It should be noted that the 1° Ab used was raised against the reductase domain of mNOS. Thus the 38 and 64 kDa proteins evidenced in the Coomassie stained gel but not found on the immunoblot could be potential interacting protein partners to bcNOS. This experiment was run twice, the first time no bound protein was found because the eluate was very dilute. The 20 fold concentration of the eluate allowed for the visualization of the bound proteins. These results were not found to be reproducible.

The homogenization pellet was found to be immunoreactive, thus purification methods containing 0.25% Triton X-100 were attempted to determine if the reactive species could be solubilized with detergent and then purified by these methods. SDS-PAGE results stained with Coomassie showed no proteins remained bound after both columns, however Western Blot analysis indicated two proteins of molecular mass 32 and 42 kDa bound both columns. Again the smaller fragment found in the immunoblot could very well be a product

of proteolytic degradation of bNOS. Table 2.2 compares the results obtained with and without Triton X-100 present.

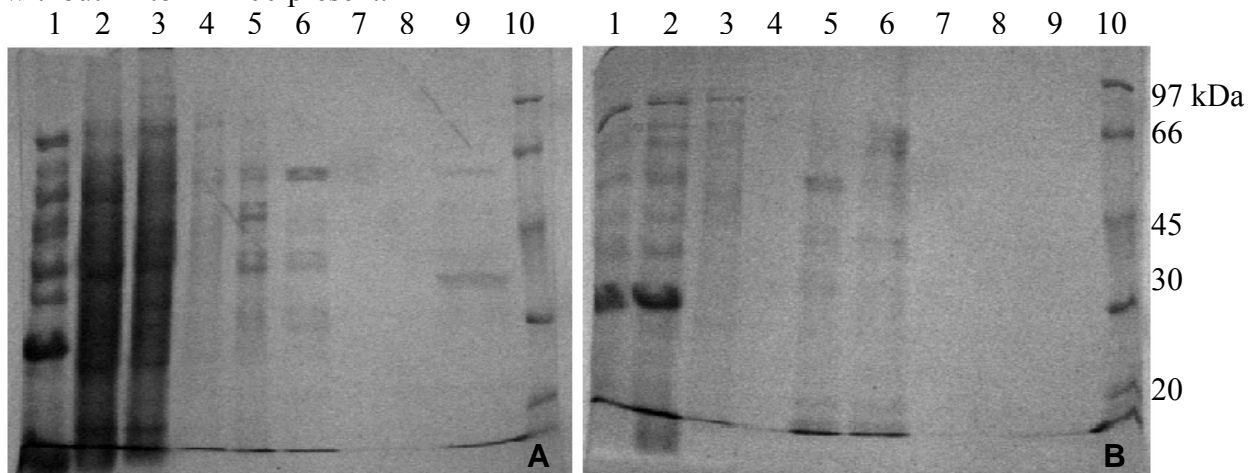


Figure 2.3—*B. cereus* lysate fractionated using ADP-sepharose and L-Arg sepharose consecutively. This figure compares these procedures performed with out (A) and with (B) 0.25 % Triton X-100. Lanes 1&2 homogenization pellet and supernatant, respectively, Lanes 3-6 fractions from ADP-sepharose column, Lanes 7-9 L-Arg-sepharose fractions, Lane 10 low molecular weight marker (20, 30, 45, 66, 97 kDa). Lanes 6 & 9 were concentrated 20x prior to analysis. Gel stained with Coomassie R-250.

Another approach attempted for this method was to perform the L-Arg sepharose column first. Since bcNOS is known to bind L-Arg this could provide evidence that those proteins that bound both columns are indeed bNOS or interacting protein partners. Fractionations done in this manner resulted in several non-specific interactions with the L-Arg-sepharose column and none with the ADP-sepharose column. This is not entirely surprising as it is still unknown if the electron-donating partner would bind NADPH.

Table 2.2 summarizes the results obtained during these attempts at isolating of intact bNOS protein complexes. The size of protein bands and the methods by which they were isolated, as discussed previously, are reviewed in this table. Since many proteins of various sizes are listed in this table, it may be useful to recall the bcNOS enzyme is 42-43 kDa

(depending on the presence of a His-tag). The presence of a band at 42-43 kDa as well as other proteins could indicate the presence of protein-protein interactions. The presence of mouse iNOS immunoreactive band confirms the 42-43 kDa protein as having NOS-like structural characteristics. Unfortunately, these results do not point conclusively to one or two probable interacting proteins.

Table 2.2- Summary table of efforts to isolate intact bNOS protein complexes from native sources.

Molecular weight of each protein isolated by the different chromatographic techniques, as described in detail in the text, are given in kDa. Replicates of the same chromatographic techniques are shown in separate rows. Results for samples resuspended in buffer containing 0.25 % Triton X-100 are also listed in separate rows.

Type of analysis	ADP sepharose	L-Arg sepharose	Mono Q	Sephacryl 300
Cell lysate resuspended in buffer without Triton				
Coomasie stain			many bands	30/32/42/60/66
	60			
	42/44/60/97			
	30/42/64	38/64		
	None			
Western with anti MiNOS^a	40/66	30/40		
	30/66	34/42		
Cell lysate resuspended in buffer with 0.25 % Triton X-100				
Coomasie stain	42/60/64	none		
Western with anti MiNOS^a	42/66	32/40		

^a C-terminal NADPH binding domain (residues 961-1144) of mouse iNOS

The ADP / L-Arg-sepharose method shows promising results, since it yielded a limited number of proteins. The ADP-sepharose column produces a protein band appropriate to bcNOS plus bands of approximated size 30, 44, 60, 64, 66, 97 kDa. Although these proteins may interact with NADPH, it is still unclear if they interact with bNOS. Since the

ability of the bNOS electron-donating partner to bind NADPH is still unknown, other methods were pursued.

2.3.3 Probing Protein-Protein Interactions of bNOS

The second approach taken to determine probable electron donors for bNOS was to ‘fish-out’ interacting proteins using the known overexpressed bNOS protein as bait. These methods entail binding His-tagged bNOS protein to a resin and allowing cell lysate to interact with the bound protein. The column is subsequently washed and any interacting proteins elute with the His-tagged protein. Three different resins were used to accomplish these studies: Ni²⁺-chelating resin, Pull-down kit Co²⁺-chelating resin, and metallic Co²⁺-chelating resin.

The Ni²⁺-chelating resin was used first due to availability. The column was overloaded with the bcNOS bait protein to ensure that proteins in cell lysate would bind only if they interacted with the bait protein and not with the resin. Figure 2.4 shows the protein fractions obtained from Ni²⁺-chelating column run with bcNOS bait and *B. cereus* cell lysate. Although faint bands of possible interacting proteins are evident, the overloading of the bait protein masks any proteins in the 40 kDa region during elution with imidazole. These methods have produced possible interacting proteins of size 32, 38, 40, 42, 45, and 60 kDa. The 42 kDa protein could be bcNOS and the other proteins are potential interacting partners. Once again, the protein bands smaller than 42 kDa may be products of protein degradation.

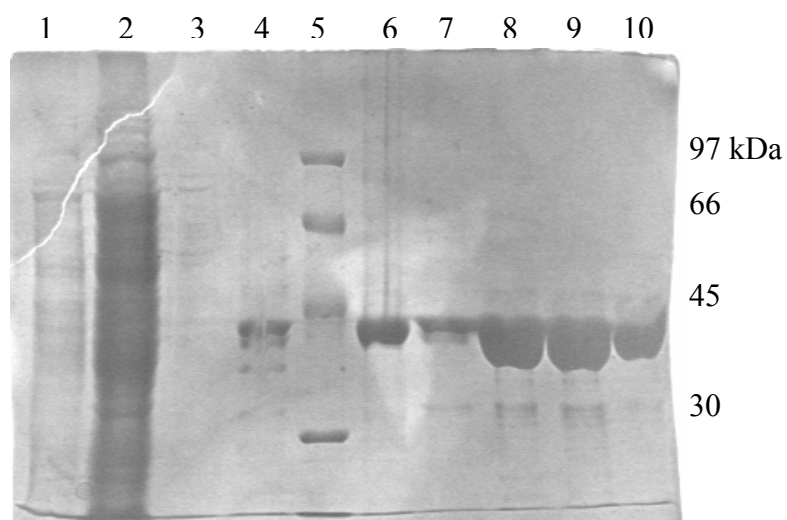


Figure 2.4– Pull-down experiment using bcNOS bound to Ni²⁺-chelating column. Lane 1 cell pellet, lane 2 cell lysate, lane 3 bcNOS cell lysate flowthrough, lane 4 buffer wash, lane 5 low molecular weight marker, lane 6 bcNOS, lane 7 cell lysate buffer wash, lanes 8-10 eluted fractions. Gel stained with Coomassie R-250.

The bound fraction from the Ni²⁺-chelating column was followed by a 2'5'-ADP-sepharose column to determine if any of proteins that bound to the His-tagged bait would also bind the ADP-sepharose resin. No proteins were detected by SDS-PAGE with Coomassie staining.

A Pull-Down kit was obtained from PIERCE in attempts to exploit its optimized conditions for 'fishing out' any interacting proteins. The main differences between this system and the homemade pull-down experiment were the method of lysing the cell culture with their proprietary detergent, the reduction in amount of cell lysate used to probe the possible interactions, and the reduction of salt in the wash buffers.

The PIERCE Pull-Down kit yielded a single protein band of approximately 40 kDa that eluted at the same time as the His-tagged bcNOS. Figure 2.5 shows a comparison of the bound fractions of the bait (previously purified bcNOS), the prey (*B. cereus* cell lysate) and

bait plus prey. Non-specific interactions with the Co^{2+} -chelating column that are found in the prey elution are minimized by overloading the column with the bait. The interaction appears to be disrupted with 500 mM salt eluting some of the bait protein as well as an additional band at 40 kDa. With subsequent elution with imidazole, the whole 38-42 kDa region is overshadowed by the abundance of bcNOS. Although the 40 kDa protein should be further analyzed, this method did not prove to be significantly more fruitful than the homemade pull-down experiment with Ni^{2+} -chelating chromatography.

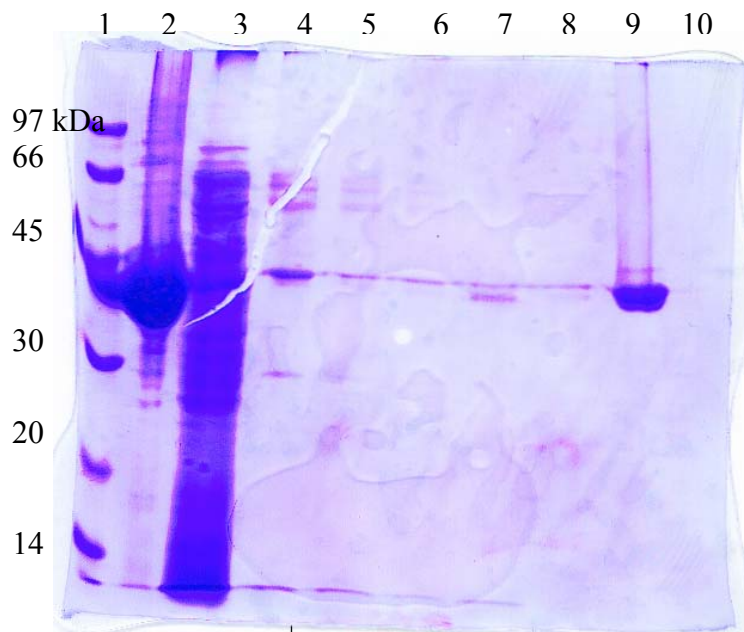


Figure 2.5 – Pull-down experiment using bcNOS bound to Co^{2+} -chelating column.

Lane 1 low molecular weight marker, lane 2 purified bcNOS, lane 3 prey flowthrough, lane 4-6 prey salt elutions 100, 250, 500mM, respectively, lane 7 bait + prey 500mM salt elution, lane 8 bait 500mM salt elution, lane 9 bait imidazole elution. Gel stained with Coomassie R-250.

Another method that was explored was the use of Dynabeads® TALON™ magnetizable beads used in Co^{2+} -based immobilized metallic affinity chromatography to isolate His-tagged proteins. This magnetic resin uses less vigorous separation conditions which is useful for pull-down experiments. This method uses the same principles for

‘fishing-out’ interacting proteins as the other two His-tagged methods however uses less vigorous methods for washing and elution. The less vigorous methods may allow protein-protein interactions that are disrupted by other methods to remain intact.

The magnetic resin resulted in significant non-specific binding. Although saturating the column with purified His-tagged bcNOS disrupts some of the non-specific binding many proteins remain. A comparison of those proteins found in the prey negative control elution and those found with the bait plus prey was performed to identify any potentially interacting partners. All potential interacting partners appear to be in the negative control. More sensitive methods for detection would be needed for this comparison.

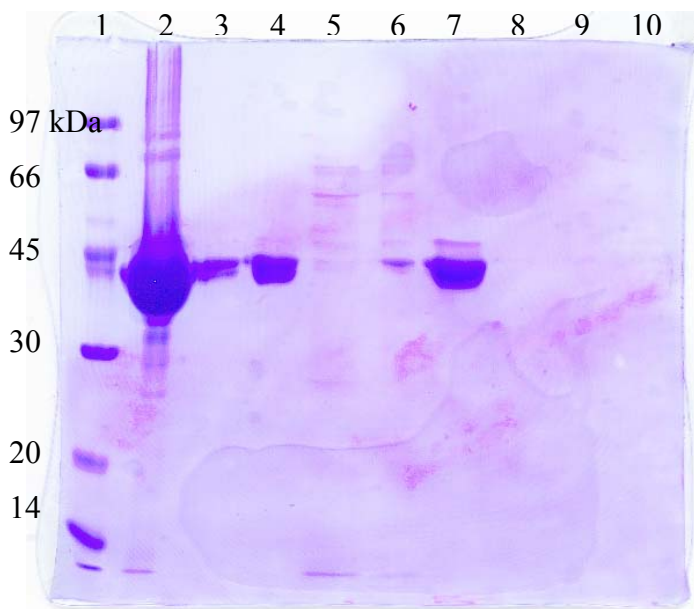


Figure 2.6– Purification fractions from magnetic resin.

Lane 1 low molecular weight marker, lane 2 previously purified bcNOS, lane 3 prey imidazole elution, lane 4 bait + prey imidazole elution, lane 5 prey 500mM salt elution, lane 6 bait + prey 500mM salt elution, lane 7-9 imidazole elution for bait, prey, and bait + prey, respectively. Gel stained with Coomassie R-250.

The results from the bcNOS pull-down experiments are summarized in Table 2.3. The Ni^{2+} - and Co^{2+} -chelating columns did not yield significant reproducible binding proteins.

The magnetic Co²⁺-chelating column produced many but reproducibly binding proteins. The less vigorous separation methods do not disrupt interactions with proteins in the cell lysate. Many of these binding proteins are interacting non-specifically with the resin, however further analysis could pull-out interacting partners not found in the negative control.

Table 2.3– Summary table of pull-down experiments using His-tagged bcNOS as bait immobilized on different metal-chelating resins.

Molecular weight of each protein isolated by the different chromatographic techniques, as described in detail in the text, are given in kDa. Replicates of the same chromatographic techniques are shown in separate rows. Results for samples resuspended in buffer containing 0.25 % Triton X-100 are also listed in separate rows.

Type of analysis	Ni ²⁺ chelating	Co ²⁺ chelating	Magnetic Co ²⁺ chelating
Cell lysate resuspended in buffer without Triton			
Coomasie stain	32/38/42		
	40/45/60		
	43		
		many bands*	
		40/42	
			many bands*
			many bands*
Cell lysate resuspended in buffer with 0.25 % Triton X-100			
Coomasie stain			many bands*
Western with anti MiNOS^a			
		inconclusive*	inconclusive*
	34/42		
	34/42		

* - non-specific binding

^aC-terminal NADPH binding domain (residues 961-1144) of mouse iNOS

2.3.4 Bacterial NOS Activity

Crude activity assays of these fractions were performed by monitoring NO production using the Griess Assay. Indications of activity were found in the homogenization pellets as well as the concentrated eluted fractions. However, since the activity readings were only

approximately twice the blank reading, this method was not pursued further. Since the binding affinity for NOHA is much higher than that of L-Arg in bacterial NOS enzymes, the substitution of NOHA for L-Arg in the enzyme mixture was attempted. This did not result in the increase in activity of the samples. Some studies also suggest that CaM is required for maximal activity (Adak, Aulak *et al.*, 2002; Adak, Bilwes *et al.*, 2002). While presently there is no known physical basis for this requirement *in vivo*, CaM was added to some assay mixtures to determine if the activity found in the samples would increase. As expected the addition of CaM did not significantly improve the apparent activity in the samples. The effect observed by Adak *et al.* in 2002 could be due the utilization of mNOS reductase as the electron donor for the bNOS assay.

Methods utilizing the addition of NADPH as an electron donor were also investigated but did not result in an increase in activity above background.

The activity assay used for assaying the fractions is presently unreliable. It would be desirable to be able to follow the activity during the purification process.

2.4 Concluding Remarks

The present studies did not yield conclusive evidence for specific interacting electron donating partner. New methods need to be pursued due to the inability to follow the elution of potential interacting partners. Since activity in the eluted fractions is undetectable and the identities of the potential interacting partners are unknown, no specific characteristics can be used to determine their presence during fractionation. Fractions often have to be concentrated 20 fold and fractions containing His-tagged proteins need to be overloaded in

order to be able to detect any potential interacting proteins by SDS-PAGE. The present method of detection of NOS activity is also not sensitive enough to follow activity within the eluted fractions from chromatographic techniques. Since chromatographic techniques often yield many fractions without a method of following the location of the target protein the processing of samples quickly becomes very labor intensive.

The ultimate goal would be to isolate several proteins of interest and to identify these interacting partners using mass spectrometry. This could prove to be difficult if these proteins of interest are found in low abundance, as the techniques we currently have to identify proteins (mass spectroscopy) require enough protein to be visualized on a Coomassie stained gel.

2.5 Future Directions

Future directions for this project could include isolation of intact protein complexes under native conditions. Two methods could be used to take this approach: (i) Expression of bNOS with a tag in the native bacterial strain, (ii) Utilization of a yeast two-hybrid system.

2.5.1 Expression of Tagged-bNOS in Native Conditions

One method of probing interactions in the native conditions is to express a tagged bcNOS in *B. cereus*. Table 2.4 lists expression vectors for use in Bacillus strains. The pMUTIN vector series with tags allows insertion of the tag under the control of the native promoter. This series of vectors may not allow for the overexpression of the target protein

but should result in the proper proportions of target protein and interacting partners. The protein complex can then be isolated by immunoprecipitation or by affinity chromatography.

Table 2.4– Bacillus expression vectors

Expression vectors	Integration locus	Selection ^a	Upstream promoter ^b	Downstream promoter ^c
pMUTIN-Flag ^d	Cloned locus	Em		Pspac
pMUTIN-FA ^d	Cloned locus	Em		Pspac
pMUTIN-GFP ^d	Cloned locus	Em		Pspac
pMUTIN-CFP ^d	Cloned locus	Em		Pspac
pMUTIN-YFP ^d	Cloned locus	Em		Pspac
pSWEET ^e	<i>amyE</i>		Pxyl	
pHCMC02 ^d	Extra chromosomal	Cr	PlepA	
pHCMC04 ^d	Extra chromosomal	Cr	Pxyl	
pHCMC05 ^d	Extra chromosomal	Cr	Pspac	
pHT304 ^f	Extra chromosomal	Em	PlacZ	

^aResistance – erythromycin (Em), chloramphenicol (Cr)

^bUpstream promoters - xylose inducible promoter (Pxyl), weakly constitutive promoter (PlepA), IPTG inducible (Pspac) & (PlacZ)

^cDownstream promoter – IPTG inducible (Pspac)

^dBGSC – Bacillus Genetic stock center

^e(Bhavsar, Zhao *et al.*, 2001)

^f(Arantes and Lereclus, 1991)

Alternatively, the pHCM vector series would allow for the overexpression of a cloned gene extra chromosomally. A fusion protein could be cloned into one of these plasmids to allow for immunoprecipitation or affinity chromatography. The expression could be carried out in the bcNOSKO strain to remove competition for the electron donating partners from the natively expressed bcNOS protein.

Extracting interacting partners from native conditions may prove to be more fruitful than trying to induce these interactions to protein already bound to a solid support.

2.5.2 Yeast 2 Hybrid System for *B. subtilis*

Another possibility for probing protein-protein interactions would be to use a yeast two-hybrid system. Yeast two-hybrid systems rely on two plasmid-borne gene fusions cotransformed into a yeast strain containing an inducible reporter gene (James, Halladay *et al.*, 1996). The bait protein is fused with a DNA binding domain specific to the reporter gene contained in the host strain. The expression library contains proteins fused to a transcriptional activation domain. Interactions of the two proteins in the host strain leads to activation of the reporter gene. Expression libraries are screened by looking for this phenotypic response.

A yeast two-hybrid system has been created recently for *B. subtilis* (Soppa, Kobayashi *et al.*, 2002). Probing protein interactions in this manner would allow for the identification of less stable interactions than those required for positive identification in this study.

Chapter 3: Investigations into the Role of bNOS

3.1 Introduction

Due to the physiological and pathological importance of mNOS it is believed that bNOS may play a critical role in bacterial systems. Although the presence of a NOS-like protein in prokaryotic systems is attracting increasing interest, a functional role has yet to be assigned to this intriguing enzyme. Possible roles for this enzyme, as described in detail in chapter 1, could include: (i) intercellular signaling to coordinate cellular/infectious activity, (ii) regulation via NO-mediated posttranslational modifications, or (iii) nitration of compounds in different biosynthetic pathways.

The methods used to investigate bNOS enzymes have focused on in vitro characterization of recombinantly expressed protein. Little effort has been devoted to the determination of a physiological role for this gene. A recent study by Gusarov and Nudler has suggested that the bNOS gene may mediate cellular adaptation to oxidative stress. They showed wild type strains of both *B. subtilis* and *S. aureus* were more resistant to oxidative stress than bNOS knockout strains. They suggest two mechanisms of cytoprotection: (i) via up-regulation of catalase, and (ii) via suppression of available cellular reducing agents, which sustain the production of damaging oxidizing agents (Gusarov and Nudler, 2005).

In order to understand the impact of this gene within bacterial systems, a genetic knockout of bNOS was obtained and characterized. One method of exploring the possible role of NOS-like enzymes in bacterial systems is to look at the differential protein expression

due to the knockout of the bNOS gene. Two-Dimensional Differential Gel Electrophoresis (2D-DIGE) allows for the determination of the change in protein expression exhibited between two samples. This technology was setup in our lab and used to identify changes in protein expression due to this genetic knockout. This will give clues to the role this gene may play in bacterial systems.

3.1.1 Gene Knockout

Genetic knockouts of the gene of interest were obtained in both *B. subtilis* and *B. cereus*. The knockouts were accomplished by insertional mutagenesis using the multi-host vector pMUTIN4 shown in Figure 3.1. This vector is uniquely designed for cloning in *E. coli* and insertional mutagenesis in other species. This vector relies on the cloning of an internal fragment of the target gene into the multi cloning site (MCS). Homologous recombination of this fragment with the chromosomal DNA results in the entire vector being inserted into the genome.

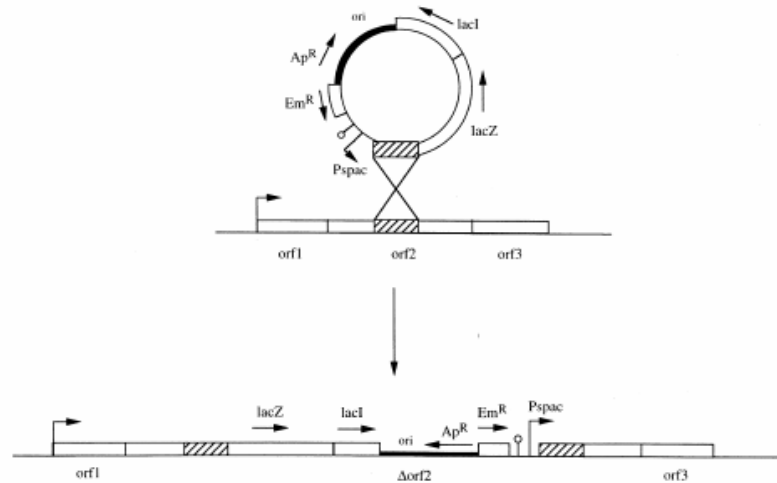


Figure 3.1– Schematic of homologous recombination of pMUTIN4 and with the targeted chromosomal DNA resulting in insertional mutagenesis.

Plasmid contains a origin of replication (ori) and an ampicilin resistance marker (Ap^R) for cloning in *E. coli*. After insertion into the target locus, the reporter gene (lacZ) and the erythromycin resistance marker (Em^R) are placed under the control of the promoter of the gene of interest. This event puts a stop codon in the middle of the gene of interest and places the downstream elements under the control of an IPTG-inducible promoter (Pspac).

This plasmid is unable to replicate in *B. subtilis*, allowing for this recombination event to occur. The pMUTIN4 vector contains a reporter gene, a selectable marker, a stop codon and an inducible promoter (Vagner, Dervyn *et al.*, 1998). The lacZ reporter gene is put under the control of the target gene’s promoter, allowing for monitoring of the expression of the target gene. The selectable marker, erythromycin resistance, allows for the selection of recombinants. Stop codons are incorporated in all three reading frames to ensure disruption of expression of the target gene. Finally, the downstream elements are placed under control of the IPTG inducible promoter, Pspac. The control of these downstream elements is key to the determination of the effects due to the single gene knockout in a polycistronic system.

3.1.2 2D Gel Methodology and Limitations

2D gel electrophoresis allows for a comprehensive study of the change in protein expression between two systems. This technique has the potential to yield a view into the physiological impact of the system that is being studied. However, this technique has some limitations. The limitations of 2D gel methods are primarily caused by the complexity of the samples being studied, requiring extensive sample preparation and troubleshooting. Sample preparations are extensive to ensure maximal protein solubility and to minimize contaminants which lead to difficulties with protein separation. Presently there are no universal parameters for 2D gel separation. Guidelines do exist for determining parameters, however, these parameters are time consuming to troubleshoot.

Perhaps the greatest challenge to 2D gel users has been gel to gel variability leading to complicating analysis and experimental variability. The introduction of the Ettan DIGE system from GE Healthcare allows for the incorporation of an internal standard in each gel allowing for gel to gel variability to be accounted for.

3.1.3 DIGE

The comparison of the proteomes of the knockout and wild type cultures was accomplished using 2D-DIGE. The introduction of the Ettan DIGE system by GE Healthcare has revolutionized 2D gel proteomic methods. Previous 2D gel methods were plagued with reproducibility issues. The Ettan DIGE system is based on matched intrinsic properties of three fluorophores which allows for multiplexing of three samples on the same

2D-gel. The multiplexing of multiple samples on the same gel allows for an internal standard to be run on each 2D-gel. This system allows for quantitative data supported by statistics to ensure that the results obtained are not due to experimental variation.

The cyanine based CyDyes™ from GE Healthcare are presently the best system for this application. The labeling procedure for the three CyDye™ DIGE fluors (Cy2, Cy3, and Cy5) shown in Figure 3.2, are designed so that the same protein labeled with different CyDye DIGE fluors will migrate to the same position on a 2D gel.

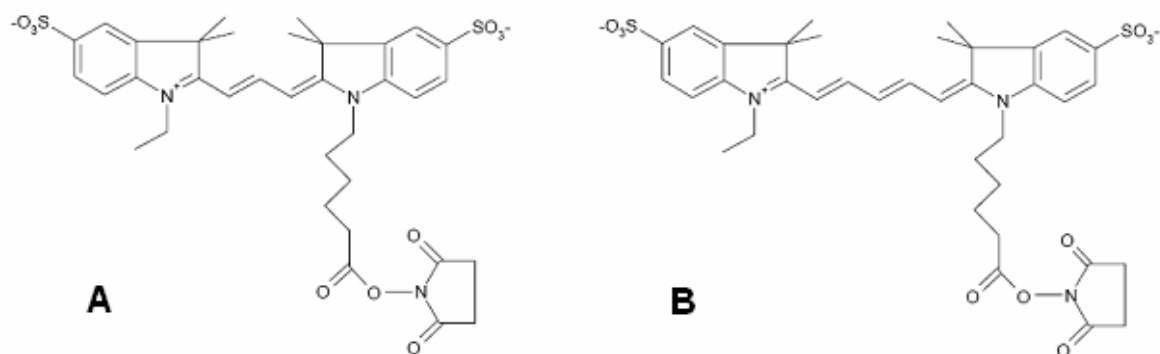


Figure 3.2-Structure of Cy3 (A) and Cy5 (B) fluors used in differential in-gel electrophoresis.
(Taken from GE Healthcare CyDye Chemistry manual)

The dyes used in DIGE are specially designed to minimize the alteration of the intrinsic properties of the proteins. The fluorescent label adds only ~500 Da to the molecular weight (MW) of the protein, creating a minimal mass shift on the electrophoresis gel. The dye is limited in the labeling reaction so that only ~1-2 % of the lysine residues (Lys) are labeled. Since the average abundance of lysine in proteins are 3-5 %, the dyes are designed such that each protein that is labeled will only be singly labeled, thus minimally affect the system that is being studied.

The three CyDyes™ in conjunction with the Typhoon 9400 variable wavelength imager, allows for the comparison of two samples and one internal standard on the same gel. The pooled internal standard, which is a pool of all samples of the system that is being studied, is used to both match the protein spot pattern and to standardize quantitation. The deconvolution of these images is possible using the DeCyder software which corrects for variability between gels using the internal standard and then overlays the gel images.

The result of these methods is a differential spectrum between the two proteomes. The Ettan DIGE system allows for the accurate determination of the change in protein expression by as little as 10 % with greater than 95 % statistical confidence. The sensitivity of the CyDyes allow for the detection of as little as 125 pg of a single protein with a linear response of up to five orders of magnitude. A minimum of three replicates is used to determine the statistical relevance of the change. The Student's T-test values are determined based on the log of the ratio of change between the two systems. Proteins that are found to be significantly differentially expressed in the two systems can be excised from the gel and are identified using mass spectrometry (MS). These methods have improved reproducibility of results which has allowed for the development of databases which are invaluable when used in combination with MS to identify protein spots.

3.2 Procedures

3.2.1 Bacterial Strains and Growth Conditions

B. subtilis wild type strain 168 (trp C2) (Burkholder and Giles, 1947) was obtained from the Bacillus Genetic Stock Centre and the isogenic mutant strain, yfIMd, was obtained from Dr. Junichi Sekiguchi, Shinshu University. *B. cereus* wild type strain 14579 was obtained from the American type culture center. All strains and plasmids are listed in Table 3.1. Cells were grown in SG media without glucose supplementation (8 g Difco Bacto Nutrient Broth, 1 g KCl, 0.25 g MgSO₄·7 H₂O, pH to 7.0 with 1 M NaOH, autoclaved, cooled to 55°C, then add 1 mM CaCl₂, 0.01 mM MnCl₂·H₂O, 1 μM FeSO₄) (Leighton and Doi, 1971) at 200 rpm and 37°C. The mutant strains were maintained in media supplemented with 1 μg/mL erythromycin and 25 μg/mL lincomycin. Cells were harvested by centrifugation (8000xg for 10 min at 4°C) according to peak expression of the yfIM gene, determined by methods outlined below. Cell pellets were washed 3 times with ice-cold TE buffer (10 mM Tris, pH 7.5, 1 mM EDTA) prior to storage at -80°C.

Table 3.1– Bacterial strains and plasmids

Bacillus strains		
<i>Bacillus subtilis</i>		
Strain or plasmid	Relevant genotype	Source*
BGSC 1A1	<i>Bacillus subtilis</i> 168 (trp C2)	BGSC
yflMd	NOS homologue knockout	Dr. Junichi Sekiguchi, Shinshu University
<i>Bacillus cereus</i>		
ATCC 14579	<i>Bacillus cereus</i> 14579	ATCC
bcNOSKO	NOS homologue knockout	This study
<i>E. coli</i> strains		
	Molecular use	
DH5 α	Used for cloning	Invitrogen
XL1-Blues	Used for PCR mutagenesis	Stratagene
Plasmids		
pMUTIN 4	Insertional mutagenesis vector	Etienne Dervyn, INRA
pHCMC02	Gram-positive expression vector	BGSC
pHCMC04	Gram-positive expression vector	BGSC
pHT 304	<i>B. cereus</i> / <i>E. coli</i> shuttle vector	Didier Lereclus, INRA

*BGSC - Bacillus Genomic Stock Center

INRA - Institut National de la Recherche Agronomique

3.2.2 Knockout Vector

An 800bp fragment generated from *B. cereus* ATCC 14579 using PCR primers B.cereus14579NOSKOF0r1 and B.cereus14579NOSKORev was obtained using the following PCR protocol using PWO polymerase (Roche): Initial denaturation 3 min at 85°, 35 cycles of 1.5 min at 95°C, 2.5 min at 68°C, and 1 min at 72°C. The final extension was carried out at 72°C for 15 min. The fragment was cloned into the pMUTIN4 vector, using the HindIII and BamHI cut sites (ratio 10:1 molecules most effective for cloning). Plasmids were cloned in *E. coli* using media containing 100 μ g/mL ampicilin.

Table 3.2 – Primers used for cloning, mutagenesis, and knockout verification.

<i>B.cereus</i> NOS knockout oligos	
B.cereus14579NOSKOfor1	5'CGGGGGAATTCTTGTTATAAGGAGCTTCATAAAGAACAA 3'
B.cereus14579NOSKORev	5' CACCTGGATCCCAGCAGTATGGTGATCAACAATACTAACTC 3'
<i>B.cereus</i> PCR mutagenesis oligos	
Cysteine mutation bc14579 For	5'GGCATGGCGTAACAGTAATCGATTGATTGGAAGACTATTTTGGAG 3'
Cysteine mutation bc 14579 Rev	5'CTCCAAAATAGTCTTCCAATCAATCGATTACTGTTACGCCATGCC 3'
Knockout verification oligos	
bsNOSFor	5' GAAGATCTCATATGGAAATACTCTGGAACGAAGCGAAAGCG 3'
bcNOSFor	5' CGGGGAAGCTTATGAGTAAAACGAAACAATTAATAGAAGAA 3'

3.2.3 PCR Mutagenesis

The Quick change method (Wang and Malcolm, 1999) was used to mutate Cys to Leu. PCR mutagenesis was performed using cysteine mutation bc14579 For and Cysteine mutation bc 14579 Rev primers and the following protocol with Expand Longtemplate polymerase (Roche): Two half reactions were setup with one primer in each. The program included a Hot start, an initial denaturation of 5 min at 95°C, 5 cycles of 1 min at 95°C, 1 min at 65°C, and 10 min at 68°C. The program was paused, and the two half reactions were mixed. The program continued with 12 cycles of 1 min at 95°C, 1 min at 65°C, and 10 min at 68°C. The final extension was carried out at 68°C for 15 min. The reaction mixture was digested with DpnI for 2 hrs at 37°C and heat inactivated for 30 min at 80°C. The reaction mixture was transformed into XL1-Blues, mini-prepped and digested with ClaI prior to sending for confirmation by sequencing.

3.2.4 Gene Knockout

Electrocompetent cells were prepared by methods outlined previously (Silo-Suh, Lethbridge *et al.*, 1994). Briefly, 100 mL LB was inoculated with 1 mL of overnight culture and then grown to an OD₆₀₀ of 0.3 (~90 min). Cells were harvested at 3000xg for 5 mins at 4°C. Cells were resuspended in 12 mL EP buffer (0.5 mM K₂PO₄/KH₂PO₄, 0.5 mM MgCl₂, 272 mM Sucrose) and centrifuged as before. Cells were then resuspended in 200 µL EP Buffer and stored on ice until use. 40 µL cells were transformed with 0.1 to 1µg of DNA in 1mm cuvettes using 1.2 & 1.8 kV. Cells were recovered in 1.5 mL LB at 30°C for 5 hours and then 100 µL & 500 µL aliquots were plated on LB plates containing 1 µg/mL erythromycin and 25 µg/mL lincomycin. Plates were grown for 2 days at 30°C.

3.2.5 Verification of Knockouts

Colony PCR screening was performed using the primers used for cloning the gene and for knocking out the gene bsNOSFor and bsNOSRev for *B. subtilis* yfIMd, and bcNOSFor and bcNOSRev for *B. cereus* bcNOSKO, knockout strains respectively. Colony PCR (1 colony resuspended in 50-100 µL of sterile MQ) using Expand Long Template Polymerase (Roche) was performed in buffer 2 using a Touchdown program with annealing temperatures 68-58°C and an extension of 15 min.

3.2.6 Expression Test

The yfIMd strain includes a β-galactosidase (β-Gal) reporter gene under the control of the yfIM promoter. The β-Gal activity was monitored by methods outlined by Yoshida *et al.*

in 2000 modified to a microtitre plate assay. Cell pellets were resuspended in 250µL Buffer Z (60 mM Na₂HPO₄, 40 mM NaH₂PO₄, 10 mM KCl, 1mM MgSO₄, 1 mM DTT, 10 µg/mL DNase I, 100 µg/mL Lysozyme) and incubated at 37°C for 1 hr. *B. cereus* cells were sonicated 3 times for 10 seconds. Tubes were centrifuged at 13, 000 rpm at 4°C for 20 min. In a microtitre plate 20 µL of sample was mixed with 80 µL Buffer Z and incubated at 4°C for 10 min. 20 µL of 4 mg/mL o-nitrophenol-β-D-galactopyranoside was added to initiate the reaction. The reaction mixture was allowed to incubate for 1 hr at r.t. before stopping with the addition of 50 µL 1 M Na₂CO₃. The absorbance was read at 420 nm and a standard curve was generated using 0-120 nmol 2-nitrophenol (stock 10 mM in EtOH). β-Gal activity was determined in nmol of product/min (mg protein)⁻¹ (Atkinson, Wray *et al.*, 1990; Yoshida, Ishio *et al.*, 2000).

3.2.7 Griess Assay

The release of NO into the medium was measured using the Griess assay (Griess, 1864; Ignarro, Buga *et al.*, 1987) modified to a microtiter plate reader assay. Briefly, 100 µL of media was incubated with 100 µL of Griess reagents at 25°C for 10 min and then read at 540 and 630 nm using a SPECTRAMax PLUS 384 microtiter plate reader. The Griess reagents comprise a 1:1 ratio of freshly prepared 0.1 % naphthylethylenediamine (N5889, Sigma-Aldrich Canada Ltd., Oakville, ON) in MQ water and freshly prepared 1 % sulphaniamide (S9251, Sigma-Aldrich Canada Ltd., Oakville, ON) in 5 % phosphoric acid (Fisher Scientific, Nepean, ON). A standard curve was generated using 0-20 µM sodium nitrite.

3.2.8 Fluorometric Nitrite Assay

Nitrite was assayed using Nitrate/Nitrite Fluorometric Assay Kit from Cayman CHEMICALS (Ann Arbor, MI). Samples were withdrawn at peak bNOS expression, as determined by β -Gal activity, and incubated in the presence of 100 μ M L-Arg for 30 min at 37°C with shaking. 10-20 μ L of the supernatant were diluted to 100 μ L prior to the addition of the DAN reagent. The reaction was incubated at room temperature for 10 min before the quenching of the reaction with 20 μ L of NaOH stock from kit. The samples were read at λ_{ex} 360 nm λ_{em} 430 nm in a microtiter plate reader.

3.2.9 2D Electrophoresis Sample Preparation

Unless otherwise stated all reagents and 2D kits were obtained from GE Healthcare (Baie d'Urfé, QC, Canada). DNase I and RNase A were obtained from Roche. Tris, Urea, DTT and CHAPS were obtained from Bioshop Canada.

The pellet of 200 mL of cells was resuspended in 2 mL of Lysis buffer (30 mM Tris, pH 8.5, 8 M Urea, 2 M Thiourea, 4 % CHAPS) and sonicated on ice 3 times for 10 seconds. Cellular debris was pelleted at 48000xg for 30 min at 4°C. The protein concentration was assessed using the 2D-Quant Kit. The supernatant was treated with nuclease solution (0.1 mg/mL DNase I, 0.025 mg/mL RNase A, 5 mM MgCl₂). Samples were flash frozen and stored at -80°C. Protein samples were precipitated using the 2-D Clean-Up Kit from GE Healthcare and resuspended in rehydration buffer (8 M Urea, 2 M Thiourea, 1 % CHAPS, 0.5 % IPG Bufer 3-10, 2 mg/mL DTT, Bromophenol blue). Samples were loaded by

rehydration loading onto 24 cm 4-7 IPG strips (GE Healthcare) for 10-20 hrs at room temperature. Analytical and preparative gel strips were loaded with 150 µg and 800 µg of protein, respectively. Isoelectric focusing was performed using the Ettan IPGphor II (GE Healthcare) with the following program: 3 hrs at 300 V, 6 hr gradient to 1000 V, 3 hr gradient to 8000 V and 6 hrs at 8000 V. Paper wicks were replaced after 6hrs during the IEF run to reduce salt build up at electrodes. After successive equilibration with SDS equilibration buffer (50 mM Tris-HCl, pH 8.8, 6 M Urea, 30 % glycerol, 2 % SDS, Bromophenol blue) containing 1 % DTT and 2.5 % Iodoacetamide, for 15 min each, IEF strips were placed on the top of a SDS-PAGE gel and overlaid with a 1 % agarose solution and bromophenol blue in SDS running buffer (25 mM Tris-HCl, 192 mM glycine, 0.1 % SDS). The lower buffer chamber was filled with 1X running buffer and the upper buffer chamber was filled with 2X running buffer. Separation in the second dimension was performed using a 15 X 25 cm 12.5 % homogeneous polyacrylamide gels at 5 W per gel for 1 hr and 17 W per gel for 3 hrs at 4°C. All solutions, including acrylamide solutions, were filtered through 0.2 µm filter prior to use.

Analytical gel samples were labeled with CyDyes™ 2, 3 and 5 according to the manufacturer's instructions (GE Healthcare). Briefly, 50 µg precipitated protein samples were rehydrated in 10 µL of lysis buffer and incubated with 200 pmol of the appropriate CyDye™ in anhydrous DMF for 30 min. The reaction was quenched with 10 mM lysine prior to addition of rehydration buffer. All procedures involving the CyDyes™ were performed at 4°C in the dark.

Each condition was run in triplicate alternating labeling with Cy3TM and Cy5TM, to account for dye effects. Each gel contained a Cy2TM labeled pooled internal standard. Gel images were generated using the Typhoon 9400 Variable Mode Imager scanning at 100 micron resolution at the appropriate wavelengths for each fluorophore: Cy2TM λ_{ex} 488 nm λ_{em} 520 nm, Cy3TM λ_{ex} 532 nm λ_{em} 580 nm, and Cy5TM λ_{ex} 633 nm λ_{em} 670 nm. The gel images were cropped in Image Quant v2.0 and analyzed using DeCyder v2.0 2-D Differential data analysis software.

Preparative gels were stained using Blue silver colloidal Coomassie G-250 stain by methods outlined by (Candiano, Bruschi *et al.*, 2004). Briefly, stain was prepared to a final concentration of 0.12 % dye, 10 % ammonium sulfate, 10 % phosphoric acid, and 20 % methanol. The stain was prepared by sequentially adding all ingredients except methanol. The solution was brought to 80 % final volume with water and mixed thoroughly prior to addition of methanol. The colloidal suspension was stored in a dark bottle and resuspended prior to each use. The solution is stable at room temperature for > 6 months but can only be reused 2-3 times. Gels were stained overnight and destained in water until the background was adequately destained.

Trouble shooting analytical gels were stained with Deep Purple Total Protein stain (GE Healthcare). Gels were fixed with fixation solution (7.5 % acetic acid in 10 % methanol) overnight. Gels were washed with wash solution (35 mM NaHCO₃, 300 mM Na₂CO₃). A 1:200 dilution of Deep Purple stain in water was then added and incubated in the dark with gentle shaking for 1 hr. Gels were washed twice in 7.5 % acetic acid for 30

min each and then imaged on the Typhoon 9400 scanner λ_{ex} 532 nm λ_{em} 610 BF scanned at 100 microns resolution.

3.2.10 IPTG-Induction of Downstream Elements

In order to distinguish between the effects due to the expression of the target gene and the downstream elements, the downstream elements were put under the control of an IPTG-inducible promoter. A comparison was made between the change in expression between the wild type and the knockout with and without IPTG-induction. Those protein spots that significantly changed ($p \leq 0.01$, $|\text{Fold change}| \geq 2$) in both the one gene knockout and the knockout with induction of the downstream elements were picked by hand and prepared for MS analysis.

3.2.11 MS Sample Prep and Analysis

Protein spots were picked by hand, destained and digested with sequencing grade trypsin (Promega, Madison, WI, USA) by methods adapted from (Wilm, Shevchenko *et al.*, 1996). Gel slices were cut into cubic millimeter fragments and washed 3 times with ultra pure water (5 min each). The gel fragments were then washed 3 times with 50 mM ammonium bicarbonate in 50% acetonitrile (10 min each). The gel fragments were dehydrated by washing with 100 % acetonitrile for 5 min prior to incubation with 10 mM DTT in 100 mM ammonium bicarbonate for 30 min at 50°C to reduce the proteins bound in the gel. All liquid was removed and the gel fragments were again dehydrated with 100 % acetonitrile prior to incubation with 55 mM iodoacetamide in 100 mM ammonium

bicarbonate in the dark for 30 min at room temperature to alkylate the proteins. The gel fragments were washed with 100 mM ammonium bicarbonate for 15 min and then dehydrated once more with 100 % acetonitrile. Proteins were then digested with 80 ng Trypsin in the presence of 100 mM ammonium bicarbonate for 16-18 hrs at 37°C.

The peptides were then extracted and purified using C₁₈ zip-tips according to manufacturer's instructions (Millipore, Bedford, MA, USA). Briefly, the peptides were extracted 3 times from the gel fragments using 5 % formic acid in 50 % acetonitrile with sonication for 5 min. Sample volume was reduced to 10 µL prior to purification with C₁₈ zip-tips. Zip-tips were equilibrated with 50 % acetonitrile (3 times) and then 0.1 % formic acid (3 times). The peptides were bound to the tip by repeated pipetting (minimum 10 times), washed twice with 0.1 % formic acid and then eluted by repeated pipetting (minimum 10 times) using 50 % acetonitrile. Formic acid was added to the samples to a final concentration of 0.2 % v/v formic acid. All plastics were washed with Acetonitrile followed by ultrapure water (HPLC grade water from Fisher) to avoid PEG contamination of peptide samples.

MS/MS data was collected using Micromass Q-TOF Ultima Global mass spectrometer in +ESI mode. Protein identification was performed using MASCOT MS/MS ion search (Matrix Sciences) to probe the MSDB protein database using raw MS/MS data.

PMF data was collected using Reflex III MALDI-TOF 337 nm Nitrogen laser (Bruker Daltonics). Protein identification was performed using ProFound PMF search (PROWL) to probe NCBI database using peptide mass maps.

3.3 Results

3.3.1 Knockout Characterization

3.3.1.1 Knockout Verification

The yfIMd knockout strain (yfIMd) was verified using the primers used to clone the bsNOS gene. These primers amplified a fragment of approximately 10 kbp. The transformation efficiency is so low in *B. cereus* the size of the internal fragment required to ensure that the homologous recombination event occurs is much larger, 800 bp instead of 200 bp in *B. subtilis*. Since the bcNOS gene is only 1000 bp there is concern that the partially expressed bcNOS gene may still be active. To rectify this, the Cys residue that is one of the heme ligands, was mutated to a Leu in the knockout vector prior to integration into the chromosome. Replacement of this ligand in mNOS enzymes results in a loss of the heme and catalytic activity (Chen, Tsai *et al.*, 1994; Richards, Claque *et al.*, 1996; Cubberley, Alderton *et al.*, 1997). The bcNOSKO was verified using analogous methods for the yfIM knockout with similar results of 11 kbp fragment.

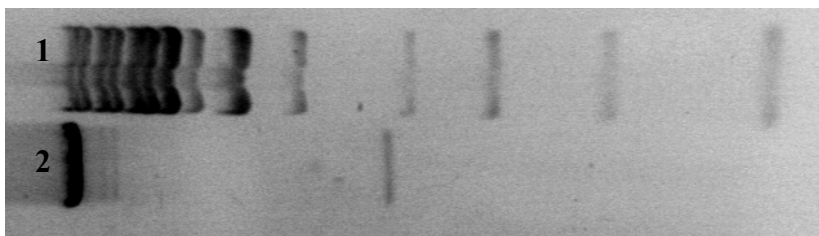


Figure 3.3 – PCR verification of NOS knockout.

Lane 1 Gene Ruler 1 kbp DNA Ladder and lane 2 shows the amplification of a faint band at 1 kbp and an intense band at 10 kbp.

Proteomic studies in *B. subtilis* were begun while the *B. cereus* NOS knockout was being generated. Efforts continued in the *B. subtilis* systems due to extensive databases that are available for this organism. The abundance of peptide mass fingerprint (PMF) data bases allows for simplification of MS analysis. These databases alleviate the need to sequence peptide fragments, allowing for the identification of proteins in a more expedited manner. The specifics of these identification methods will be discussed in more detail in section 3.3.4.

3.3.1.2 Evaluation of bNOS expression in liquid media

The ideal growth media for the induction of bsNOS was initially determined using the β -Gal reporter gene. Since expression of this gene had been shown to be stress-induced, various media were initially tested. *S. aureus* NOS has been previously shown to be induced in nutrient broth containing 0.125 % methanol (Choi, Seo *et al.*, 1998). The yfIMd knockout was shown to express the β -Gal reporter gene only in sporulative media (<http://bacillus.genome.jp/>). The knockout yfIMd strain cultures were grown in SG, MM, DSM, MeOH, starvation (long growth in SG) media and β -Gal activity was determined for aliquots withdrawn hourly. The most significant activity was found in the cultures grown in SG and MeOH media. Since there was no significant difference found between these two conditions, subsequent growth trials were done using SG media.

Growth trials were performed to determine when this gene was expressed and if NO was released into the media. Both wild type and knockout cultures were grown and analyzed for β -Gal activity and for the presence of nitrite using the Griess assay. The expression of β -

Gal activity, as evidenced in Figure 3.4, indicates that this gene is expressed in late exponential phase and early lag phase.

Other growth trials, including those posted on the web by the Sekiguchi group (<http://bacillus.genome.jp/>), also show expression in late exponential phase and early lag phase. Samples for 2D-DIGE analysis were withdrawn late in log phase, as indicated by the arrow in Figure 3.4, to ensure yfIM was being expressed at the time of analysis.

Although the expression of the gene was evidenced by the β -Gal activity, no changes in nitrite levels were detectable in the supernatant using the Griess assay. Figure 3.4 also shows the nitrite levels in the supernatant measured using the Griess assay. There is no consistent trend exhibited between the knockout and the wild type system. This could be indicative that the NO produced is used in biosynthesis and not released into the media or that the amount released is lower than the detection limits for this assay.

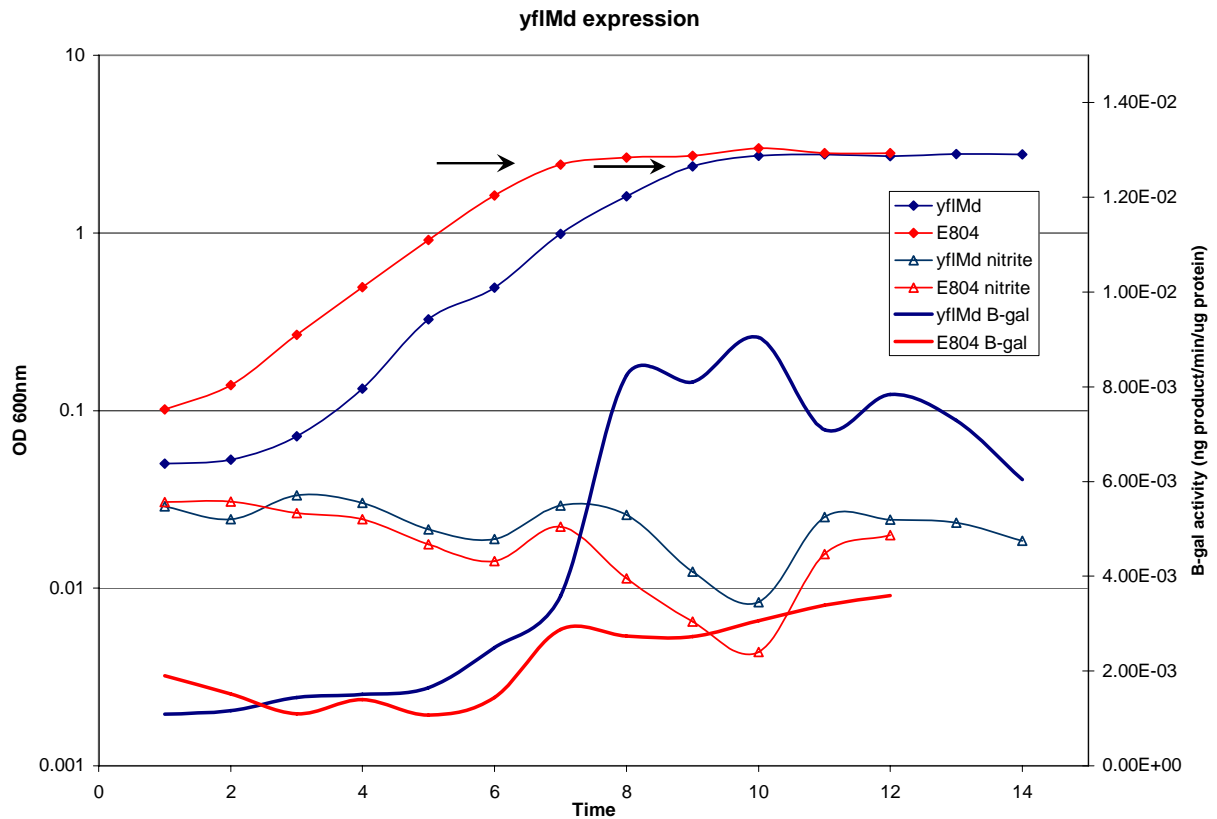


Figure 3.4— Expression of yfiM during cell growth cycle exhibited by the β-galactosidase reporter gene activity.

Arrows indicate the time of extraction of samples for 2D gel electrophoresis based on maximal activity of the reporter gene (β-Gal). Nitrite levels, as determined by the Griess assay, are shown on the primary axis and are given in μM.

A more sensitive method for detection of nitrite was used to investigate the later proposal. A Fluorometric assay kit from Cayman CHEMICALS was used to detect differential nitrite levels between the knockout and wild type strains of *B. cereus*. The assay showed slightly higher nitrite levels in the wild type strain compared to those found in the knockout, 3.31 μM and 2.66μM, respectively. The relative difference between the wild type and the knockout are comparable to that shown previously by Gusarov and Nudler in 2005. Gusarov and Nudler compared the nitrite levels in the media of *B. subtilis* wild type and

bsNOS knockout strains and found the nitrite levels to be 20 % higher in the culture of the wild type strain.

A comparative analysis is required to differentiate the increase in nitrite levels due to the low levels of nitrite and the presence of other nitrite sources. Other sources of nitrite are found in the growth media and within the cell. The most common source of nitrite in many denitrifying bacteria is Nitrate reductase and has been shown to be present in *B. subtilis*. Although bacteria are able to produce NO via denitrifying pathways, the production of NO is tightly regulated with NO reductase to maintain the steady state of NO at nanomolar levels (Cutruzzola, 1999). Since nitrate reductase is repressed under conditions of nitrogen and oxygen excess (Ogawa, Akagawa *et al.*, 1995; Nakano, Hoffmann *et al.*, 1998), little nitrite should be derived from these pathways. Since the nitrite levels are so low a comparative analysis gives confidence to the change in nitrite levels being real.

3.3.2 2D Gel Trouble Shooting

Initial 2D gel runs followed the recommendations of the manufacturer. Amersham Biosciences recommended a rehydration buffer of 8 M Urea, 2 % CHAPS, 2 % IPG Buffer for maximal protein loads. These recommended parameters resulted in very little protein entering the 2D gel. The little protein that was able to enter the gel formed large horizontal streaks.

Several parameters were varied in attempts to introduce more protein into the 2D gel. Different methods of sample loading, increased amount of protein loaded and increased amount of detergent, all resulted in similarly streaky gels. Precipitation of the protein sample

prior to loading and increasing the IEF time from the recommend 25 kVhr to 80 kVhr, not only increased the amount of protein entering the gel but also increased the amount of streaks.

Next the rehydration buffer was changed to a buffer used by Buttner et al. 2001 in a study of *B. subtilis*. The rehydration buffer, containing 8 M urea, 2 M thiourea, 1% CHAPS, 20 mM DTT, 0.5 % IPG buffer, significantly improved the solubility of the samples.

Decreasing the amount of protein loaded and changing the IEF program to ramp up the voltage slowly while decreasing the total volt hours resulted in more distinct spots on the 2D gel, shown in Figure 3.5, however there was still significant streaking evident throughout.

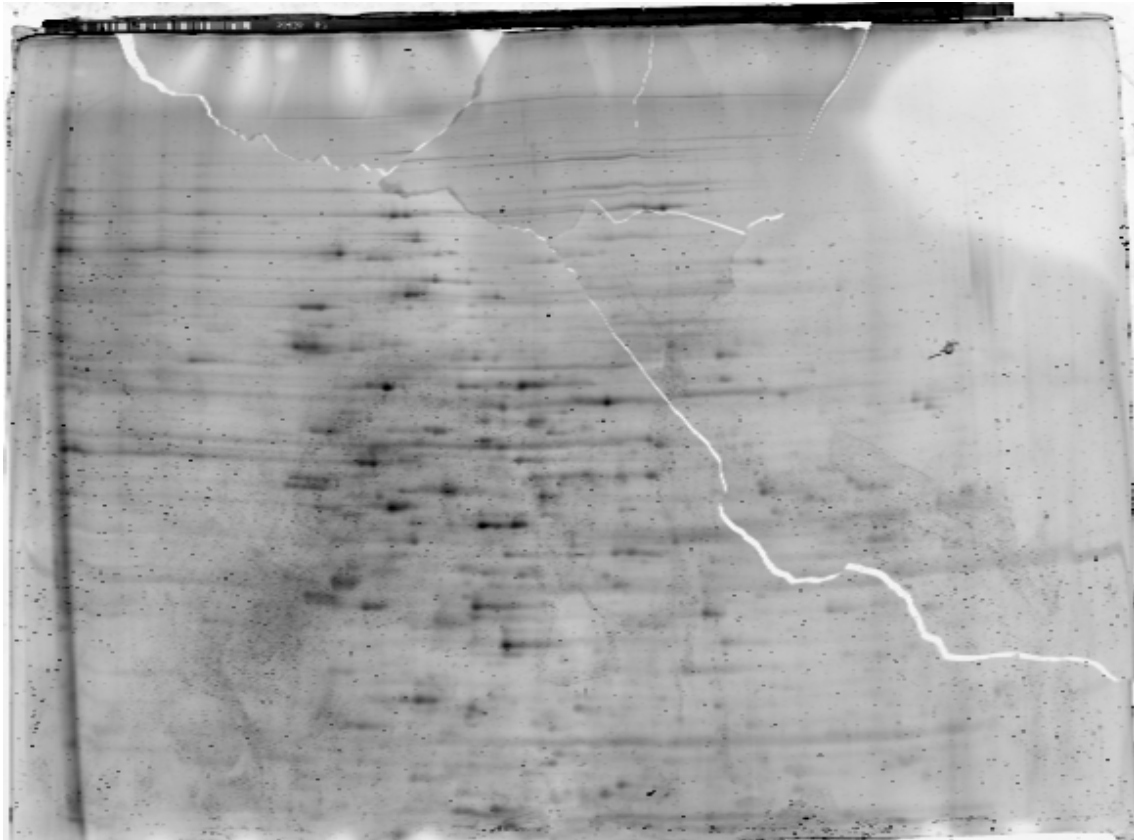


Figure 3.5– Analytical trouble shooting 2D gel image

B.subtilis 168 sample, 200 μg of total protein separated on pH 4-7 IPG and 10 % SDS PAGE. Gel stained with Deep Purple total protein stain.

To further remove the salt from the sample and reduce salt build up at the electrodes, the cells were washed three times in TE buffer before harvesting and the paper wicks were replaced after 6 hours of IEF. The samples were also treated with a nuclease solution to reduce interference of DNA and RNA in the IEF. These measures improved the system to such an extent that well resolved proteins were obtained. Figure 3.6 shows the results of a preparative gel of a protein sample from a wild type culture that has been induced with IPTG containing 600 μg of total protein.

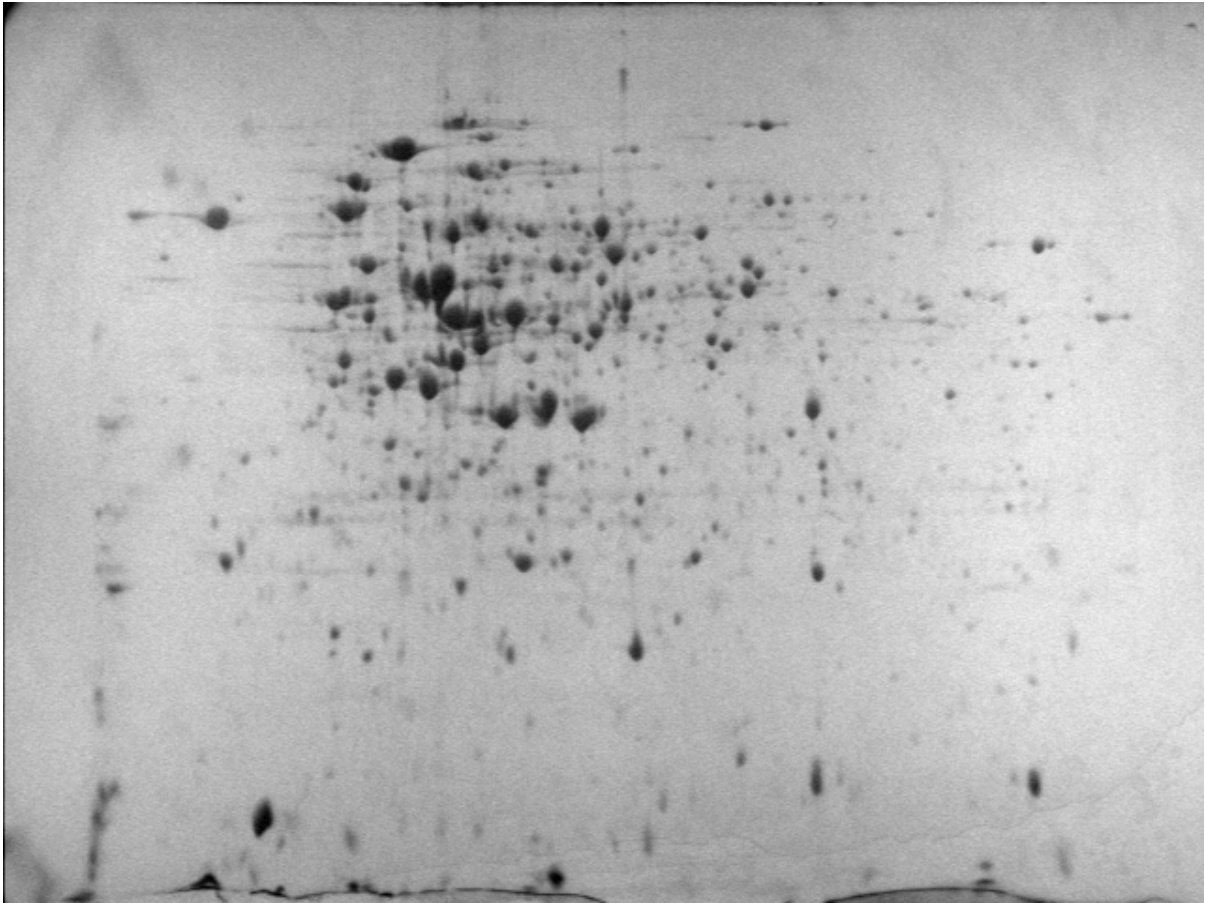


Figure 3.6 – 2D Preparative gel of wild type sample with IPTG.
B. subtilis 168 sample, 600 μ g of total protein separated on pH 4-7 IPG and 12.5 % SDS PAGE. Gel stained with Blue silver stain.

For more examples of trouble shooting 2D gel parameters the reader is referred to Section 3.4.1 and a discussion forum on the GE Healthcare website. This is an invaluable tool for 2D gel users.

3.3.3 Differential in-gel Electrophoresis Analysis

Ettan DIGE system was used to determine the change in protein expression due to the bNOS gene in *B. subtilis*. The Ettan DIGE system allows for the multiplexing of multiple

samples on each gel, allowing for an internal standard to be run on each gel. The differential analysis of two samples can then be accomplished in an accurate quantitative manner by comparative analysis to this standard. Over 1500 spots were detected and matched in the differential analysis compared to the 4100 open reading frames found in the *B. subtilis* genome, showing a good representation of the *B. subtilis* proteome.

The DeCyder software allows for easy analysis of large proteomic data sets. After the initial scan of the gels using the Typhoon variable wavelength scanner, the gel images are cropped and input into the DeCyder software. The software detects and quantitates the protein spots on all of the gel images. The software contains Differential In-gel Analysis (DIA) algorithms that detect spots based on matched images from the same gel. This DIA not only ensures that all spots are represented in all the gels but also allows for quantitative comparison of spot volumes to the internal standard.

The software also contains a Biological Variation Analysis (BVA) module which allows for inter-gel matching of protein spots and quantitative comparison of protein spots from multiple gels. Once the gel images are input into the BVA, the gel that contains the greatest number of identified spots is chosen as the master gel and all other gel images are matched to the master. At this point it is important for the user to ensure that the spot patterns have been matched appropriately. Although the software automatically adapts the gel images to match the pattern of the master gel, spot matching can be adapted manually if needed. Figure 3.7 is a screen view of the Match table of the BVA module, showing the vectors that were used to skew each gel to fit the master gel.



Figure 3.7– Screen capture of the match table of the DeCyder 2D gel analysis software.
 (Refer to text for details)

Once spot matching is complete, statistical analysis can be performed on the differential protein abundance levels between the systems. Directing the software to compare to systems yields a Protein table in the BVA module that lists abundance ratios with statistical significance values attached. The protein table, shown in Figure 3.8, allows the user to select proteins of interest and toggle between matched spots to ensure proper matching. The lower left hand corner displays a 3D image of the spot pattern, showing relative protein abundances as peaks. The upper right hand corner shows a graph of relative

abundance for a selected spot across all of the matched gels. This gives the user an indication of the biological variance within the systems.

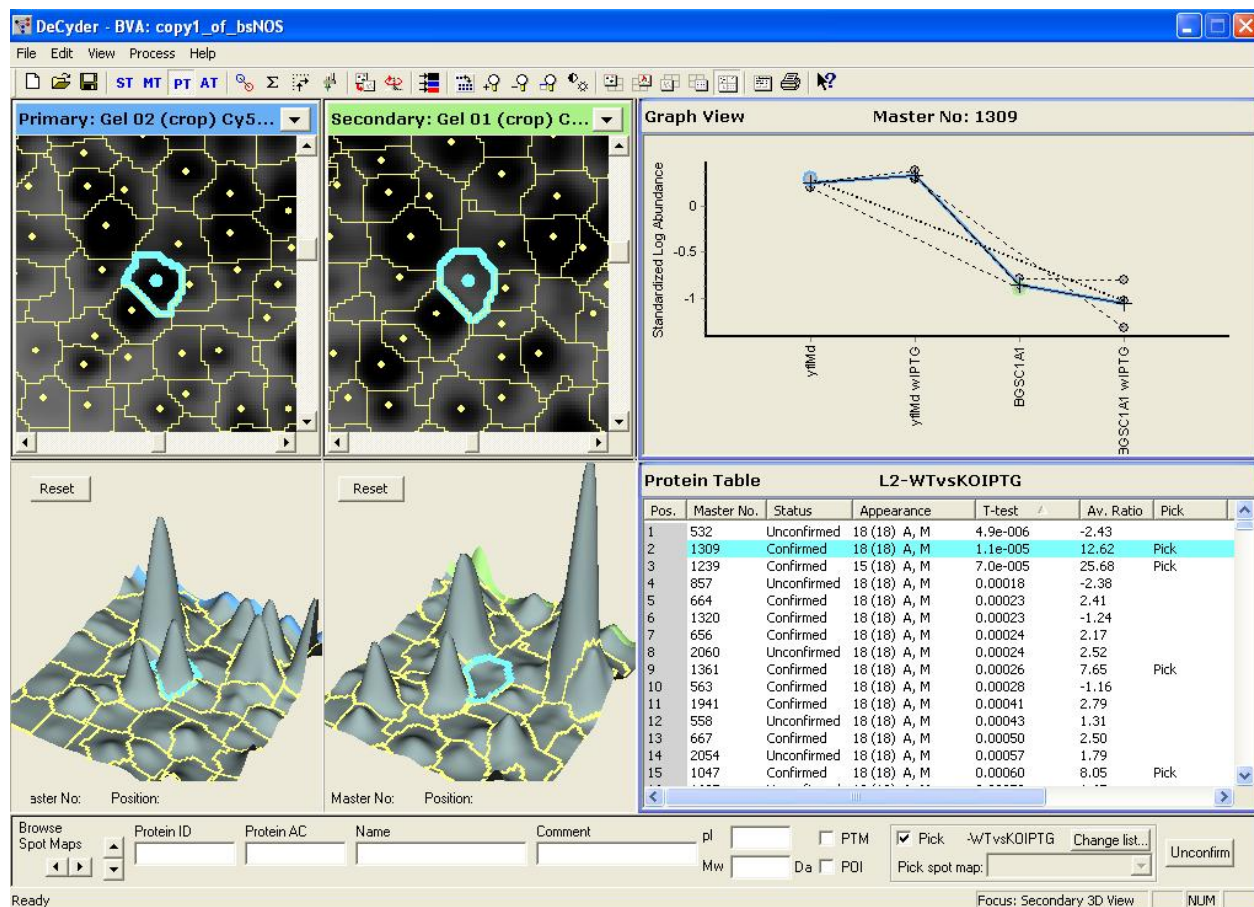


Figure 3.8– Screen capture of the Protein table view of the DeCyder 2D gel analysis software. (Refer to text for details)

The system under analysis compares the wild type *B. subtilis* strain 168 to the yfIMd bNOS knockout strain. Since the downstream elements in the knockout strain were placed under the control of an IPTG-inducible promoter, IPTG was added to make the system a one gene knockout. To account for the change within the system due to IPTG induction, 4 systems were compared in the DIGE analysis: (i) knockout, (ii) wild type, (iii) knockout with

IPTG, and (iv) wild type with IPTG. Triplicates of each system and a pooled internal standard were run together in a 6 gel DIGE experiment. A minimum of 6 gels are required in this system for determination of statistical significance of the change in protein expression between the 4 systems. Data analysis compared the change in expression between the knockout and the wild type, with and without IPTG, independently. Statistical analysis 1 compared the wild type and the knockout systems both without IPTG, showing the effects due to the knockout of the promoter of the gene of interest. Statistical analysis 2 compared the wild type system and the knockout system with IPTG, showing the effects due to the knockout of the gene of interest plus any effects due to the presence of IPTG. A comparison between these two sets of data allows for the exclusion of the changes due to the downstream element.

The proteins that changed significantly between the two systems were determined to be due solely to the effects of the gene of interest. Figure 3.9 shows a visual representation of the data obtained from one gel, comparing the wild type and the knockout system. Proteins that are up-regulated in the knockout are shown in green, proteins that are down-regulated are shown in red, and proteins that do not change in expression are shown in yellow.

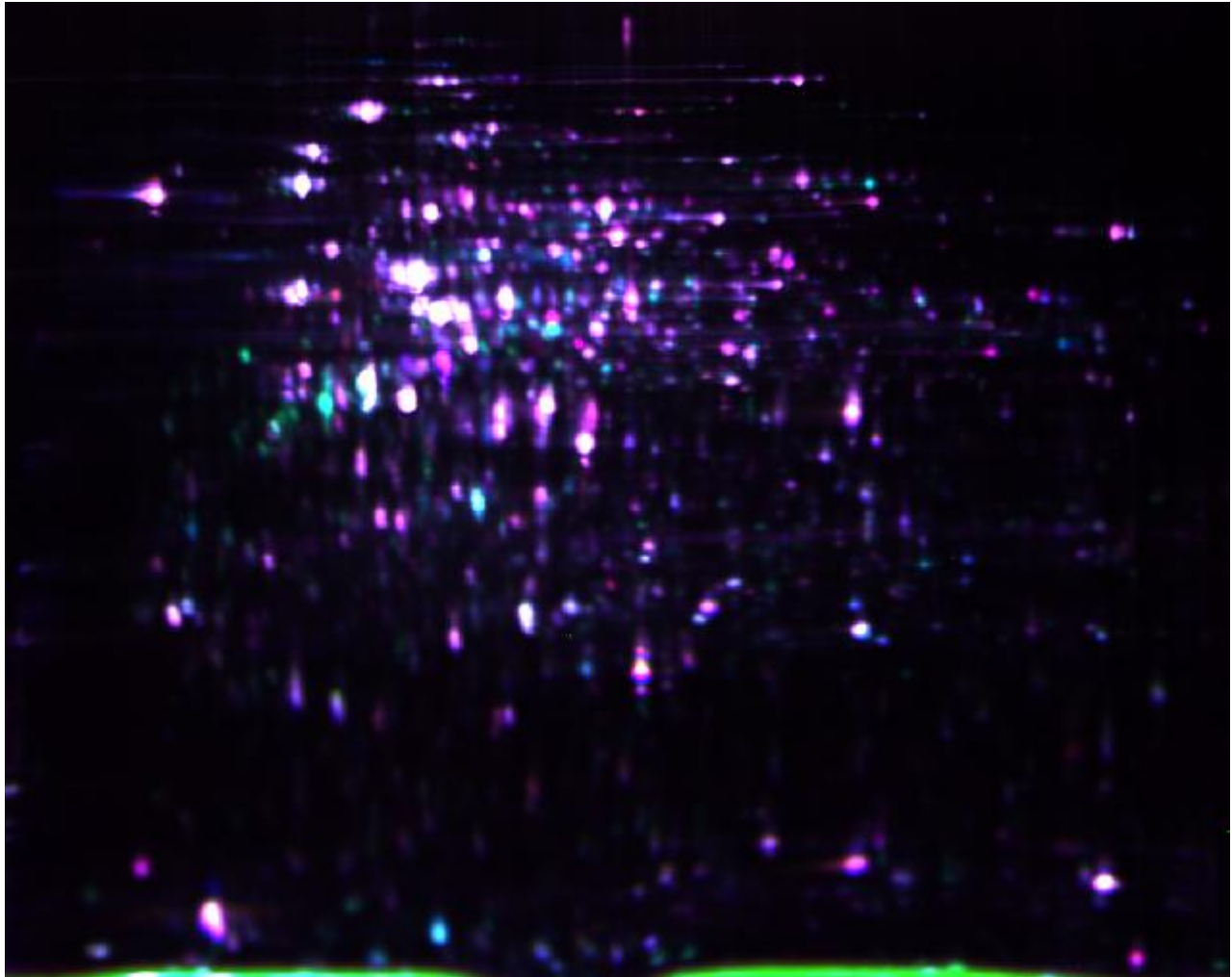


Figure 3.9– Tricolour comparison of the change in protein expression due to bNOS knockout in *Bacillus subtilis*.

Proteins that are coloured red are down-regulated in the knockout. Proteins that are coloured green are up-regulated in the knockout. The expression of those proteins that are coloured yellowish/white do not change between the two systems. The Differential in Gel Electrophoresis analysis was performed on bacterial cultures harvested at the end of log phase. *B. subtilis* 168 sample, 150 µg of total protein separated on pH 4-7 IPG and 12.5 % SDS PAGE. Samples, pooled internal standard, yfIMd and wild type, were labeled with 200 pmol of Cy2, Cy3 and Cy5, respectively.

3.3.4 Protein Identification

Proteins can be identified using two different techniques: via PMF or via MS/MS ion search. Both methods rely on the trypsin digestion of a protein spot picked from a gel but

use different methods for determination of protein identity. The trypsin digestion fractionates the protein in a characteristic pattern known as a PMF. PMF identification is based off a discrete section of the MS spectra of the trypsin digested sample searched against databases that have been generated for known proteins. This method can use MALDI MS which is less sensitive to contaminants, more sensitive for protein detection and amenable to a high through-put work-flow. MS/MS ion searching relies on the generation of MS/MS data for the digested peptides. It is the MS/MS of these peptides that is used in the database search to determine the protein identity. The MS/MS of the peptide essentially allows for the sequencing of the peptide by comparison of the mass difference in the fragmentation to the mass of individual amino acid residues. This method is invaluable to identify proteins from organisms whose genomes have not been sequenced, as a BLAST search can be performed to the peptide sequence to find homologues and tentatively assign function to these proteins. This technique is however significantly more time consuming, more expensive and more sensitive to contaminants.

The current statistical requirements for significance, $p \leq 0.05$ and a $|\text{fold change}| \geq 2$, yield a pick list of 73 proteins shown in Appendix A Table 1. Of these 73 proteins 16 proteins have been identified, among which 2 were identical. Table 3.3 shows the results of the proteins identified thus far.

Table 3.3– Proteins determined to change significantly due to the knockout of bNOS in *B. subtilis*.

Essential ^a	Fold change ^b	% sequence coverage ^c	BSORFID ^d	Protein Identity	Pathway ^e
no	-4.0	34	dhaS	Aldehyde dehydrogenase	Glycolysis / Gluconeogenesis Ascorbate and aldarate metabolism Fatty acid metabolism Bile acid biosynthesis Valine, leucine and isoleucine degradation Lysine degradation Arginine and proline metabolism Histidine metabolism Tryptophan metabolism beta-Alanine metabolism Glycerolipid metabolism Pyruvate metabolism Propanoate metabolism Butanoate metabolism Limonene and pinene degradation
no	-13.2	34	acoB	acetoin dehydrogenase E1 component (TPP-dependent beta subunit)	Glycolysis / Gluconeogenesis Valine, leucine and isoleucine biosynthesis Pyruvate metabolism Butanoate metabolism
no	-16.4	47	citH	Malate dehydrogenase	Citrate cycle (TCA cycle) Pyruvate metabolism Glyoxylate and dicarboxylate metabolism Carbon fixation Reductive carboxylate cycle (CO2 fixation)
no	-8.4	56	sdhA	succinate dehydrogenase flavoprotein subunit	Citrate cycle (TCA cycle) Oxidative phosphorylation Benzoate degradation via CoA ligation Butanoate metabolism Reductive carboxylate cycle (CO2 fixation)
no	-2.8	51	etfB	Electron transfer flavoprotein beta subunit	Membrane bioenergetics (electron transport chain and ATP synthase)

Table 3.3 – continued

Essential	Fold change	% Sequence coverage	BSORFID	Identification	Pathway
no	-2.1	35	ArgC	N-acetyl-glutamate-gamma-semialdehyde dehydrogenase	Urea cycle and metabolism of amino groups
no	-5.7	6	carB	Carbamoyl-phosphate synthase large chain carbamoyl-phosphate transferase-arginine (subunit B)	Pyrimidine metabolism Glutamate metabolism
no	2.5	61	rocG	Glutamate Dehydrogenase	Glutamate metabolism Nitrogen metabolism
no	2.2	53	serA	Phosphoglycerate dehydrogenase	Glycine, serine and threonine metabolism
no	2.6	39	AroA	3-deoxy-7-phosphoheptulonate synthase	Phenylalanine, tyrosine and tryptophan biosynthesis
no	-10.8	22	hutU	urocanate hydratase	Histidine metabolism
no	-5.2	38	HutG	Formimino glutamase	Histidine metabolism
no	3.3	25	mtnK	methylthioribose kinase	Metabolism of amino acids and related molecules
no	15.3	26	mtnS	Translational initiation factor eIF-2B alpha chain homolog	Metabolism of amino acids and related molecules
yes	-6.2	138	nusA	transcription termination factor	Transcription elongation protein nusA.

^aA systematic study generating knockouts to every gene in the *B. subtilis* genome has been used to determine the requirement for specific proteins for cell viability. This information can be accessed at <http://bacillus.genome.jp/>

^bFold change - the relative abundance change of the proteins spots from a comparison of wild type vs. knockout. Fold changes less than 1 are represented as the negative inverse ratio.

^cPercentage of amino acid sequenced used to identify the protein by mass spectrometry.

^dBSORFID – gene name as given on <http://bacillus.genome.jp/>

^ePathways identified given by KEGG that utilize the protein identified by mass spectrometry

We can be confident that those changes exhibited in the knockout system are not due to polar effects because the closest locus that has been identified to be affected is more than 42 kbp downstream. Not only are there more than 10 terminator sequences between these two loci, but none of the other genes located between these loci have been identified to be influenced by the knockout. Thus the changes identified in this system are not due to polar effects introduced by the integration of the knockout vector into the chromosomal DNA.

Two protein spots that were determined to change significantly due to the bNOS knockout were identified to be aldehyde dehydrogenase when analyzed by MS. Both protein spots were down regulated in the knockout by 4.0 and 3.7 fold, respectively. These proteins pictured in Figure 3.10, appear to have the same MW but distinct pI values, as illustrated by the differential migration in the horizontal direction. Raggiaschi *et al.* in 2006 used a 2D-DIGE system to look at the migrational due to phosphorylation of protein samples. They determined phosphorylation patterns in rat cortical neurons by analysis of a normal and phosphatase treated sample. They showed 2D-DIGE to be a useful tool for identifying PTM via a shift in pI values. Further studies using Western Blot analysis are required to confirm the presence of PTM within this system.

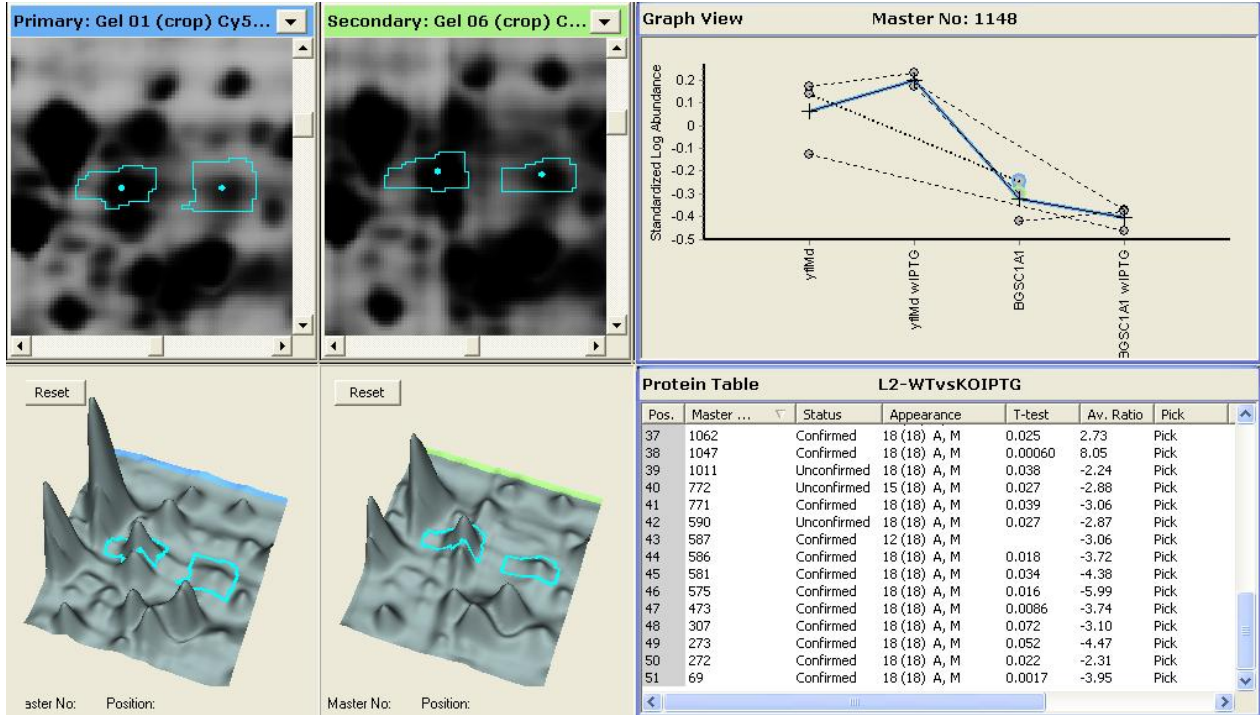


Figure 3.10– Comparison of two protein spots which resulted in the same MS identification. The molecular weight of the two proteins appears to be maintained while there is a distinct shift in the pIs, illustrated by the horizontal shift in migration pattern.

The identification of more proteins on this pick list will continue. The challenge of identifying these proteins has been primarily due to their low abundance. In order to identify more proteins from the pick list shown in Table 1 in Appendix A, protein spots from multiple gels will need to be pooled to have enough protein to identify the spot by mass spectrometry. Furthermore, although the parameters used for statistical significance are relatively normal, many proteomics studies pick a lower cut-off for significance of fold change. Lowering the change cut-off to 50% (fold change of 1.5) could allow the inclusion of proteins with higher abundance that would have a more significant impact on the cell, shown in Appendix A Table 2. This cut-off is still significantly higher than that suggested by the manufacturer, GE

Healthcare, as they claim their product is capable of quantitatively determining a 10 % change between two systems with greater than 95 % statistical confidence.

3.4 Discussion

3.4.1 2D Electrophoresis

Proteomic analysis using 2D gel electrophoresis requires reproducibly distinct separation of proteins within a sample. It is ideal to keep sample preparation to a minimum for reproducibility reasons but it cannot be stressed enough that every step in sample preparation is critical.

2D gel electrophoresis is often plagued with streaking problems. Procedures are often unique to the sample being run and require sample specific trouble shooting. Streaking issues are particularly evident in samples obtained from microorganisms with complex cell walls (Herbert, Grinyer *et al.*, 2006). There are two types of streaking in 2D gels, horizontal and vertical streaking, both with unique causes and solutions. An example of both horizontal and vertical streaking is pictured in Figure 3.11.

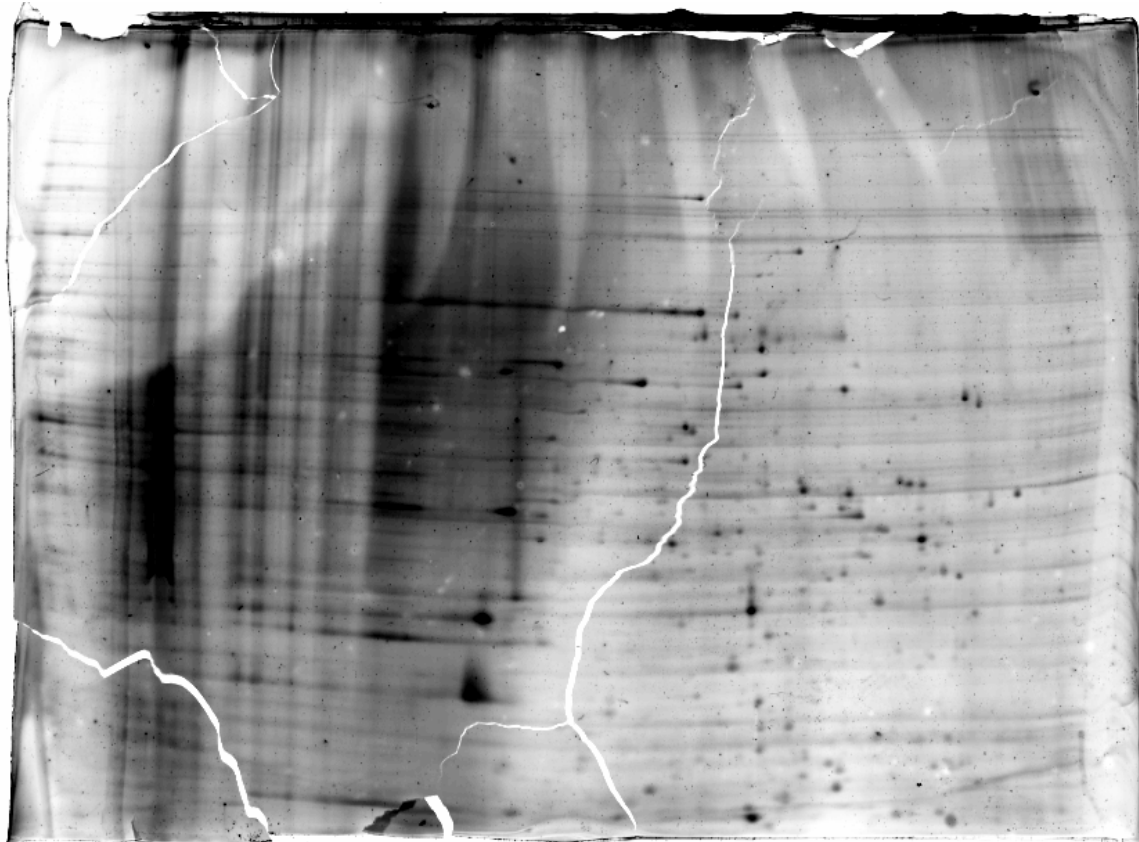


Figure 3.11– 2D gel of *B. subtilis* pH 4-7 demonstrating both horizontal and vertical streaking. *B. subtilis* 168 sample, 200 µg of total protein separated on pH 4-7 IPG and 10 % SDS PAGE. Gel stained with Deep Purple total protein stain.

Horizontal streaking has two primary causes: (i) increased conductivity of the sample and (ii) precipitation of proteins during IEF. Increased conductivity in the sample can result from the presence of salts, polysaccharides, nucleic acids and macromolecules (Vandahl, Christiansen *et al.*, 2002). The presence of salts is perhaps the most common cause of horizontal streaking. Salts can be removed by washing the cells prior to lysis, precipitation of the sample, and by switching of the paper wicks during prolonged IEF times (Gorg, Obermaier *et al.*, 2000). Polysaccharides and nucleic acids can interact with the carrier ampholytes and the proteins, interfering with IEF conditions. These contaminants can be

removed by precipitation and nuclease treatment of the samples. Macromolecules can actually increase the viscosity of the solution to such an extent that the pores in the IEF gel can be obstructed (Gorg, Weiss *et al.*, 2004). Macromolecules can be removed from the sample by ultracentrifugation or by using protein extraction methods that do not solubilize these contaminants (Herbert, Grinyer *et al.*, 2006).

The other main cause of horizontal streaking is poor solubilization of the sample. Poor solubilization of protein can be a result of high protein loads and differing detergent requirements for specific samples. Increased protein loads are particularly desirable for preparative gels when excising protein spots for identification by MS. Samples are often hard to resuspend after precipitation and are at their limit of solubility. Thus proteins often precipitate out of solution during sample loading. To rectify this problem, gel strips can be rehydrated with rehydration buffer and samples can be loaded with a low current (Sabouchi-Schutt, Astrom *et al.*, 2000). Alternatively, protein fractionation allows for the splitting of different proteins into different samples prior to sample application (Lilley, Razzaq *et al.*, 2001). Fractionation allows for an increased amount of total protein to be loaded, which is distributed over multiple gels. Another cause of poor solubility of the sample could be a result of the inadequacy of the detergent. Currently CHAPS is the most commonly used detergent due to background smearing associated with detergents such as Triton X-100 and Nonidet P-40 (Gorg, Obermaier *et al.*, 2000). However, some samples, particularly those with high amounts of lipids, may have different detergent requirements. There are many alternative detergents, the only requirement is that the detergent be zwitterionic or nonionic

so it does not interfere with IEF. Which detergent is best for a given sample can still not be predicted (Vandahl, Christiansen *et al.*, 2002).

Horizontal streaking can also result from depletion of reducing agent or carbamylation within the protein sample. Reducing agents such as DTT or DTE are essential to disruption of disulfide bonds. Since the pKa of DTT and DTE are 8.5 and 9, respectively, streaking can result due to depletion of reducing agent at the basic end of the IEF strip (Gorg, Weiss *et al.*, 2004). This can be rectified by either placing DTT soaked paper wicks at the cathodic end of the IEF gel, to provide a constant in flux of reducing agent, or by stabilizing the disulfides as mixed disulfides using hydroxyethyl-disulfide (HED) reagent (Gorg, Weiss *et al.*, 2004) (Destreak, GE Healthcare). Carbamylation results from the interaction of isocyanate, a degradative product of urea, and primary amines and can affect the migration of proteins during IEF (Gorg, Weiss *et al.*, 2004). Protein carbamylation can be avoided by ensure the sample is never heated above 37°C.

One final cause of horizontal streaking results from an inadequate IEF program. Protocols suggest a range of 35-120 kVhr for IEF programs (Sabounchi-Schutt, Astrom *et al.*, 2000). The real challenge arises in determination of an adequate IEF program due to the fact that overfocusing and underfocusing both result in streaking (Gorg, Obermaier *et al.*, 2000). Thus trouble shooting this parameter can be frustrating and time consuming.

Vertical streaking is normally caused by inefficient transfer of protein from the IEF strip to the SDS gel. There are several causes of this phenomenon. This could be caused by poor equilibration in the SDS equilibration buffer. Making up fresh buffer and increasing

equilibration time may rectify this problem. A poor transfer of protein into the 2D dimension may also be solved by decreasing the voltage during the transfer (the first hour of electrophoresis in the second dimension). The most common cause of streaking in the vertical direction is caused by depletion of SDS in the upper buffer chamber. This could be caused by leaking in the upper buffer chamber. It is recommended that the seals are checked and that fresh buffers are made.

3.4.2 Perspectives on the Role of NOS in Bacteria

A broader scope is required before definitively outlining the role of NOS in bacterial systems. Until more proteins can be identified we can use the proteins that have been identified to speculate on a plausible role.

The proteins identified thus far can be grouped into three categories: (i) glucose metabolism, (ii) amino acid metabolism, (iii) nitrogen metabolism, and (iv) transcriptional factors.

3.4.2.1 Glucose Metabolism and Alternative Carbon Source Utilization

Several of the proteins identified thus far suggest a down-regulation of glucose metabolism in the knockout. This is exhibited by the down-regulation of enzymes involved in glycolysis, the TCA cycle, and membrane bioenergetics. This down regulation of glucose metabolism is exhibited in Figure 3.12. Two enzymes are believed to show the down-regulation of glycolysis: (i) aldehyde dehydrogenase (dhaS) and (ii) phosphoglycerate dehydrogenase (serA). dhaS is involved in the conversion of pyruvate to acetyl-CoA

(Kanehisa, Goto *et al.*, 2006) is down-regulated 4.0 fold in the yfIMd strain. Whereas, serA is involved in the conversion of 3-P-Glycerate to serine (Kanehisa, Goto *et al.*, 2006). This enzyme is up-regulated in the yfIMd strain showing the alternate usage of this glycolytic intermediate for amino acid biosynthesis.

The down-regulation of the TCA cycle is shown in the repression of malate dehydrogenase (citH) and succinate dehydrogenase (sdhA) by 16.4 and 8.4 fold, respectively. These two proteins catalyze the conversion of malate to oxaloacetate (Jin, De Jesus-Berrios *et al.*, 1996) and succinate to fumarate (Melin, Magnusson *et al.*, 1987) in the TCA cycle. Glutamate dehydrogenase (rocG) catalyzes the conversion of 2-oxoglutarate to glutamate (Belitsky and Sonenshein, 1998). This process is up-regulated in the yfIMd strain showing the alternate usage of TCA cycle intermediates.

The repression of proteins involved in the electron transport chain is exhibited in the down-regulation of the electron transfer flavoprotein (etfB) and as well as sdhA by 2.8 and 8.4 fold, respectively. Both these enzymes are involved in oxidative phosphorylation (Kanehisa, Goto *et al.*, 2006). sdhA interacts directly with ubiquinone donating electrons into the electron transport chain. etfB accepts electron from other dehydrogenases and transfers them to the respiratory chain via ETF-ubiquinone oxidoreductase.

It is interesting to note that the down-regulation of alternative carbon source utilization is also evident in the knockout strain. This is exhibited by the down-regulation of acetoin dehydrogenase (acoB) by 13.2 fold in the knockout strain

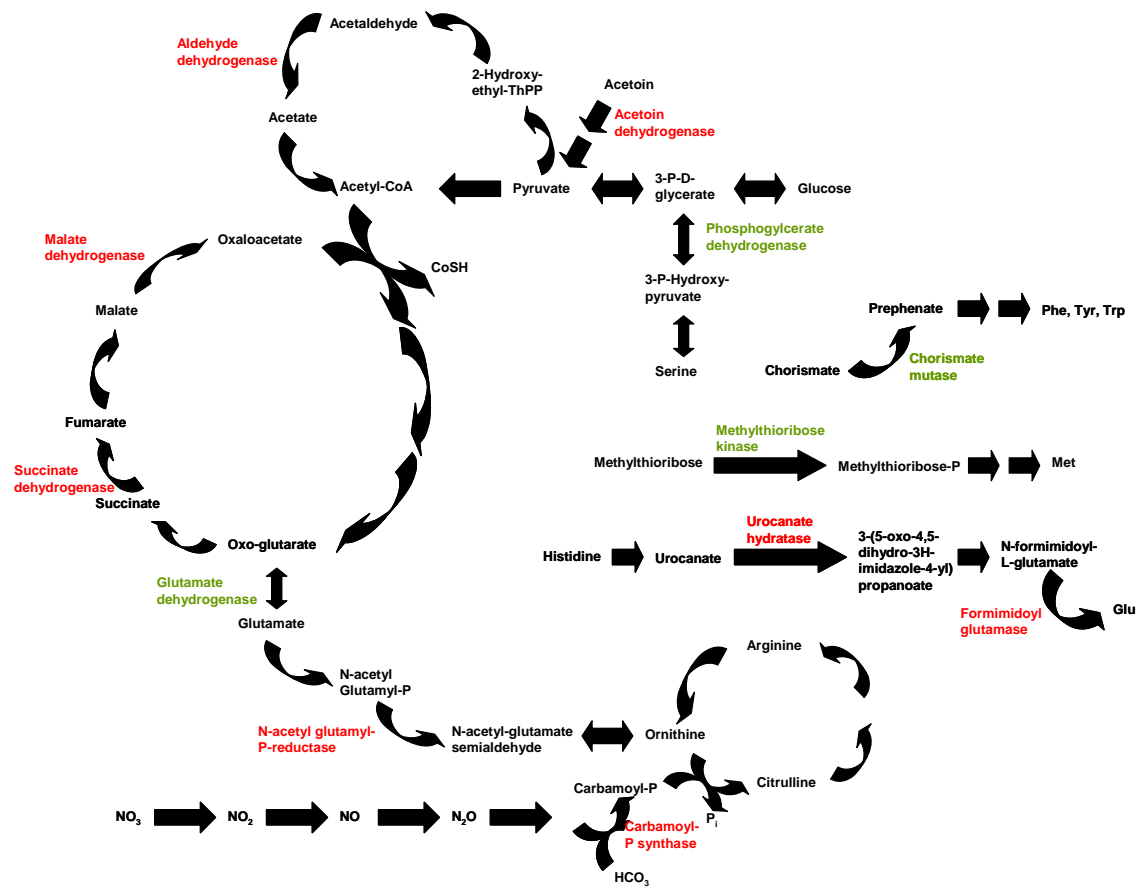


Figure 3.12 – Summary of metabolic pathways affected by the yfIMd knockout.

Those proteins shown in red are down-regulated in the knockout strain. Those proteins shown in green are up-regulated in the knockout strain.

One interesting aspect of the change in protein expression between these two systems is the down regulation of glucose metabolism and alternative carbon source utilization. Samples were taken at the end of the cultures growth cycle at which point glucose is depleted in the media and the culture generally shifts to using alternative carbons sources, such as acetoin (Butt, Bernhardt *et al.*, 2000). Both glucose and acetoin utilization appear to be down-regulated.

Since the yfIMd strain appears to affect similar genes as those in glucose starvation but with differing effects, it appears that the yfIM gene may somehow work to modulate the glucose starvation response.

3.4.2.2 Amino Acid Metabolism

Amino acid metabolism is also significantly repressed in the yfIMd strain. The yfIMd strain exhibits both a down-regulation of amino acid catabolism and an up-regulation of amino acid biosynthesis is exhibited in Figure 3.12. The down-regulation of histidine catabolism (Kimhi and Magasanik, 1970) is shown by the repression of both urocanate hydratase (hutU) and formimino glutamase (hutG) by 10.8 and 5.2 fold, respectively. The up-regulation of amino acid biosynthesis is shown by the induction of chorismate mutase (aroA), methylthioribose kinase (mtnK), and serA by 2.6, 3.3, and 2.2, fold respectively. These enzymes contribute to pathways that are involved in biosynthesis of Phe, Tyr, Trp, Met, Gly, Ser, and Thr (Sekowska, Mulard *et al.*, 2001; Kanehisa, Goto *et al.*, 2006).

The up-regulation of rocG may also contribute to amino acid biosynthesis as the product glutamate is the main amino donor for transamination reactions.

The significance of up-regulation of amino acid biosynthesis is unknown, however the glucose starvation response also showed a repression of catabolic pathways (Butt, Bernhardt *et al.*, 2000). This may indicate that yfIM is involved in regulation of the glucose starvation response or in the regulation of the synthesis of specific amino acids required for an adaptive response to the lack of *NO in the knockout.

3.4.2.3 Nitrogen Metabolism

Nitrogen metabolism is also significantly affected in the yfIMd strain. The down-regulation of nitrogen metabolism is shown in the repression of N-acetyl-glutamate-semialdehyde dehydrogenase (argC) and Carbamoyl-phosphate synthase (carB) by 2.1 and 5.7 fold, respectively (Kanehisa, Goto *et al.*, 2006). These enzymes are involved in reactions that feed into the urea cycle. Interestingly, these reactions are allosterically inhibited by L-Arg. If the physiological substrate for bNOS is actually L-Arg, a build-up of L-Arg in the knockout would result in the repression of this process.

This study shows that the expression of the yfIM gene significantly affects nitrogen metabolism. The yfIMd knockout results in the down-regulation of the urea cycle and amino acid catabolism and the up-regulation of amino acid biosynthesis. As mentioned in section 3.3.1.2, there are other contributing factors to nitrogen metabolism, however, the use of a comparative system should keep these factors consistent between the wild type and the knockout.

Perhaps the down-regulation of nitrogen metabolism is a result of the decreased production of ^1NO and nitrogen containing metabolic intermediates fueled into the urea cycle for bioprocessing. Alternatively the up-regulation of amino acid biosynthesis in the knockout could be a result of the absence of ^1NO as a regulative factor. The apparent up-regulation of amino acid biosynthesis relative to the wild type, could be a result of the down-regulation of amino acid biosynthesis in the wild type. This would be a reasonable assumption since the down-regulation of protein synthesis has been observed in cells at the end of log phase in a proteomic study by Bernhardt *et al.* in 2006.

3.4.2.4 Transcriptional Factors

Two of the proteins identified thus far are transcriptional factors. nusA is a general transcriptional termination factor (Ingham, Dennis *et al.*, 1999), which has been shown to be essential in *B. subtilis* (Ingham, Dennis *et al.*, 1999). nusA is down-regulated in the yfIMd strain. mtnS is a transcriptional factor that is part of the S box Regulon which controls sulfur metabolism and biosynthesis of Cys and Met (Grundy and Henkin, 1998). mtnS is up-regulated in the knockout strain and may thus further contribute to the up-regulation of amino acid biosynthesis.

The down-regulation of the transcriptional factor nusA could add weight to the potential role of ^1NO as a regulative factor. The apparent down-regulation of this general transcriptional terminator in the knockout relative to the wild type could be a result of the up-regulation of this transcriptional factor in the wild type. This could result in increased protein synthesis supporting the above hypothesis.

3.4.2.5 Quorum-Sensing Precursor Generation

Another interesting difference between the two systems is seen in the induction of two genes from the S box regulon, *mtnS* and *mtnK*. These genes are implicated in the recycling of methylthioribose (MTR), a precursor for quorum-sensing molecules (Sekowska, Mulard *et al.*, 2001). Again these genes are normally induced under glucose starvation but are induced to an even greater extent in the *yflMd* strain. It appears that *yflM* may regulate the cell's response to glucose starvation. *B. subtilis* uses a LuxS quorum-sensing signaling molecule to regulate spore morphogenesis, biofilm formation, and swarming. MTR is fed into the pathway producing LuxS (Singh, Shi *et al.*, 2006). Quorum-sensing acts in a cell density dependent manner and would be found at high cell densities like those found at the end of the log phase. Perhaps this apparent up-regulation of quorum-sensing in the knockout relative to the wild type could be a result of the down-regulation in the wild type. Again these effects could be a result of the *yflM* gene or its product NO contributing to a regulative mechanism at the end of log phase. Although the use of NO donors would allow the distinction between these two effects, the reintroduction of NO in this unregulated manner would be more appropriate to a phenotypic analysis.

Exactly how these interactions occur is still unknown. These studies do not allow us to differentiate between whether the *bsNOS* gene or its NO product is the influencing factor. Neither do they allow for the differentiation between whether the change in expression is due

to a change in *de novo* protein synthesis or protein degradation. Future studies are required to determine the specifics of these interactions.

3.5 Future Directions

Although the present analysis has shed some light on the role of NOS in bacterial systems, the identification of more proteins is required for a better understanding. The identification of more proteins requires the pooling of protein spots of low abundance proteins from multiple gels and the picking of spots of higher abundance whose relative change may be less but whose change in expression would have a more significant impact on the cell. The identification of more proteins will either confirm or disprove hypotheses presented in this paper.

This study was conducted at the point in the growth curve that showed the highest expression of the bsNOS gene as determined by β -Gal expression tests. Since it has been suggested that the role of this gene may partially be regulative, it would be interesting to compare the change in protein expression between these two systems during different stages of growth. Similar methods have been used with *B. subtilis* and *S. aureus* to determine the change in protein expression due to the sigB regulon (Butt, Bernhardt *et al.*, 2000) and the hemB gene (Kohler, von Eiff *et al.*, 2003), respectively.

In conjunction with the proteomic study at different stages of growth, it would be beneficial to look at the change in translation due to this genetic knockout. The changes in translational activity more accurately shows regulation as it focuses on those proteins that are being actively expressed. Studies using L-[³⁵S]methionine incorporation would be used to

monitor translation of proteins. Samples would be analyzed using the 2D gel methods outlined in this thesis to separate proteins. Visualization of gels would be preformed using autoradiography and is compatible with DeCyder software used for the current study. Previous work used similar methods to monitor the change in the translation, in response to environmental stress (Mostertz, Scharf *et al.*, 2004).

3.5.1 [•]NO-mediated Posttranslational Modification

Another extension of this project would be to look at the change in [•]NO-mediated PTM within the two systems. Since the bNOS enzyme is suspected to produce [•]NO it has been suggested that it may play a role in [•]NO-mediated PTM. There are four possible kinds of [•]NO-mediated PTMs: (i) binding to metal centers, (ii) nitrosylation of thiol and amine groups, (iii) nitration of tyrosine, tryptophan, amine, carboxylic acid, and phenylalanine groups, and (iv) oxidation of thiols and tyrosine (Green, Wagner *et al.*, 1982). The significance of a change in PTM within a proteome is becoming increasingly evident with the analysis of the proteomes of cells in diseased states. Thus the change in protein nitration and nitrosylation will also be investigated using a similar system to the DIGE analysis. Several mechanisms have been previously used to explore the PTM within proteomes. Most PTM work has been done on phosphorylation and methylation and the principles from these studies will be used to design the current system (Raggiaschi, Lorenzetto *et al.*, 2006). PTM analysis can be accomplished using two different approaches: immunoprecipitation/Biotin-switch method or Western Blot analysis.

The immunoprecipitation or Biotin-switch method allows removal of [•]NO-mediated PTM proteins from the system. The change in the S-nitrosyl/nitrotyrosyl-proteome can then be assessed either by looking at the absence of these proteins in the overall proteome or in the appearance of proteins in the isolated fraction. The S-nitroso proteome of *Mycobacterium tuberculosis* was analyzed using the Biotin-switch method (Rhee, Erdjument-Bromage *et al.*, 2005). This method selectively replaces the NO moieties of target cysteine nitrosothiols with a disulfide linkage to a biotin derivative allowing the isolation of these proteins by streptavidin affinity chromatography. These methods produced 29 S-nitroso proteins that were separated by 1D gel electrophoresis and identified by MS. To get an overall picture of the [•]NO-mediated PTM proteome both the S-nitroso and Nitrotyrosyl-proteomes would be isolated. Coupling the biotin-switch methods with immunoprecipitation method followed by electrophoresis would allow for analysis of the NO-mediated PTM of the proteome. Difficulties in this method could result from loss of proteins during processing. Conditions needed for maximal solubility within the proteome may also not be able to be maintained during biotin-switch and immunoprecipitation procedures, resulting in an incomplete view of the proteome.

Another method used, and perhaps the most obvious one, for PTM analysis is Western Blot analysis of 2D gels. This may seem like the simplest method however, this would be least reproducible method. Differences due to gel to gel variability combined with variations introduced during the transfer process will amplify any differences between runs. Antibodies to nitrotyrosine have been used to analyze the distribution of tyrosine nitration in

rat tissue extracts (Aulak, Miyagi *et al.*, 2001) and human pituitary tissue extracts (Zhan and Desiderio, 2004). These methods produced 40 and 16 nitrotyrosine-immunoreactive proteins, respectively. The Biotin-switch method can be adapted for immunoblotting purposes and thus the \cdot NO-mediated PTM proteome can be analyzed on the same membrane. Comparison of two systems may lead to difficulties due to gel to gel variability, however reproducible 2D-Western analysis could be accomplished using a fluorescently labeled 2^o antibody and the DeCyder software, analogous to the 2D-DIGE analysis. Further analysis of the change in protein expression over time between the two systems would not only shed light on the role of bNOS enzymes but could also add to the evidence that \cdot NO-mediated PTM contributes to intracellular signaling.

Appendix A

Table 1 - Pick list for proteins $p \leq 0.05$ and $|\text{fold change}| \geq 2$

Pos.	Master No. ^a	Appearance ^b	WT vs KO ^c		WTvsKOIPTG ^d	
			T-test	Fold change ^e	T-test	Fold change ^e
1	69	18 (18) A, M	0.0017	-3.95	0.0019	-4.91
2	87	18 (18) A, M	0.0098	-2.63	0.003	-2.86
3	272	18 (18) A, M	0.022	-2.31	0.0022	-3.32
4	281	18 (18) A, M	0.0027	-2.11	0.00083	-2.12
5	473	18 (18) A, M	0.0086	-3.74	0.0005	-3.89
6	509	18 (18) A, M	0.0077	-2.21	0.00094	-2.7
7	522	18 (18) A, M	0.014	-2.05	0.00097	-2.5
8	532	18 (18) A, M	4.90E-06	-2.43	0.0076	-2.48
9	575	18 (18) A, M	0.016	-5.99	0.0024	-10.84
10	581	18 (18) A, M	0.034	-4.38	0.00054	-8.4
11	586	18 (18) A, M	0.018	-3.72	0.0012	-6.6
12	590	18 (18) A, M	0.027	-2.87	0.0072	-3.51
13	595	18 (18) A, M	0.0091	-2.7	0.011	-5.32
14	664	18 (18) A, M	0.00023	2.41	0.0065	2.21
15	667	18 (18) A, M	0.0005	2.5	0.0038	2.25
16	771	18 (18) A, M	0.039	-3.06	0.0093	-3.98
17	772	15 (18) A, M	0.027	-2.88	0.037	-3.72
18	924	18 (18) A, M	0.0058	-2.45	0.0053	-2.26
19	985	12 (18) A, M	0.0071	-3.01	0.006	-3.65
20	1011	18 (18) A, M	0.038	-2.24	0.0031	-3.14
21	1047	18 (18) A, M	0.0006	8.05	0.00028	9.48
22	1058	18 (18) A, M	0.05	2.12	0.037	2.51
23	1062	18 (18) A, M	0.025	2.73	0.0037	3.39
24	1070	18 (18) A, M	0.014	-3.17	0.0045	-3.57
25	1137	18 (18) A, M	0.042	5.2	0.049	4.68
26	1148	18 (18) A, M	0.023	2.52	0.00059	3.29
27	1175	18 (18) A, M	0.0049	-4.99	0.0022	-6.17
28	1239	15 (18) A, M	7.00E-05	25.68	4.50E-05	31.99
29	1309	18 (18) A, M	1.10E-05	12.62	8.80E-06	15.31
30	1310	15 (18) A, M	0.028	2.74	0.04	2.72
31	1337	15 (18) A, M	0.015	2.46	0.0041	2.7
32	1339	15 (18) A, M	0.03	-2.64	0.045	-2
33	1343	15 (18) A, M	0.045	-6.26	0.00099	-10.45
34	1357	18 (18) A, M	0.0097	2.5	0.00034	2.57
35	1358	15 (18) A, M	0.041	3.58	0.02	3.43
36	1361	18 (18) A, M	0.00026	7.65	8.70E-06	7.57
37	1410	18 (18) A, M	0.00096	4.87	0.002	3.81

38	1412	18 (18) A, M	0.0027	-3.56	0.038	-2.09
39	1417	15 (18) A, M	0.0013	3.53	0.0014	3.67
40	1441	15 (18) A, M	0.023	-3.08	0.0045	-4.05
41	1458	12 (18) A, M	0.00037	3.69	0.00092	3.27
42	1467	18 (18) A, M	0.046	-3.58	0.024	-4.15
43	1526	18 (18) A, M	0.024	-5.33	0.0032	-8.39
44	1531	15 (18) A, M	0.042	-3.3	0.0075	-4.18
45	1573	18 (18) A, M	0.0059	-3.9	0.0028	-5.22
46	1581	18 (18) A, M	0.04	-2.33	0.00081	-2.34
47	1586	18 (18) A, M	0.037	-2.35	0.011	-2.84
48	1601	15 (18) A, M	0.012	-2.05	0.041	-2.14
49	1765	15 (18) A, M	0.034	-7.86	0.0067	-11.39
50	1808	15 (18) A, M	0.0055	-2.94	0.022	-2.88
51	1815	18 (18) A, M	0.024	-2.58	0.0058	-2.47
52	1852	15 (18) A, M	0.014	-2.63	0.0037	-3.29
53	1869	18 (18) A, M	0.037	-2.18	0.003	-2.46
54	1875	18 (18) A, M	0.019	3.57	0.022	3.42
55	1941	18 (18) A, M	0.00041	2.79	0.00033	2.65
56	1989	18 (18) A, M	0.027	2.46	0.047	2.15
57	1995	15 (18) A, M	0.027	3.19	0.02	3.81
58	2017	15 (18) A, M	0.0063	-6.28	0.0073	-5.64
59	2050	18 (18) A, M	0.02	2.4	0.01	2.25
60	2112	15 (18) A, M	0.0044	-5.5	0.0018	-6.08
61	2114	18 (18) A, M	0.02	3.08	0.0063	2.6
62	2206	18 (18) A, M	0.011	-2.54	0.0078	-2.7
63	2277	15 (18) A, M	0.019	-2.24	0.014	-2.63
64	2316	15 (18) A, M	0.04	-2.96	0.003	-3.55
65	2349	18 (18) A, M	0.004	-3.04	0.0085	-2.46
66	2356	18 (18) A, M	0.041	-3.56	0.0059	-3.92
67	2432	15 (18) A, M	0.0035	-3.92	0.0026	-5.08
68	2532	15 (18) A, M	0.041	-2.62	0.013	-2.74
69	2555	18 (18) A, M	0.047	-2.33	0.0026	-3.24
70	2575	18 (18) A, M	0.011	-6.26	0.0036	-6.41
71	2589	18 (18) A, M	0.0089	-2.21	0.022	-2.14
72	2601	18 (18) A, M	0.05	2.52	0.04	2.62
73	2643	12 (18) A, M	0.017	-4.8	0.047	-3.23

^aMaster No. – based on protein number assigned in DeCyder software

^bAppearance shows the number of gels that contain the specific protein spot

^cWT vs KO – Statistical analysis comparing wild type to knockout

^dWT vs KOIPTG - Statistical analysis comparing wild type to knockout with IPTG

^e Fold change - the relative abundance change of the proteins spots from a comparison of wild type vs. knockout. Fold changes less than 1 are represented as the negative inverse ratio.

Table 2 - Pick list for proteins $p \leq 0.01$ and $|\text{fold change}| \geq 1.5$

Pos.	Master No. ^a	Appearance ^b	WT vs KO ^c		WT vs KOIPTG ^d	
			T-test	Fold change ^e	T-test	Fold change ^e
1	69	18 (18) A, M	0.0017	-3.95	0.0019	-4.91
2	87	18 (18) A, M	0.0098	-2.63	0.003	-2.86
3	281	18 (18) A, M	0.0027	-2.11	0.00083	-2.12
4	473	18 (18) A, M	0.0086	-3.74	0.0005	-3.89
5	509	18 (18) A, M	0.0077	-2.21	0.00094	-2.7
6	532	18 (18) A, M	4.90E-06	-2.43	0.0076	-2.48
7	656	18 (18) A, M	0.00024	2.17	0.004	1.87
8	664	18 (18) A, M	0.00023	2.41	0.0065	2.21
9	667	18 (18) A, M	0.0005	2.5	0.0038	2.25
10	779	18 (18) A, M	0.00082	1.77	0.0015	1.97
11	807	18 (18) A, M	0.0086	1.84	0.0036	1.86
12	924	18 (18) A, M	0.0058	-2.45	0.0053	-2.26
13	947	18 (18) A, M	0.00074	1.73	0.0076	1.59
14	985	18 (18) A, M	0.0071	-3.01	0.006	-3.65
15	1047	18 (18) A, M	0.0006	8.05	0.00028	9.48
16	1066	18 (18) A, M	0.0074	1.66	0.0032	1.58
17	1151	18 (18) A, M	0.009	1.89	0.00083	2.09
18	1157	18 (18) A, M	0.0024	1.89	0.00062	2.05
19	1175	18 (18) A, M	0.0049	-4.99	0.0022	-6.17
20	1239	15 (18) A, M	7.00E-05	25.68	4.50E-05	31.99
21	1309	18 (18) A, M	1.10E-05	12.62	8.80E-06	15.31
22	1357	18 (18) A, M	0.0097	2.5	0.00034	2.57
23	1361	18 (18) A, M	0.00026	7.65	8.70E-06	7.57
24	1410	18 (18) A, M	0.00096	4.87	0.002	3.81
25	1417	15 (18) A, M	0.0013	3.53	0.0014	3.67
26	1422	18 (18) A, M	0.0078	1.71	0.0052	1.79
27	1573	18 (18) A, M	0.0059	-3.9	0.0028	-5.22
28	1627	18 (18) A, M	0.00072	1.67	0.0017	1.68
29	1878	18 (18) A, M	0.003	1.96	0.0011	2.25
30	1941	18 (18) A, M	0.00041	2.79	0.00033	2.65
31	2017	15 (18) A, M	0.0063	-6.28	0.0073	-5.64
32	2054	18 (18) A, M	0.00057	1.79	0.00029	1.75
33	2057	18 (18) A, M	0.0027	1.52	0.0042	1.72
34	2060	18 (18) A, M	0.00024	2.52	0.0013	1.92
35	2112	15 (18) A, M	0.0044	-5.5	0.0018	-6.08
36	2334	18 (18) A, M	0.0064	1.54	0.00012	1.57
37	2349	18 (18) A, M	0.004	-3.04	0.0085	-2.46
38	2417	18 (18) A, M	0.0046	1.9	0.0016	1.84
39	2432	15 (18) A, M	0.0035	-3.92	0.0026	-5.08
40	2613	18 (18) A, M	0.0035	1.68	0.0044	1.61

^{a,b,c,d}Please refer to description in previous table.

Bibliography

- Adak, S., K. S. Aulak and D. J. Stuehr (2002). "Direct evidence for nitric oxide production by a nitric-oxide synthase-like protein from *Bacillus subtilis*." *J. Biol. Chem.* **277**(18): 16167-71.
- Adak, S., A. M. Bilwes, K. Panda, D. Hosfield, K. S. Aulak, J. F. McDonald, J. A. Tainer, E. D. Getzoff, B. R. Crane and D. J. Stuehr (2002). "Cloning, expression, and characterization of a nitric oxide synthase protein from *Deinococcus radiodurans*." *Proc. Natl. Acad. Sci. U S A* **99**(1): 107-12.
- Adak, S., Q. Wang and D. J. Stuehr (2000). "Arginine conversion to nitroxide by tetrahydrobiopterin-free neuronal nitric-oxide synthase. Implications for mechanism." *J. Biol. Chem.* **275**(43): 33554-33561.
- Altschul, S. F., W. Gish, W. Miller, E. W. Myers and D. J. Lipman (1990). "Basic local alignment search tool." *J. Mol. Biol.* **215**: 403-410.
- Andrew, P. J. and B. Mayer (1999). "Enzymatic function of nitric oxide synthases." *Cardiovasc Res* **43**(3): 521-31.
- Arantes, O. and D. Lereclus (1991). "Construction of cloning vectors for *Bacillus thuringiensis*." *Gene* **108**: 115-119.
- Atkinson, M. R., L. V. Wray and S. H. Fisher (1990). "Regulation of Histidine and Proline Degradation Enzymes by Amino Acid Availability in *Bacillus subtilis*." *J. Bacteriol.* **172**(9): 4758-4765.
- Aulak, K. S., T. Koeck, J. W. Crabb and D. J. Stuehr (2004). "Dynamics of protein nitration in cells and mitochondria." *Am J Physiol Heart Circ Physiol* **286**: H30-H38.
- Aulak, K. S., M. Miyagi, L. Yan, K. A. West, D. Massillon, J. W. Crabb and D. J. Stuehr (2001). "Proteomic method identifies proteins nitrated *in vivo* during inflammatory challenge." *Proc Natl Acad Sci U S A* **98**(21): 12056-12061.
- Belitsky, B. R. and A. L. Sonenshein (1998). "Role and regulation of *Bacillus subtilis* glutamate dehydrogenase genes." *J. Bacteriol.* **180**: 6298-6305.
- Bhavsar, A. P., X. Zhao and E. D. Brown (2001). "Development and Characterization of a Xylose-Dependent System for Expression of Cloned Genes in *Bacillus subtilis*: Conditional Complementation of a Teichoic Acid Mutant." *Appl. Envir. Microbiol.* **67**(1): 403-410.
- Bird, L. E., J. Ren, J. Zhang, N. Foxwell, A. R. Hawkins, I. G. Charles and D. K. Stammers (2002). "Crystal structure of SANOS, a bacterial nitric oxide synthase oxygenase protein from *Staphylococcus aureus*." *Structure (Camb.)* **10**(12): 1687-1696.
- Bogdan, C. (2001). "Nitric oxide and the immune response." *Nature Immunol.* **2**(10): 907-916.
- Buddha, M. R. and B. R. Crane (2005). "Structure and activity of an aminoacyl-tRNA synthetase that charges tRNA with nitro-tryptophan." *Nat Struct Mol Biol* **12**(3): 274-275.

- Buddha, M. R., K. M. Keery and B. R. Crane (2004). "An unusual tryptophanyl tRNA synthetase interacts with nitric oxide synthase in *Deinococcus radiodurans*." *Proc Natl Acad Sci U S A* **101**(45): 15881-6.
- Buddha, M. R., T. Tao, R. J. Parry and B. R. Crane (2004). "Regioselective nitration of tryptophan by a complex between bacterial nitric-oxide synthase and tryptophanyl-tRNA synthetase." *J Biol Chem* **279**(48): 49567-70.
- Burkholder, P. R. and N. H. Giles (1947). "Induced biochemical mutations in *Bacillus subtilis*." *Amer. J. Bot.* **34**: 345-348.
- Butt, E., M. Bernhardt, A. Smolenski, P. Kotsonis, L. G. Frohlich, A. Sickmann, H. E. Meyer, S. M. Lohmann and H. H. Schmidt (2000). "Endothelial nitric-oxide synthase (type III) is activated and becomes calcium independent upon phosphorylation by cyclic nucleotide-dependent protein kinases." *J. Biol. Chem.* **275**(7): 5179-5187.
- Candiano, G., M. Bruschi, L. Musante, G. M. Ghiggeri, B. Carnemolla, P. Orecchia, L. Zardi and P. G. Righetti (2004). "Blue silver: A very sensitive colloidal Coomassie G-250 staining for proteome analysis." *Electrophoresis* **25**: 1327-1333.
- Chen, P. F., A. L. Tsai and K. K. Wu (1994). "Cysteine 184 of endothelial nitric oxide synthase is involved in heme coordination and catalytic activity." *J. Biol. Chem.* **269**(40): 25062-25066.
- Chen, Y. and J. P. Rosazza (1995). "Purification and characterization of nitric oxide synthase (NOS_{Noc}) from a *Nocardia* species." *J Bacteriol* **177**(17): 5122-8.
- Choi, D. W., Y. H. Oh, S. Y. Hong, J. W. Han and H. W. Lee (2000). "Identification and Characterization of Nitric Oxide Synthase in *Salmonella typhimurium*." *Arch. Pharm. Res.* **23**(4): 407-412.
- Choi, W. S., M. S. Chang, J. W. Han, S. Y. Hong and H. W. Lee (1997). "Identification of nitric oxide synthase in *Staphylococcus aureus*." *Biochem Biophys Res Commun* **237**(3): 554-8.
- Choi, W. S., D. W. Seo, M. S. Chang, J. W. Han, S. Y. Hong, W. K. Paik and H. W. Lee (1998). "Methylesters of L-Arginine and N-Nitro-L-arginine Induce Nitric Oxide Synthase in *Staphylococcus aureus*." *Biochem. Biophys. Res. Commun.* **246**: 431-435.
- Crane, B. R., A. S. Arvai, R. Gachhui, C. Wu, D. K. Ghosh, E. D. Getzoff, D. J. Stuehr and J. A. Tainer (1997). "The structure of nitric oxide synthase oxygenase domain and inhibitor complexes." *Science* **278**(5337): 425-431.
- Crane, B. R., A. S. Arvai, D. K. Ghosh, C. Wu, E. D. Getzoff, D. J. Stuehr and J. A. Tainer (1998). "Structure of nitric oxide synthase oxygenase dimer with pterin and substrate." *Science* **279**(5359): 2121-2126.
- Cubberley, R. R., W. K. Alderton, A. Boyhan, I. G. Charles, P. N. Lowe and R. W. Old (1997). "Cysteine-200 of human inducible nitric oxide synthase is essential for dimerization of haem domains and for binding of haem, nitroarginine and tetrahydrobiopterin." *Biochem. J.* **323**(Pt 1): 141-146.
- Cutruzzola, F. (1999). "Bacterial nitric oxide synthesis." *Biochim Biophys Acta* **1411**: 231-249.

- Garcin, E. D., C. M. Bruns, S. J. Lloyd, D. J. Hosfield, M. Tiso, R. Gachhui, D. J. Stuehr, J. A. Tainer and E. D. Getzoff (2004). "Structural basis for isozyme-specific regulation of electron transfer in nitric-oxide synthase." *J Biol Chem* **279**(36): 37918-27.
- Ghosh, D. K. and J. C. Salerno (2003). "Nitric oxide synthases: domain structure and alignment in enzyme function and control." *Front Biosci* **8**: d193-209.
- Gorg, A., C. Obermaier, G. Boguth, A. Harder, B. Scheibe, R. Wildgruber and W. Weiss (2000). "The current state of two-dimensional electrophoresis with immobilized pH gradients." *Electrophoresis* **21**: 1037-1053.
- Gorg, A., W. Weiss and M. J. Dunn (2004). "Current two-dimensional electrophoresis technology for proteomics." *Proteomics* **4**: 3665-3685.
- Green, L. C., D. A. Wagner, J. Glogowski, P. L. Skipper, J. S. Wishnok and S. R. Tannenbaum (1982). "Analysis of nitrate, nitrite, and [¹⁵N]nitrate in biological fluids." *Anal. Biochem.* **126**(1): 131-138.
- Griess, J. P. (1864). "On a new series of bodies in which nitrogen is substituted for hydrogen." *Phil. Trans. Res. Soc. (London)* **154**: 667-731.
- Grundy, F. J. and T. M. Henkin (1998). "The S box regulon: a new global transcription termination control system for methionine and cysteine biosynthesis genes in gram-positive bacteria." *Mol. Microbiol.* **30**: 737-749.
- Gusarov, I. and E. Nudler (2005). "NO-mediated cytoprotection: Instant adaptation to oxidative stress in bacteria." *Proc Natl Acad Sci U S A* **102**(39): 13855-13860.
- Gustafsson, M. C. U., O. Roitel, K. R. Marshall, M. A. Noble, S. K. Chapman, A. Pessegueiro, A. J. Fulco, M. R. Chessman, C. v. Wachenfeldt and A. W. Munro (2004). "Expression, Purification, and Characterization of *Bacillus subtilis* Cytochromes P450 CYP102A2 and CYP102A3: Flavochrome Homologues of P450 BM3 from *Bacillus megaterium*." *Biochemistry* **43**: 5474-5487.
- Herbert, B. R., J. Grinyer, J. T. McCarthy, M. Isaacs, E. J. Harry, H. Nevalainen, M. D. Traini, S. Hunt, B. Schultz, M. Laver, A. R. Goodall, J. Packer, J. L. Harry and K. L. Williams (2006). "Improved 2-DE of microorganisms after acidic extraction." *Electrophoresis* **27**: 1630-1640.
- Hong, I.-s., Y. K. Kim, W. S. Choi, D. W. Seo, J. W. Yoon, J.-W. Han, H. Y. Lee and H. W. Lee (2003). "Purification and characterization of nitric oxide synthase from *Staphylococcus aureus*." *FEMS Microbiol. Lett.* **222**: 177-182.
- Hulo, N., A. Bairoch, V. Bulliard, L. Cerutti, E. De Castro, P. S. Langendijk-Genevaux, M. Pagni and C. J. Sigrist (2006). "The PROSITE database." *Nucleic Acids Res.* **34**: D227-D230.
- Ignarro, L. J., G. M. Buga, K. S. Wood, R. E. Byrns and G. Chaudhuri (1987). "Endothelium-derived relaxing factor produced and released from artery and vein is nitric oxide." *Proc. Natl. Acad. Sci. U S A* **84**(24): 9265-9269.
- Ignarro, L. J., J. N. Degnan, W. H. Baricos, P. J. Kadowitz and M. S. Wolin (1982). "Activation of purified guanylate cyclase by nitric oxide requires heme. Comparison of heme-deficient, heme-reconstituted and heme-containing forms of soluble enzyme from bovine lung." *Biochim Biophys Acta* **718**: 49-59.

- Ingham, C. J., J. Dennis and P. A. Furneaux (1999). "Autogenous regulation of transcription termination factor Rho and the requirement for Nus factors in *Bacillus subtilis*." *Mol. Microbiol.* **31**: 651-663.
- Ischiropoulos, H. (2003). "Biological selectivity and functional aspects of protein tyrosine nitration." *Biochem Biophys Res Commun* **305**(3): 776-83.
- Jaffrey, S. R., H. Erdjument-Bromage, C. D. Ferris, P. Tempst and S. H. Snyder (2001). "Protein S-nitrosylation: a physiological signal for neuronal nitric oxide." *Cell Biol Nature* **3**: 193-197.
- James, P., J. Halladay and E. A. Craig (1996). "Genomic Libraries and a Host Strain Designed for Highly Efficient Two-Hybrid Selection in Yeast." *Genetics* **144**: 1425-1436.
- Jin, S., M. De Jesus-Berrios and A. L. Sonenshein (1996). "A *Bacillus subtilis* malate dehydrogenase gene." *J. Bacteriol.* **178**: 560-563.
- Kanehisa, M., S. Goto, M. Hattori, K. F. Aoki-Kinoshita, S. Kawashima, T. Katayama, M. Araki and M. Hirakawa (2006). "From genomics to chemical genomics: new developments in KEGG." *Nucleic Acids Res.* **34**: D354-D357.
- Karow, D. S., D. Pan, R. Tran, P. Pellicena, A. Presley, R. A. Mathies and M. A. Marletta (2004). "Spectroscopic characterization of the soluble guanylate cyclase-like heme domains from *Vibrio cholerae* and *Thermoanaerobacter tengcongensis*." *Biochemistry* **43**(31): 10203-11.
- Kers, J. A., M. J. Wach, S. B. Krasnoff, J. Widom, K. D. Cameron, R. A. Bukhalid, D. M. Gibson, B. R. Crane and R. Loria (2004). "Nitration of a peptide phytotoxin by bacterial nitric oxide synthase." *Nature* **429**(6987): 79-82.
- Kimhi, Y. and B. Magasanik (1970). "Genetic basis of histidine degradation in *Bacillus subtilis*." *J. Biol. Chem.* **245**: 3545-3548.
- Kleerebezem, M. and L. E. Quadri (2001). "Peptide pheromone-dependent regulation of antimicrobial peptide production in Gram-positive bacteria: a case of multicellular behavior." *Peptides* **22**(10): 1579-1596.
- Koeck, T., D. J. Stuehr and K. S. Aulak (2005). "Mitochondria and regulated tyrosine nitration." *Biochem. Soc. Trans.* **33**(6): 1399-1403.
- Kohler, C., C. von Eiff, G. Peters, R. A. Proctor, M. Hecker and S. Engelmann (2003). "Physiological Characterization of a Heme-Deficient Mutant of *Staphylococcus aureus* by a Proteomic Approach." *J. Bacteriol.* **185**(23): 6928-6937.
- Lawson, R. J., C. v. Wachenfeldt, I. Haq, J. Perkins and A. W. Munro (2004). "Expression and Characterization of the Two Flavodoxin Proteins of *Bacillus subtilis*, YkuN and YkuP: Biophysical Properties and Interactions with Cytochrome P450 BioI." *Biochemistry* **43**: 12390-12409.
- Leighton, T. J. and R. H. Doi (1971). "The stability of messenger ribonucleic acid during sporulation in *Bacillus subtilis*." *J. Biol. Chem.* **246**(10): 3189-3195.
- Li, H. and T. L. Poulos (2005). "Structure-function studies on nitric oxide synthases." *J Inorg Biochem* **99**(1): 293-305.

- Lilley, K. S., A. Razzaq and P. Dupree (2001). "Two-dimensional gel electrophoresis: recent advances in sample preparation, detection and quantitation." *Curr Opin Chem Biol* **6**: 46-50.
- MacMillan-Crow, L. A., J. P. Crow, J. D. Kirby, J. S. Beckman and J. A. Thompson (1996). "Nitration and inactivation of manganese superoxide dismutase in chronic rejection of human renal allografts." *Proc Natl Acad Sci U S A* **93**: 11853-11858.
- Melin, L., K. Magnusson and L. Rutberg (1987). "Identification of the promoter of *Bacillus subtilis* *sdh* operon." *J. Bacteriol.* **169**: 3232-3236.
- Midha, S., R. Mishra, M. A. Aziz, M. Sharma, A. Mishra, P. Khandelwal and R. Bhatnagar (2005). "Cloning, expression, and characterization of recombinant nitric oxide synthase-like protein from *Bacillus anthracis*." *Biochem Biophys Res Commun* **336**(1): 346-356.
- Mitchell, D. A., P. A. Erwin, T. Michel and M. A. Marletta (2005). "S-Nitrosation and Regulation of Inducible Nitric Oxide Synthase." *Biochemistry* **44**(12): 4636-4647.
- Mostertz, J., C. Scharf, M. Hecker and G. Homuth (2004). "Transcriptome and proteome analysis of *Bacillus subtilis* gene expression in response to superoxide and peroxide stress." *Microbiology* **150**: 497-512.
- Mungrue, I. N., D. S. Bredt, D. J. Stewart and M. Husain (2003). "From molecules to mammals: what's NOS got to do with it?" *Acta Physiol Scand* **179**(2): 123-35.
- Murataliev, M. B., R. Feyereisen and F. A. Walker (2004). "Electron transfer by diflavin reductases." *Biochim. Biophys. Acta.* **1698**: 1-26.
- Nakano, M. M., T. Hoffmann, Y. Zhu and D. Jahn (1998). "Nitrogen and Oxygen Regulation of *Bacillus subtilis* *nasDEF* Encoding NADH-Dependent Nitrite Reductase by TnrA and ResDE." *J Bacteriol* **180**(20): 5344-5350.
- Nioche, P., V. Berka, J. Vipond, N. Minton, A. L. Tsai and C. S. Raman (2004). "Femtomolar sensitivity of a NO sensor from *Clostridium botulinum*." *Science* **306**(5701): 1550-3.
- Ogawa, K.-I., E. Akagawa, K. Yamane, Z.-W. Sun, M. LaCelle, P. Zuber and M. M. Nakano (1995). "The *nasB* Operon and *nasA* Gene Are Required for Nitrate/Nitrite Assimilation in *Bacillus subtilis*." *J Bacteriol* **177**(5): 1409-1413.
- Pant, K., A. M. Bilwes, S. Adak, D. J. Stuehr and B. R. Crane (2002). "Structure of a nitric oxide synthase heme protein from *Bacillus subtilis*." *Biochemistry* **41**(37): 11071-9.
- Pant, K. and B. R. Crane (2006). "Nitrosyl-Heme Structures of *Bacillus subtilis* Nitric Oxide Synthase Have Implications for Understanding Substrate Oxidation." *Biochemistry* **45**: 2537-2544.
- Radi, R. (2004). "Nitric oxide, oxidants, and protein tyrosine nitration." *Proc Natl Acad Sci U S A* **101**(12): 4003-8.
- Raggiaschi, R., C. Lorenzetto, E. Diodato, A. Caricasole, S. Gotta and Terstappen (2006). "Detection of phosphorylation patterns in rat cortical neurons by combining phosphatase treatment and DIGE technology." *Proteomics* **6**: 748-756.

- Ravi, K., L. A. Brennan, S. Levic, P. A. Ross and S. M. Black (2004). "S-nitrosylation of endothelial nitric oxide synthase is associated with monomerization and decreased enzyme activity." *Proc Natl Acad Sci U S A* **101**(8): 2619-24.
- Rhee, K. Y., H. Erdjument-Bromage, P. Tempst and C. F. Nathan (2005). "S-nitroso proteome of *Mycobacterium tuberculosis*: Enzymes of intermediary metabolism and antioxidant defense." *Proc Natl Acad Sci U S A* **102**(2): 467-472.
- Richards, M. K., M. J. Claque and M. A. Marletta (1996). "Characterization of C415 mutants of neuronal nitric oxide synthase." *Biochemistry* **35**(224): 7772-7780.
- Roman, L. J., P. Martasek and B. S. Masters (2002). "Intrinsic and extrinsic modulation of nitric oxide synthase activity." *Chem. Rev.* **102**(4): 1179-1190.
- Sabounchi-Schutt, F., J. Astrom, I. Olsson, A. Eklund, J. Grunewald and B. Bjellqvist (2000). "An Immobilized DryStrip application method enabling high-capacity two-dimensional gel electrophoresis." *Electrophoresis* **21**: 3649-3656.
- Sagami, I., Y. Sato, T. Noguchi, M. Miyajima, E. Rozhkova, S. Daff and T. Shimizu (2002). "Electron transfer in nitric-oxide synthase." *Coord. Chem. Rev.* **226**: 179-186.
- Salerno, J. C., D. E. Harris, K. Irizarry, B. Patel, A. J. Morales, S. M. Smith, P. Martasek, L. J. Roman, B. S. Masters, C. L. Jones, B. A. Weissman, P. Lane, Q. Liu and S. S. Gross (1997). "An autoinhibitory control element defines calcium-regulated isoforms of nitric oxide synthase." *J. Biol. Chem.* **272**(47): 29769-29777.
- Schopfer, F. J., P. R. Baker and B. A. Freeman (2003). "NO-dependent protein nitration: a cell signaling event or an oxidative inflammatory response?" *Trends Biochem Sci* **28**(12): 646-54.
- Sekowska, A., L. Mulard, S. Krogh, J. K. Tse and A. Danchin (2001). "MtnK, methylthioribose kinase, is a starvation-induced protein in *Bacillus subtilis*." *BMC Microbiol.* **1**: 15-25.
- Sekowska, A., L. Mulard, S. Krogh, J. K. Tse and A. Danchin (2001). "MtnK, methylthioribose kinase, is a starvation-induced protein in *Bacillus subtilis*." *BMC Microbiol.* **1**: 15-24.
- Sibille, N., M. Blackledge, B. Brutscher, J. Coves and B. Bersch (2005). "Solution Structure of the Sulfite Reductase Flavodoxin-like Domain from *Escherichia coli*." *Biochemistry* **44**: 9086-9095.
- Siddhanta, U., A. Presta, B. Fan, D. Wolan, D. L. Rousseau and D. J. Stuehr (1998). "Domain swapping in inducible nitric-oxide synthase. Electron transfer occurs between flavin and heme groups located on adjacent subunits in the dimer." *J. Biol. Chem.* **273**(30): 18950-18958.
- Silo-Suh, L. A., B. J. Lethbridge, S. J. Raffel, H. He, J. Clardy and J. Handelsman (1994). "Biological Activities of Two Fungistatic Antibiotics Produced by *Bacillus cereus* UW85." *Appl. Envir. Microbiol.* **60**(6): 2023-2030.
- Singh, V., W. Shi, S. C. Almo, G. B. Evans, R. H. Furneaux, P. C. Tyler, G. F. Painter, D. H. Lenz, S. Mee, R. Zheng and V. L. Schramm (2006). "Structure and Inhibition of Quorum Sensing Target from *Streptococcus pneumoniae*." *Biochemistry* **45**: 12929-12941.

- Snyder, S. H. and D. S. Brecht (1992). "Biological roles of nitric oxide." *Sci. Am.* **266**(5): 68-71, 74-77.
- Soppa, J., K. Kobayashi, M.-F. Noirot-Gros, D. Oesterheit, S. D. Ehrlich, E. Dervyn, N. Ogasawara and S. Moriya (2002). "Discovery of two novel families of proteins that are proposed to interact with prokaryotic SMC proteins, and characterization of the *Bacillus subtilis* family members ScpA and ScpB." *Mol Microbiol* **45**(1): 59-71.
- Strume, M. H., M. Kleerebezem, J. Nakayama, A. D. Akkermans, E. E. Vaughn and W. H. de Vos (2002). "Cell to cell communication by autoinducing peptides in gram-positive bacteria." *Antonie Van Leeuwenhoek* **81**((1-4)): 233-243.
- Stuehr, D. J., J. Santolini, Z. Q. Wang, C. C. Wei and S. Adak (2004). "Update on mechanism and catalytic regulation in the NO synthases." *J Biol Chem* **279**(35): 36167-70.
- Stuehr, D. J., C. C. Wei, Z. Wang and R. Hille (2005). "Exploring the redox reactions between heme and tetrahydrobiopterin in the nitric oxide synthases." *Dalton Trans.* **21**: 3427-3435.
- Sudhamsu, J. and B. R. Crane (2006). "Structure and Reactivity of a Thermostable Prokaryotic Nitric-oxide Synthase That Forms a Long-lived Oxy-Heme Complex." *J. Biol. Chem.* **281**(14): 9623-9632.
- Vagner, V., E. Dervyn and S. D. Ehrlich (1998). "A vector for systematic gene inactivation in *Bacillus subtilis*." *Microbiology* **144** (Pt 11): 3097-104.
- Vandahl, B., G. Christiansen and S. Birkelund (2002). Preparation of Bacterial Samples for 2-D PAGE. *The Protein Protocols Handbook*. J. M. Walker. Totowa, NJ, Humana Press: 19-26.
- Wang, W. and B. A. Malcolm (1999). "Two-stage PCR protocol allowing introduction of multiple mutations, deletions and insertions using QuikChange Site-Directed Mutagenesis." *Biotechniques* **4**: 680-682.
- Wang, Z. Q., C. C. Wei, M. Sharma, K. Pant, B. R. Crane and D. J. Stuehr (2004). "A conserved Val to Ile switch near the heme pocket of animal and bacterial nitric-oxide synthases helps determine their distinct catalytic profiles." *J Biol Chem* **279**(18): 19018-25.
- Waters, C. M. and B. L. Bassler (2005). "Quorum Sensing: Cell-To-Cell Communication in Bacteria." *Annu. Rev. Cell. Dev. Biol.* **21**: 319-346.
- Wilm, M., A. Shevchenko, T. Houthaeve, S. Breit, L. Schweigerer, T. Fotsis and M. Mann (1996). "Femtomole sequencing of proteins from polyacrylamide gels by nano-electrospray mass spectrometry." *Nature* **379**(6564): 466-469.
- Yoshida, K.-i., I. Ishio, E. Nagakawa, Y. Yamamoto, M. Yamamoto and Y. Fujita (2000). "Systematic study of gene expression and transcription organization in the *gntZ-ywaA* region of the *Bacillus subtilis* genome." *Microbiology* **146**: 573-579.
- Yumakura, F. and K. Ikeda (2006). "Modification of tryptophan and tryptophan residues in proteins by reactive nitrogen species." *Nitric Oxide* **14**: 152-161.
- Zemojtel, T., R. C. Wade and T. Dandekar (2003). "In search of the prototype of nitric oxide synthase." *FEBS Lett* **554**(1-2): 1-5.

Zhan, X. and D. M. Desiderio (2004). "The human pituitary nitroproteome: detection of nitrotyrosyl-proteins with two-dimensional Western blotting, and amino acid sequence determination with mass spectrometry." *Biochem Biophys Res Commun* **325**: 1180-1186.